CHALMERS
UNIVERSITY OF TECHNOLOGY

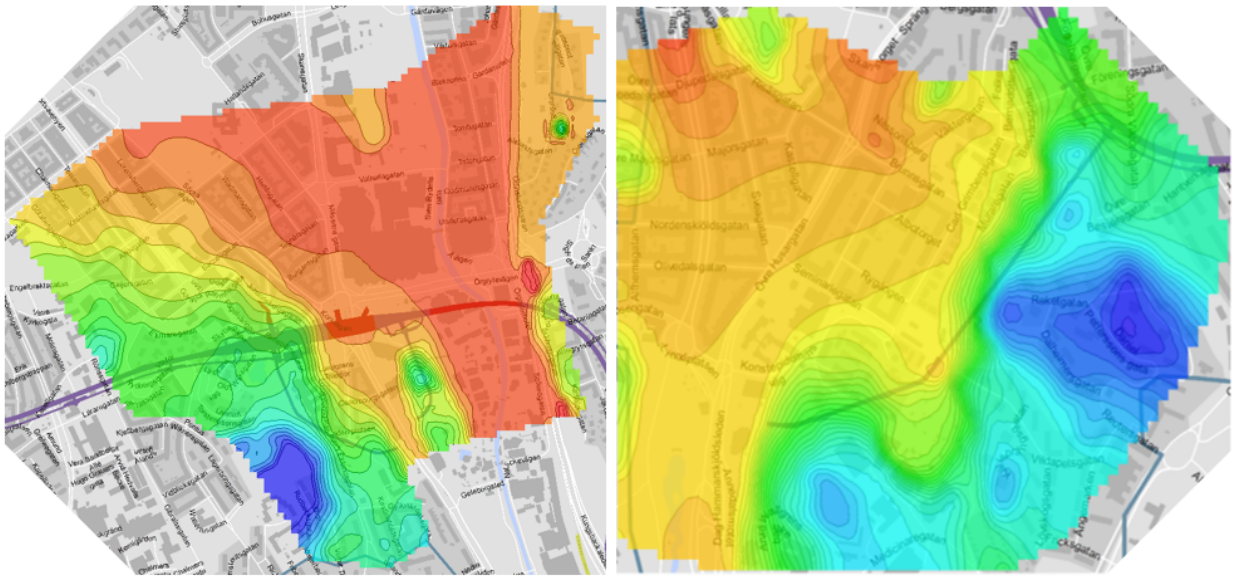

Parameter uncertainties in groundwater modelling

A study on the effect of calibration method on parameter uncertainties in an inverse stochastic groundwater model

Master's thesis in Infrastructure and Environmental Engineering

VILHELM BERLING
JONAS STRÖMBERG

Department of Architecture and Civil Engineering
Chalmers University of Technology
Master's Thesis ACEX30
Gothenburg, Sweden 2020

Master's thesis ACEX30-XX-XX

Parameter uncertainties in groundwater modeling

A study on the effect of calibration method on parameter uncertainties in an inverse stochastic groundwater model

VILHELM BERLING
JONAS STRÖMBERG

CHALMERS
UNIVERSITY OF TECHNOLOGY

Department of Architecture and Civil Engineering
Division of Geology and Geotechnics
Engineering geology
Chalmers University of Technology
Gothenburg, Sweden 2020

Parameter uncertainties in groundwater modeling.
A study on the effect of calibration method on parameter uncertainties in an inverse stochastic groundwater model.
VILHELM BERLING
JONAS STRÖMBERG

Supervisors: Jonas Sundell, Trafikverket
Johanna Merisalu, Department of Architecture and Civil Engineering
Jenny Palmenäs, Bergab

Examiner: Lars Rosén, professor in the Division of Geology and Geotechnics

Department of Architecture and Civil Engineering
Division of Geology and Geotechnics
Engineering Geology
Chalmers University of Technology
SE-412 96 Gothenburg
Telephone +46 31 772 1000

Cover: Groundwater heads in the two model areas.

Department of Architecture and Civil Engineering
Gothenburg, Sweden 2020

Parameter uncertainties in groundwater modelling
A study on the effect of calibration method on parameter uncertainties in an inverse stochastic groundwater model
Master's thesis in Infrastructure and Environmental Engineering
Vilhelm Berling
Jonas Strömberg
Department of Architecture and Civil Engineering
Division of Geology and Geotechnics
Engineering Geology
Chalmers University of Technology

Abstract

Numerical models can be used to forecast the effects of underground constructions on groundwater conditions. Such forecasts always includes uncertainties, with values of used parameters being one common source of uncertainty. This study aims to assess how these parameter uncertainties and the resulting model outcome uncertainty are affected by either calibrating an inverse stochastic groundwater model against historic mean head observations or against a disturbance of the hydrogeological conditions. Two sections of the planned train tunnel Västlänken through Gothenburg are used as case studies to evaluate the effect that calibration method has on uncertainties. The first modelled section, Linné service tunnel uses historical mean head observations for the first case of calibration and leakage to the partially constructed tunnel with the effect on groundwater levels for the second calibration case. The other modelled section, Korsvägen, uses the same type of observations for the first calibration case, while the second case uses the effects of a pumping test. It was seen that the model over Linné service tunnel resulted in larger uncertainties for calibration case two compared to case one, while the model over Korsvägen resulted in less uncertainties for calibration case two compared to case one. This study shows that calibration method effects uncertainties deriving from used parameters and that more observations does not always mean less uncertainty.

Keywords: Stochastic groundwater modelling, GMS MODFLOW, inverse calibration, parameter uncertainty, PEST, Null Space Monte Carlo

Acknowledgements

The work with this study was done during the spring of 2020 on behalf of Trafikverket in cooperation with Bergab. We would like to recognize our gratitude to our supervisor Jonas Sundell at Trafikverket for the support during all our struggles with the modelling. We would also like to say many thanks to Bergab for supplying us with computers, office space and material for the modelling. All the employee's at Bergab's Gothenburg office should have a big thanks for supporting us with your knowledge as well as nice conversations. A special thanks to Jenny Palmenäs, who especially in the beginning of modelling process provided invaluable help with GMS. We would also like to give a thank to our supervisor at Chalmers, Johanna Merisalu.

Vilhelm Berling & Jonas Strömberg, Gothenburg, June 2020

Contents

1
Introduction

Groundwater leakage can cause great problems. When constructing rock tunnels, the goal is to achieve a watertight solution around the tunnel construction in order to reduce the impact on the groundwater conditions. A lowering of the groundwater levels beneath a clay layer in an urban environment can reduce the pore water pressure in the soil, inducing settlements and potentially causing damage to building foundations (Chilton, 1999). Settlements due to rock tunneling is a common worldwide problem in urban environments. An example is the construction of the Rödbo rock tunnel in Gothenburg, with lowered groundwater levels in wells, decreased pore pressure in clay leading to large settlements (Ahlberg & Lundgren, 1977). A further example is a case in Seoul, where a reduction of groundwater levels induced by rock tunneling led to large settlements, even though pre- and post grouting was implemented (Yoo, Lee, Kim, & Kim, 2012).

To assess the effects that an underground construction has on a groundwater system, numerical models can be used. Gustafson (2009) states three different purposes of such modelling; analysing and understanding the system, forecasting system behavior and quantify system components. This has for example been used in the planned construction of the train tunnel Västlänken through Gothenburg where it is a part of the basis for assessment of the projects effect on groundwater conditions (Sundkvist, 2016). A numerical groundwater model was also used in the Ormen tunnel project in Stockholm, where the expected drawdown from the 3.7 km long rock tunnel in a highly urbanised area was studied. However, large hydrogeological systems in a heterogenic environment contains a lot of uncertainties, which for example has been shown in a previous study on Varbergstunneln (Sundell, 2018). Many different kinds of uncertainties are present in groundwater modelling and Walker et al. (2003) has divided them into context-, model-, input-, parameter- and model outcome uncertainty. The uncertainties are often assessed in a model outcome uncertainty analysis. One such method being the utility Null Space Monte Carlo (NSMC), that introduces uncertainty to the model parameters, enabling analyses of model outcome uncertainty (Doherty, 2018). Sparse observational data sets are a usual cause of parameter uncertainty when developing groundwater models. Using more data to calibrate a model should according to Bayes theorem decrease this uncertainty, but studies by Tiedeman, Hill, D'Agnese, and Faunt (2003) and Beven (2005) has shown that more data used for calibration does not always decrease model outcome uncertainty, highlighting the importance of using the right type of calibration data for the right type of model.

In this study, an inverse probabilistic hydrogeological model is developed to asses how parameter uncertainties are affected by using different kinds of observations for calibration of the model. The study will use the ongoing construction of the train tunnel Västlänken through Gothenburg as a case study. Two models are developed for each of two sections of Västlänken; service tunnel Linné and section Korsvägen. The models are developed with the software GMS MODFLOW and calibrated with the utility package PEST (Parameter ESTimation) and PEST NSMC for the stochastic modeling.

The study will assess the use of different observations in model calibration in a model used to forecast the effects tunnel leakage will have on the hydrogeological system of the areas. Two calibrated models are developed for each area with two observation cases. The first case is with historical hydrogeological conditions from before tunnel construction and the second case is with disturbed hydrogeological conditions. 20 calibrated models of each case is created with PEST NSMC. The expected tunnel leakage is then simulated and the spread of the outcome can be observed and compared between the cases. The second case for service tunnel Linné is observed groundwater levels and measured tunnel leakage at a time when 495 meter of tunnel is constructed, while the second case for Korsvägen is a pumping test with observed effects on groundwater levels in the area.

The study is performed on behalf of Trafikverket in association with Bergab - Berggeologiska undersökningar AB.

1.1 Purpose

The study aims to assess how different types of observational data used to calibrate an inverse probabilistic groundwater model affects parameter uncertainties and the resulting model outcome uncertainty. With a model calibrated against historical mean groundwater head observations compared to one calibrated against a disturbance of the groundwater conditions, it is intended to compare the accuracy of the groundwater drawdown forecast caused by tunneling. This aims to enable an evaluation of the uncertainties in model output and calibrated parameters in the differently calibrated models.

1.2 Specification of research question

- Can advanced hydrogeological modelling in conjunction with observations during construction improve forecasts of groundwater drawdown caused by tunneling?
- How does re-calibration with additional observational data change the uncertainties in the predictions of an inverse stochastic groundwater model?

1.3 Limitations

The analysis will be limited to only two segments of Västlänken, service tunnel Linné and Korsvägen station with surroundings. Calibration of the models is done by varying hydraulic conductivity, recharge and conductance of draining structures, with only recharge and hydraulic conductivity being calibrated with PEST and NSMC. This study will look into the potential disturbances of the water balance of the lower soil and rock aquifer, with all modelling being performed for stationary conditions. The uncertainty explored in the thesis is solely linked to parameter uncertainty of recharge and hydraulic conductivity of rock and glacial till.

The tunnel parts built through soil will be regarded as watertight, meaning that only leakage to the rock tunnels will be considered. The sand and/or gravel layer in between the clay that can be found in the geologic setting around Korsvägen will not be included in the hydrogeological model. The geologic model developed at Bergab, which gives the soil stratigraphy of the area will be used to perform the numerical modelling, meaning that no own evaluation of the stratigraphy is done in this study. Forecasts of the effects of tunnel leakage is done without taking any protective measures apart from the sealing of the tunnel into account. Only steady state modelling is performed.

The number of inversely calibrated models created with NSMC, for each method of calibration, for the two different areas are limited to 20. This was due to the fact that this project was carried out during 20 weeks and that the calibration of 20 models took over 72 hours to perform.

1.4 Disposition

Six different chapters makes up the thesis, with the first being this introductory chapter. The second chapter is a background that firstly describes some basic theory of groundwater and tunnel leakage, as well as a description of the softwares used to create the models. The background then describes the construction and geologic- and hydrogeologic settings of the Västlänken project and the two studied sections.

Chapter three is the method, that first gives an overview of the working process before going into details of the used methods. The chapter ends with a more detailed description of how the models for the two different areas has been developed.

The results chapter (4), shows the outcome of the modelling as variation of parameters and forecast groundwater head and spread of drawdown and leakage to planned structures.

In the discussion chapter, (5) the results are evaluated and a comparison is done between the different cases. The final chapter, conclusion (6) summarises the key findings of the thesis.

2
Background

2.1 Theory

2.1.1 Groundwater flow

Groundwater flow is the movement of water trough the pores and fractures of rock and sediment in the saturated zone caused by an equalization of energy differences. The flow takes place in the direction of declining hydraulic head and can for low flow velocities, which is mostly the case for groundwater flow, be described by Darcy's law, equation 2.1. It relates the groundwater flow, Q to the hydraulic conductivity, K, the cross sectional area, A, which water passes through and the hydraulic gradient, where the hydraulic gradient is the difference in hydraulic head between two points dh, divided by the distance between them, dl (Fetter, 2014).

$$Q = -KA\frac{dh}{dl} \tag{2.1}$$

2.1.2 Groundwater recharge

Recharge to an aquifer naturally takes place by infiltration of precipitation, either directly trough the ground or by leakage from surface waters or other aquifers. The amount of the precipitation that infiltrates the ground surface mainly depends on the permeability of the soil and rock layers, but other factors such as the position of the water table and the type of precipitation also has an influence. Human activities may however alter the natural recharge. Underground constructions draining an aquifer and leakage from water pipes are examples that increases recharge, while impervious surfaces decreases it (Knutssons & Morfeldt, 2002).

2.1.3 Tunnel leakage

All construction taking place in the saturated zone will to some degree affect the groundwater conditions and can cause drawdown of the groundwater level. A lowered groundwater table can for example lead to damaging settlements, degradation of wooden pile foundations that ends up above the water table, drainage of water dependent habitats, larger depth to the water table possibly affecting water uptake by plants and wells running dry (Hölting & Coldewey, 2019). In the case of building tunnels through rock, leakage will inevitably occur, but the amount varies depending on the geological and hydrogeological conditions in conjunction with drawdown re-

ducing measures. The effect of tunnel leakage in bedrock aquifers can propagate into adjacent soil aquifers, leading to drawdown of groundwater levels in these aquifers as well. This potential groundwater lowering in soil aquifers can in cases where the soil is of a compressible material lead to subsidence. If this takes place in an urban environment, there could be damage to infrastructure and buildings caused by the drawdown induced settlement (Sundell, 2018).

2.2 Groundwater modelling

A groundwater model is an interpretation of a real world hydrogeological system. This study uses a mathematical model, which describes the behavior of the system using a set of equations. Mathematical models can be divided into data-driven or process based. Data driven models uses empirical or statistical data to formulate equations describing the hydrogeology, while process based models uses the laws of physics. Subdivision between the process based models can also be done between deterministic and stochastic models, where a model is stochastic if any of the used parameters are described probabilistically. The mathematical models can be solved with either analytical or numerical solutions. Analytical solutions does often required a high degree of simplification to achieve a closed form solution, while the numerical solutions can handle more complex problems, which most commonly is solved by using the finite difference- or finite element method (Andersson, Hunt, & Woessner, 2015). A process-based stochastic numerical finite difference model will be used for the analysis in this paper.

2.2.1 Modelling process

Literature suggests modelling to be an iterative process, where a simple model initially is constructed and continuously revised as new field data is collected (Fetter, 2014). A suggested modelling workflow for a forecasting model is shown below in figure 2.1 (Anderson, Woessner, & Hunt, 2015), with field data being critical in the conceptual design and calibration process. A forecasting model uses a calibrated model to predict the result of a proposed measure, whilst a back-casting model recreates past conditions (Anderson et al., 2015). For this paper a forecasting model is used.

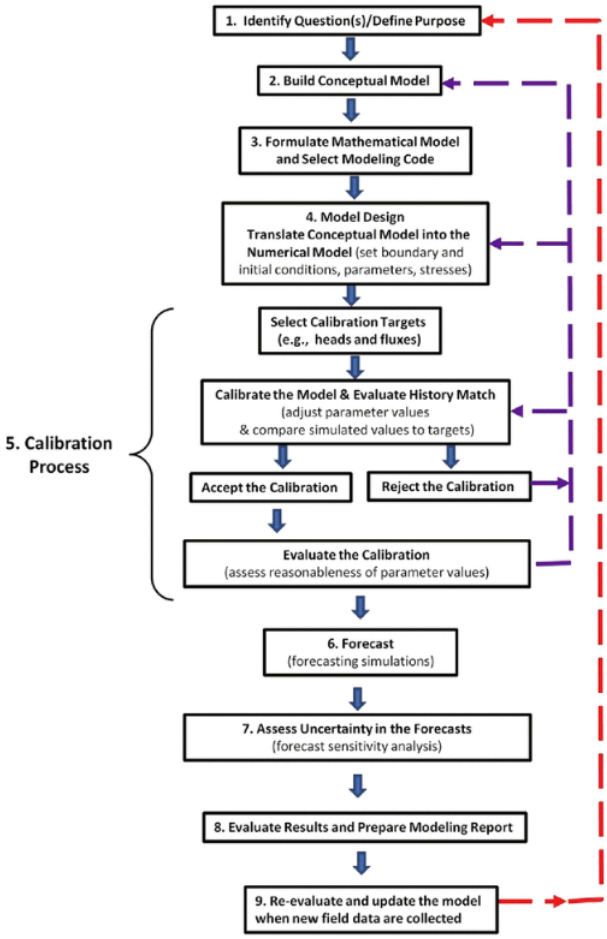

Figure 2.1: Suggested workflow for a forecasting groundwater model (Anderson et al., 2015).

2.2.2 Conceptual model

A conceptual model characterizes the hydrogeological framework and the hydrologic system of an area. It is used to develop the mathematical problem and numerical model, so the level of detail in the conceptual model is determined by the modelling purpose. In literature a conceptual model is defined to as: *"a qualitative representation of a groundwater system that conforms to hydrogeological principles and is*

based on geological, geophysical, hydrological, hydrochemichal, and other ancillary information" (Andersson et al., 2015).

2.2.3 Model calibration

When calibrating a model, runs of the model are performed so that the model to a certain degree reproduces known field observations, such as groundwater heads (Fetter, 2014). Calibration can be manual or automatic. Manual calibration is a forward problem where parameters are manually varied and the effects are observed. Automatic calibration is an inverse problem, with the effects known and causes unknown. The solution to an inverse problem is calculated from observations, see figure 2.2, also called back calculation (Gustafson, 2009). For this, software such as PEST can be used (Doherty, 2018).

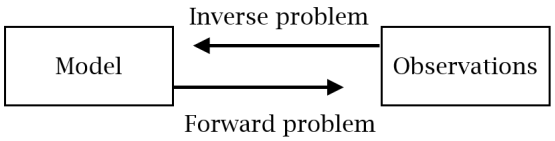

Figure 2.2: The relation between an inverse problem, model and observations.

2.2.4 Uncertainties in groundwater modelling

All attempts to make a model out of a real world problem involves uncertainties of different kinds. One way of differentiating between various kinds of uncertainty is described by Walker et al. (2003) as following:

- Context uncertainty
  - relates to the boundaries of the modelled system.
- Model uncertainty
  - stems from both the conceptual model and the computer model.
- Input uncertainty
  - comes from the external driving forces and the used reference system.
- Parameter uncertainty
  - originates from used data and calibration methods.
- Model outcome uncertainty
  - the compiled uncertainty affecting the model outcome.

It is essential to perform post calibration analysis of model out come uncertainty in order to use the model in any decision-making process (Doherty, 2018). Earlier literature treating model uncertainty notes that complex groundwater models has a loss of data in the calibration against incomplete datasets with the potential of considerable magnitudes of error in model predictions (Moore & Doherty, 2006) (Gallagher & Doherty, 2007).

2.2.5 Boundary conditions

There are three different types of boundary conditions in groundwater modelling; specified head-, specified flow- and head-dependent boundary (Andersson et al., 2015). A specified head boundary is when the head along the boundary is set to constant value that can vary along the border. The second type, specified flow boundary is when a derivative of the head is specified for the boundary. The last one, head-dependent boundary is when flow over the boundary is decided by Darcy's law using a gradient with a specified head outside the model boundary and a head computed by the model next to the boundary.

2.2.6 MODFLOW

MODFLOW is a numerical model that simulates groundwater flow by using a block centered finite difference approach. MODFLOW uses packages to perform specific tasks.
The packages are divided into three categories (XMS Wiki, 2017):

- Flow package - performs the flow calculations.
- Solver - solves the finite difference equations.
- Optional packages - performs external influences, for example drain, recharge and evapotranspiration.

The groundwater modelling code MODFLOW is based on the following differential equation that describes flow through a porous media (Harbaugh, 2005):

$$\frac{\delta}{\delta x}\left(k_{xx}\frac{\delta h}{\delta x}\right)+\frac{\delta}{\delta y}\left(k_{yy}\frac{\delta h}{\delta y}\right)+\frac{\delta}{\delta z}\left(k_{zz}\frac{\delta h}{\delta z}\right)+W=S_s\frac{\delta h}{\delta t} \tag{2.2}$$

K_{xx}, K_{yy} and K_{zz}: Hydraulic conductivity in the x, y and z direction
h: Piezometric head
W: Volumetric flux per unit volume corresponding to sources and/or sinks
S_s: Specific storage
t: Time

MODFLOW solves equation 2.2 by using finite differences where a finite set of discrete points is used to describe the equation, with the partial derivatives being substituted by the difference in head between the points. The time dependency of the head in equation 2.2 is discretized by calculating the head for different time steps, which allows the finite difference formulation to be created.

The continuity equation is used to formulate the finite differences, which describes the flow balance for a cell as following:

$$\sum Q_i = SS\frac{\Delta h}{\Delta t}\Delta V \tag{2.3}$$

Q_i: Flow rate into the cell.
Δh: Change in head over a time step Δt.
ΔV: Volume of the cell.

SS: Volume of water that can be injected per unit volume of aquifer material per unit change in head.

Flow into one cell from one face of an adjacent cell can be described as following:

$$q_{i,j-1/2,k} = KR_{i,j-1/2,k}\Delta c_i \Delta v_k \frac{h_{i,j-1/2,k} - h_{i,j,k}}{\Delta r_{j-1/2}} \tag{2.4}$$

Where:
$q_{i,j-1/2,k}$: The flow rate through the face between cells i,j-1,k and i,j,k.
$KR_{i,j-1/2,k}$: The hydraulic conductivity along the row between nodes i,j-1,k and i,j,k.
$\Delta c_i \Delta v_k$: The area of the cell faces normal to the direction of the flow.
$h_{i,j,k}$: The head at the nodes i,j-1,k and i,j,k.
$r_{j-1/2}$: The distance between the nodes i,j-1,k and i,j,k.

The groundwater flow equations in MODFLOW can be solved by several options. One of them is the Newton method (NWT), which can handle wetting and drying of cells that can occur in problems dealing with unconfined aquifers (Niwsonger, Panday, & Ibaraki, 2011).

2.2.7 PEST

PEST is a non-linear model independent parameter estimation software package developed by John Doherty, first released in 1994. It is used to accelerate model calibration by back-calculating parameters in order to reduce the residual error between model output values and input measurements (Doherty, 2018). Input measurements can for example be observations of groundwater levels, output values being computed model groundater levels. (Doherty, 2018).

Back calculation of parameters is an inverse problem, which PEST solves by writing sets of model parameter input values, adjusted within a user defined parameter set interval. PEST runs the model and compares the output values to the input measurements, see figure 2.3 (*PEST Model-independence*, n.d.). This process is iterated as many times as needed to find the solution with the lowest residual error between measurements and model output (SSPA, n.d.). User defined parameter sets can for example be hydraulic conductivity, with a specified parameter value interval that the PEST output file is constrained to stay within.

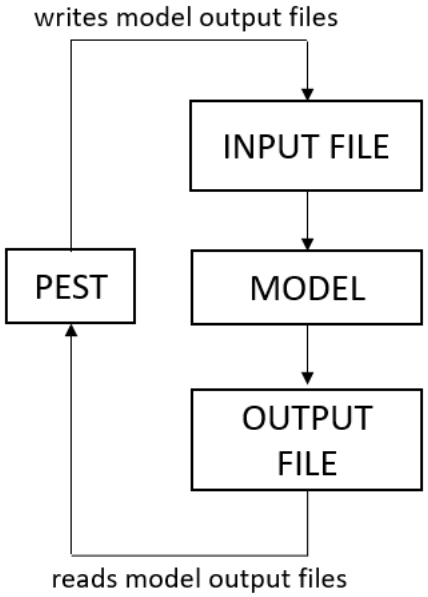

Figure 2.3: Pest interaction with model input and output files.

The PEST-suite includes different software programs which can be used both for model pre-calibration and post-calibration uncertainty analysis of the model, such as NSMC.

2.2.8 Null space monte carlo

The unique solution computed by PEST is only one of many. With the PEST program Null Space Monte Carlo, PEST can perform post-prediction uncertainty analysis, by creating multiple calibrated models.
Dohertey (2020) explains the null space of model calibration as:

$$X \times \lambda P = 0 \tag{2.5}$$

λ: Vector
P: Parameters
X: Matrix representing model under calibration

Where λP defines the null space of X. If the model is well calibrated with that set of parameters P, any λP within the null space calibrates the model as well. With NSMC, PEST generates many non-unique parameter sets within the null space of the model (Doherty, 2020). This allows the user to asses the uncertainty of the calibrated model (Doherty, 2018).

2.3 Project Västlänken

Västlänken is an eight kilometer long railway project in Göteborg with 6.6 kilometer of railway in an underground tunnel . The tunnel route alternates between soil/clay

and rock. In soil/clay the tunnel is built by excavating the soil and constructing the tunnel in concrete. In rock, the tunnel is built by drilling and blasting, see figure 2.4 for the extent of the two building methods. Three underground stations will be constructed, Centralen, Haga and Korsvägen. Additional working tunnels are built at Haga, Korsvägen and Skår. These are later to be used as service tunnels during the operating phase of the railway (Wallroth et al., 2016). Figure 2.4 also shows the two sections, Linné and Korsvägen marked with red boxes, that are used for the numerical modelling.

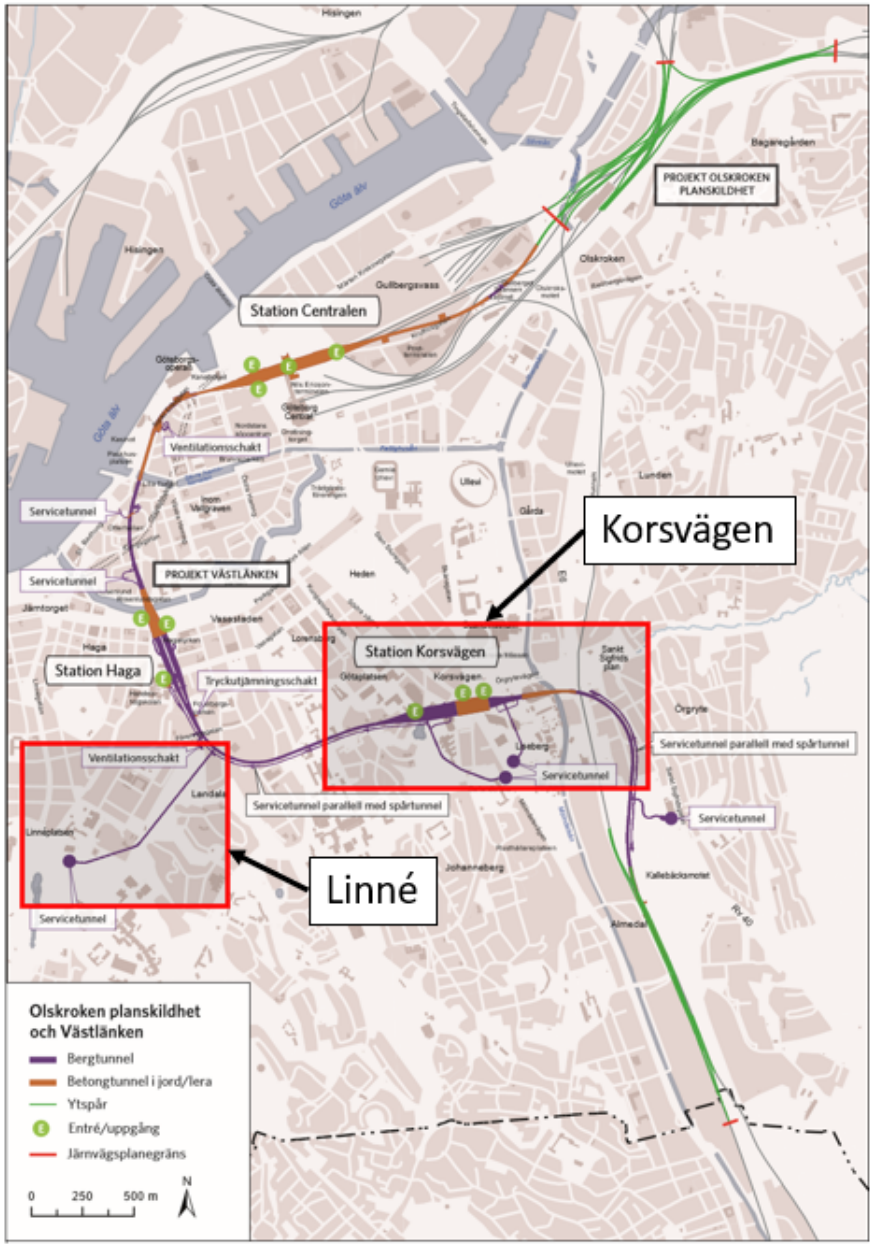

Figure 2.4: Västlänken route and type of tunnel (Sundkvist, 2016). Adapted with permission.

2.3.1 Construction of rock tunnels

The tunnel driving method for the rock tunnels in Västlänken is conventional drilling and blasting. This is performed in three steps: pre-grouting, blasting and removal of blasted rock. The rock is then reinforced by additional grouting or bolting. Pre-grouting is when the outer radius of the rock face is drilled and injected with a grouting agent in order to reduce the groundwater leakage. The extent of grouting is dependent on the hydrogeological settings and the groundwater leakage limits that are to be met to ensure that groundwater heads does not decrease to potentially harmful levels. The grouting of the tunnel will however not seal the fractures of the rock completely and leakage will occur after finished construction of the tunnel (Trafikverket, 2014).

2.3.2 Geologic setting

Soil generally covers the low laying valleys in the project area, while the higher elevated areas have exposed rock surfaces or only a thin soil cover. The stratigraphy of the valleys are in general the following: Filling material at the top, followed by a thick clay layer ranging from up to 100m thick near Göta älv to about 30m around Korsvägen. Below the clay follows a layer of coarser glacial till that lies upon the bedrock. Soil layers of significant thickness in the higher laying areas mostly consists of glacial till and can be found in depressions. The filling material consists of a varying mix of anthropogenic materials and natural soils, while the glacial till is an unsorted material with particle sizes ranging from clay to boulders (Sundkvist & Wallroth, 2016).

2.3.3 Hydrogeology

Groundwater flow can generally be said to follow the topography of the ground surface, flowing from higher to lower elevated places. Local geologic features and draining underground constructions does however influence flow patterns, leading to deviations from the topographic setting. The project stretches over areas with both groundwater in rock and soil.

Water in rock is transmitted through fractures and the hydraulic conductivity is dependent on the properties of the fractures, meaning that the ability to transmit water varies a lot in short distances. The hydraulic conductivity of the rock aquifers has been evaluated depending on its quality, with $4 * 10^{-8}$ - $2 * 10^{-7}$m/s for intact bedrock, $1 - 2 * 10^{-7}$m/s for rock near surface and $2 * 10^{-7}$ - $5 * 10^{-6}$m/s in weakness zones. There are however places with both lower and higher hydraulic conductivity than these values. Groundwater recharge in rock mainly takes place at the higher laying areas, while groundwater flows out at the lower laying rock areas. The natural recharge to the rock aquifers are approximately 100mm/year, but underground structures, such as the planned tunnel can increase recharge rates up to 200mm/year (Sundkvist & Wallroth, 2016). This is in line with a study by Raposo, Molinero, and Dafonte (2010), showing that a tunnel increased aquifer recharge by up to 75% compared to the undisturbed situation.

Through soil, the groundwater flows in the pores and the groundwater in soil in the area can be divided into two types of aquifers: An upper open aquifer found on top of the clay in frictional soils and a lower confined aquifer in the glacial till located under the clay, on top of the bedrock. The lower aquifers are found in the valleys and depressions. In places where the bedrock is greatly fractured, the soil and rock form a combined aquifer. The upper and lower aquifer is to a great extent separated by the low permeable clay layer, but are in contact in the outskirts of the aquifers where clay layers are thin or absent and in some cases connected through man made structures. Both aquifer types has some connections to surface water bodies in the area. The groundwater level in the soil generally follows the ground surface topography, expect for some areas where artesian pressure exists or man made structures either drains or recharges the aqfuifers. Runoff from the high laying rock areas flows down the valley sides recharging the soil aquifers in the valleys. There is in general a flow of groundwater from the borders of the aquifer towards the middle, which continues in the longitudinal direction of the aquifers.

2.3.4 Linné service tunnel

Linné service tunnel will connect the main tunnel to surface. The tunnel is driven trough rock from the opening at Linnéplatsen at +20 m.a.s.l. and follows a 920 meter long route in a north-east direction towards Landala, see figure 2.5, where it will connect to the main tunnel at about -20 m.a.s.l (Ramböll, 2014)

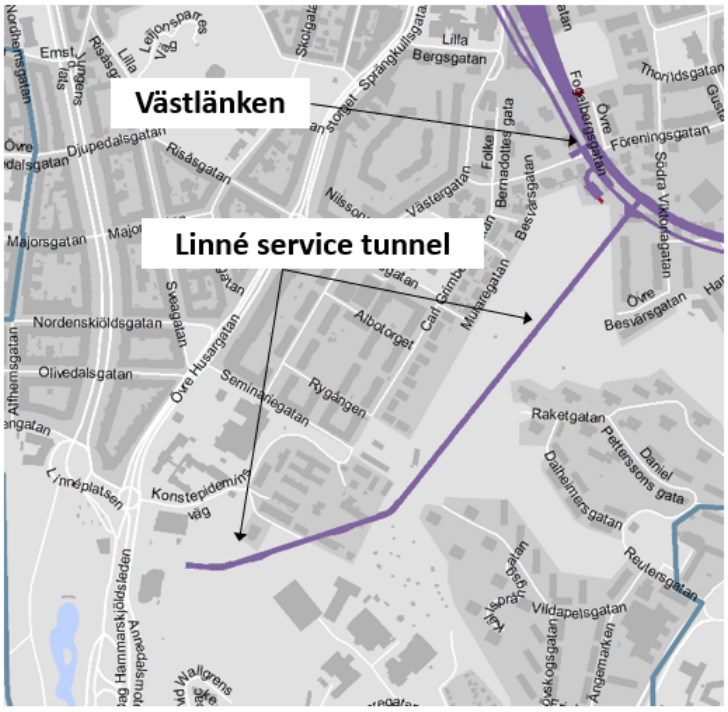

Figure 2.5: Linne service tunnel and Västlänken tunnel with property map background.

2.3.4.1 Geologic setting

The bedrock level in the area has top elevations of 50 to 70 m.a.s.l. at Sahlgrenska and Skansberget, with depressions down to -10 m.a.s.l. at Annedal. Weakness zones are found on the tunnel route with a north-west, north-north-west direction and inclination to the west. A large area of deformation zones is also found around Konstepedemien with fractures in a NNW-SSE direction (Lithén & Wadsten, 2016).

The soil stratigraphy consists of a top layer of filling material, followed by a thick layer of clay and a few meters of glacial till on top of bedrock, see figure 2.6.

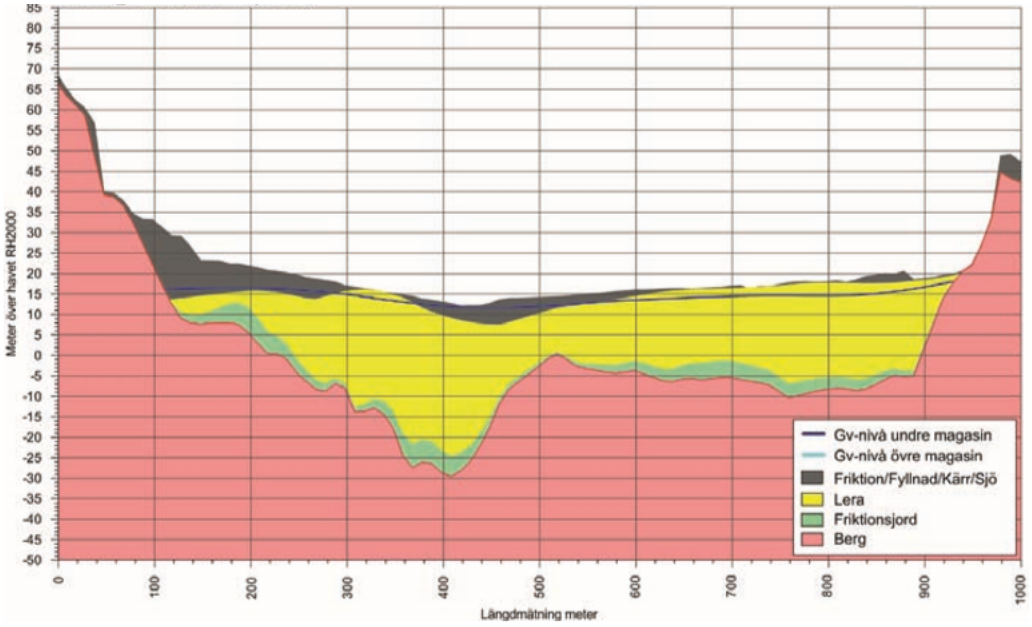

Figure 2.6: Soil stratigraphy profile of aquifer Olivedal-Annedal, along Nordenskiöldsgatan in western direction toward Landala (Sundkvist & Wallroth, 2016).

2.3.4.2 Hydrogeology

As seen in figure 2.7, a confined lower homogeneous aquifer is located in the glacial till, with the bedrock slopes acting as hydraulic boundaries. A pumping test in Annedal shows that the hydraulic transmissivity of the aquifer is $3 * 10^{-5} m^2/s$ (Sundkvist & Wallroth, 2016).

Figure 2.7: Lower soil aquifer. Groundwater head, flow direction and water divides (Sundkvist & Wallroth, 2016).

.

The area around Annedal contains underground constructions which affects the groundwater conditions, leading to reduced groundwater levels in the lower aquifer and hydraulic conductive fracture zones. There is no protective infiltration active (Sundkvist & Wallroth, 2016).

The leakage requirements for the service tunnel is 30 l/min, with a leakage condition permit for Västlänken of 40 l/min. The actual leakage during the construction will be measured at specific measuring mounds in the tunnel. Specific values for leakage budget and values from measuring mounds are found in appendix A.2. The values

from the measuring mounds are regarded as uncertain (Vestin & Lindström, 2020). At time of writing of this study the tunnel has been driven 495 m, with drawdown reported in three groundwater wells, see appendix A.1. The location of the wells are seen i figure 2.8.

Figure 2.8: Location of wells with documented drawdown.

2.3.5 Korsvägen

The main train tunnel of Västlänken passes through the studied area in a west to east direction, as can be seen in figure 2.9. The part to the west will be built through rock, which includes the western part of the Korsvägen station. 140m of the station will be constructed in soil, with the tunnel entering rock for about 160m at the eastern exit of the station, before passing through a 260m long section built through soil in the Mölndalsån Valley. The tunnel enters into rock again in the easternmost part of the area. A service tunnel will also run parallel to the main tunnel west of the station. The bottom of the tunnel will be located at an elevation of about -17 m.a.s.l. at the westernmost section with an upward inclination towards the east that reaches an elevation of about -12 m.a.s.l. at the station. There is a downward inclination east of the station with the tunnel reaching a depth of -20 m.a.s.l. on the east side of the Mölndalsån valley.

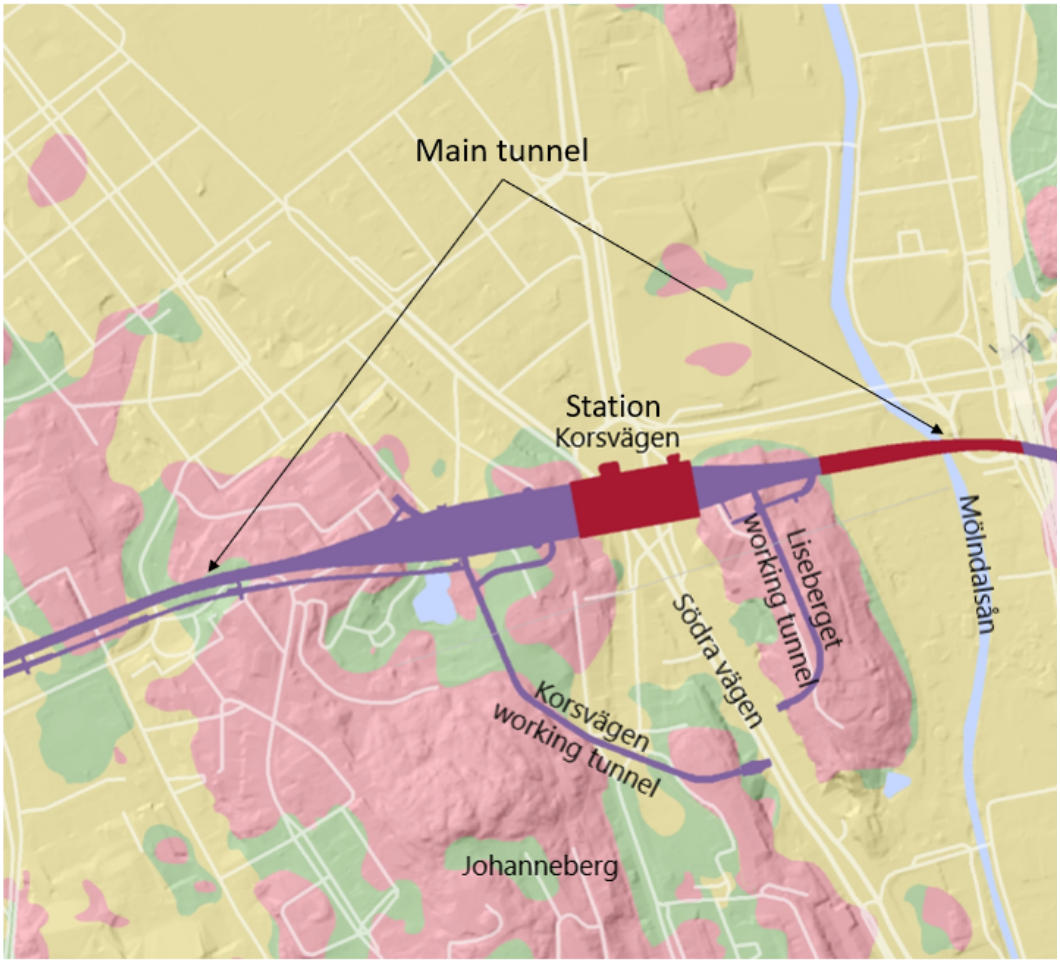

Figure 2.9: Location of tunnels, red=concrete tunnel, purple=rock tunnel, pink=rock outcrop, yellow=cohesive soil, green=frictional soil (Sundkvist & Wallroth, 2016). Adapted with permission.

Two service tunnels are being constructed to support the construction of Västlänken around Korsvägen station. The tunnels will be built through rock and enters the underground approximately 400 meters south of Korsvägen along Södra vägen at opposite sides of the street. Both tunnels turns towards the north connecting with the main tunnel, exact placement can be seen in figure 2.9. Service tunnel Liseberget (207) is the tunnel to the east, which will be about 300 meters long and service tunnel Korsvägen (206) is the one to the west, which will be about 550 meters long. Both tunnels enters the underground at about 8 m.a.s.l and reaches a final depth of approximately -12 m.a.s.l. The tunnel entries are located in a valley going in a north-north-west direction surrounded by two ridges, stretching in the same direction, Liseberget to the east and Johanneberg to the west, while Korsvägen and the area further north has a flat ground surface. East of Liseberget runs a valley in a north to south direction along Mölndalsån, with a flat ground surface and further east is another ridge.

2.3.5.1 Geologic setting

Gneiss of different kinds with a great degree of foliation makes up the bedrock in the studied area. The level of the bedrock differs greatly in the area, reaching an altitude of 70 m.a.s.l west of Korsvägen, while elevations lower than -30 m.a.s.l are present north of Korsvägen and there are even lower levels, below -60 m.a.s.l close to Mölndalsån. There is a general pattern of higher bedrock levels at Liseberget that continues to the north surrounded by lower elevations following Mölndalsån and Södra vägen. Two sets of weakness zones are present in the area: One vertical weakness zone with a northeast to southwest direction passing trough the main tunnel at the point where Korsvägen working tunnel connects. A set of weakness zones with a south-southwest to north-northwest direction with an inclination to the west is present in the valleys. Korsvägen working tunnel partially follows this zone and the main tunnel passes trough two weakness zones belonging to this set. The hydrogeology in rock PM (Lithén & Wadsten, 2016) gives two dominating fracture sets, SG1 (140±30 / 60±15) and SG2 (310±20 / 35±15) for the rock between Korsvägen and Haga stations and three sets for Liseberget, SG1 (170±20 / 45±15), SG2 (350±20 / 50±15) and SG3 (85±20 / 85±15), but there are also fractures with random directions. The bedrock has also been seen to be fractured at the transition zones between soil and rock outcrop.

Figure 2.10: Soil map with groundwater head in the lower soil aquifer, pink=rock outcrop, yellow=cohesive soil, green=glacial till (Sundkvist & Wallroth, 2016). Adapted with permission.

The stratigraphy and soil types around Korsvägen are the typical for Gothenburg, with soil in the lower laying parts and rock outcrop or thin soil layers at higher parts. Soil covers the flat areas north of Korsvägen and the valleys along Södra vägen and Mölndalsån, while rock outcrop dominates at Liseberget and Johanneberg. The section showed in figure 2.11 can be said to represent the area quite well, with these features continuing in a north-northwest to south-southeast direction. The soil filled depressions are Södra vägen valley to the left and Mölndalsån valley to the right, surrounded by areas with rock outcrop. Filling material covers most of the soil layers in the area, which is followed by a clay layer, often of large thickness. A layer of glacial till separates the clay from the bedrock. Higher laying areas with soil cover

does mainly consist of glacial till or filling material on top of the bedrock. It should however be noted that a layer or lenses of gravel and sand are present inside the clay layer, which will not be included in the model.

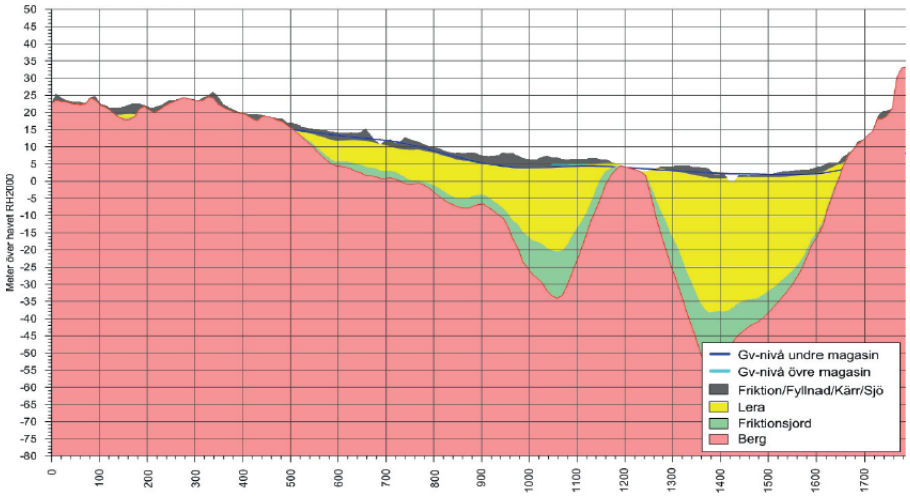

Figure 2.11: Profile with soil types from west of Vasa kyrka stretching east-northeast past Liseberg station. Pink=bedrock, green=glacial till, yellow=clay, grey=filling/peat material (Sundkvist & Wallroth, 2016)

.

The tunnels are built in an urban area, meaning that much of the surroundings are a built environment with a lot of impermeable surfaces. Especially the area north of Korsvägen is highly exploited with paved streets or buildings covering the vast majority of the area. Liseberget is only sparsely built with a lot of natural ground surfaces, Johanneberg has more built environment, but also large areas with natural ground surfaces.

One major surface water body exists in the area in form of Mölndalsån that runs to the north in the eastern edge of the studied area. Two types of soil groundwater reservoirs are present in the area: An upper unconfined aquifer in the filling material and a lower confined aquifer in the glacial till below the clay. The lower aquifer can be divided into one aquifer in Mölndalsåns valley and one at Korsvägen. They are to delimited by the high laying rock areas to the west and east and separated by the higher bedrock elevations running north from Liseberget, but this ridge does not disconnect the two aquifers hydraulically. There is in general declining head towards the north in the lower aquifer, with steep gradients in the soil filled depression that stretches into the Johanneberg rock area and a groundwater divide sits in the valley west of Liseberget. There is also a groundwater reservoir in the fractures of the rock, which has been seen to have approximately the same groundwater head as the lower soil aquifer.

The hydraulic conductivity in the rock can in general be represented by "rock west of Mölndalsån" (Lithén & Wadsten, 2016), with an arithmetic mean of $1,8 * 10^{-7}$ m/s and a standard deviation of $1,5 * 10^{-6}$m/s. Higher hydraulic conductivity can be expected in weakness zones, but investigations performed did not provide

enough information to give quantitative estimate. Hydraulic conductivity in the lower aquifer in has been evaluated to range from approximately 10^{-5} to 10^{-4} m/s according to Sundkvist and Wallroth, (2016).

2.3.5.2 Groundwater lowering

The working tunnels will be built as described in section 2.3.1, sealing fractures through grouting before blasting. There will still be a leakage to the tunnel during both the construction- and operational phase when the permanent structures are in place. Sundkvist and Wallroth, (2016) declares leakage rates after construction used during the planning phase of the project for different stretches of Västlänken. A 340m long section west of Korsvägen is assumed to leak 100l/min and for a 550m long section east of Korsvägen the corresponding value is 105l/min.

An existing tram tunnel, Chalmerstunneln enters the rock just south of the Korsvägen service tunnel. The tunnel is approximately 1050m long and has a total leakage of around 26 l/min. There is also a train tunnel, Gårdatunneln with a station in rock to the east of Korsvägen. It was built without any grouting and it has been seen to affect the local groundwater conditions. Gårdatunneln could be assumed to lower the groundwater level to its drainage level (Lissel, 2016). There is an underground shelter at Korsvägen that could have an effect on the groundwater.

3
Method

3.1 Working process

Two cases, case one and case two, with different observations are used for calibration of each area. For Linné, observations used for case one was long term mean groundwater levels from before construction of the service tunnel. In case two, groundwater level observations and tunnel leakage from when the tunnel had been driven 495 m are used to calibrate the model. For Korsvägen, case one was calibrated using groundwater level observations from before tunnel construction. Case two was calibrated using the same observations as in case one and also the observed effects at the end of a pumping test.

The modelling process is iterative and new steps or simulations in the modelling is built on the previous model step. The entire modelling procedure was completed once for the first case. Then for the second case, the same parameterized working model used for inverse PEST calibration is reused, but updated with new observations. The working process has followed the flow chart in figure 3.1.

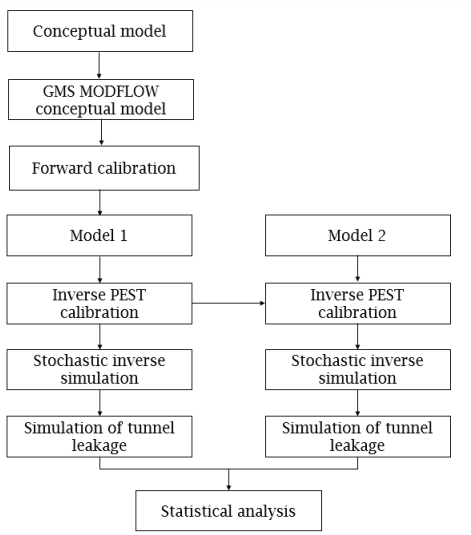

Figure 3.1: Thesis working process.

First, data was collected to develop a conceptual model describing the physical and hydrogeological conditions of the area. With the conceptual model finished, a GMS MODFLOW conceptual model could be created, defining soil layer properties in a 3D grid and hydrogeological properties as arcs and polygons. In the manual calibration step the historical observations of mean groundwater levels and estimated parameter values were added. The model was then manually calibrated by executing forward calculations and varying parameter values until the model converged and the calculated groundwater levels were somewhat similar to the observed. For the inverse automatic parameter estimation calibration step, the manually calibrated model was parameterized with pilot points and parameter intervals. Pilot points are 2D scatter points representing a parameter. During inverse calibration the parameter is interpolated between the points, and each point achieves a value between the set parameter interval. PEST was run and a calibrated model was achieved. The model solution is however unique, and to analyse how the solutions could vary, stochastic inverse simulations with Null Space Monte Carlo was performed based on the PEST calibrated model. 20 unique randomly parameterized parameter sets of the model was generated. To see the effect from the tunnel, drain arcs simulating tunnel leakage was added to the model and a forward stochastic simulation was run on the 20 calibrated models.

3.2 Data collection

The data used for creating the models was mainly gathered from Trafikverket reports about Västlänken, with the greatest source of information being the Hydrogeology PM by Sundkvist and Wallroth (2016). This information was used to develop the conceptual model, including boundary conditions, hydraulic conductivity and recharge. The geology and stratigraphy of the area are based on rasters supplied by Bergab, that describes the location of the interfaces between the stratigraphic units. The position of existing underground structures and the planned tunnels was also supplied by Bergab as rasters. Groundwater head observations used for calibration was collected from Trafikverkets measuring database, TMO.

3.3 Conceptual model

Eklund's hydrogeolgic type settings (2002) were used to characterize the surroundings of the tunnels. The type settings can be seen below:

- Hydrogeologic system
  - Soil type
  - Location in relation to HK
  - Stratigraphy
  - Hydrology
  - Land use
- Parameter system
  - Groundwater recharge
  - Groundwater head

- Hydraulic conductivity
- Porosity
- Storage coefficient
- Field capacity
- Hydraulic gradient

The hydraulic conductivity of the filling material and clay was set to constant values, while the glacial till, fractured bedrock and bedrock was defined by ranges, which can be seen in table 3.3 for the Korsvägen model and in table A.1 for the Haga model. Hydraulic conductivity of the clay is an assumed value that should be sufficiently low that a negligible amount of water passes through it. Due to the large spatial variability in the composition of the filling material it was assigned a reasonable assumed value. The glacial till range is based on grading analysis by Lithén, Wadsten, Östergaard, and Persson (2016) and the bedrock range on energy wells and hydraulic tests in boreholes by Lithén and Wadsten (2016). The fractured bedrock range is based on the bedrock range, but has somewhat higher values. All materials was assumed to have a vertical anisotropy of 3, meaning 3 times larger conductivity in the horizontal direction than the vertical.

Five different materials makes up the models, with filling material at the top, followed by clay, glacial till, fractured bedrock and bedrock. The fractured bedrock was not included in the stratigraphy model that was provided by Bergab, but was created to account for the fact that the top of the bedrock often has a higher hydraulic conductivity than the underlying bedrock. A two meter thick layer of fractured bedrock was therefore allowed a higher hydraulic conductivity than the bedrock. The vertical cell layers were assigned with one of the materials, except for the bedrock that was divided into different smaller layers and one larger layer reaching down to the bottom elevation of the model. This division was done to ensure that the drainage of the tunnels would not occur in a large cell reaching down to the bottom of the model.

3.4 Groundwater modelling

The numerical modeling in this study was done using the software Groundwater Modelling System 10.3.5 (GMS).

3.4.1 GMS conceptual model

The first step of the numerical modelling procedure was to create the geologic units. It was done by converting stratigraphy rasters into Triangulated Irregular Network (TIN) surfaces, which was used to create solids by filling the voids between the TINs. Materials that could be assigned to the different solids were then created. A 3D-grid had to be generated to convert the solids into a MODFLOW compatible grid format. The MODFLOW model was created using the boundary matching option in GMS (AQUAVEO, 2017a) with a minimum cell thickness of 0.3m and a grid cell size of 20x20m. The conceptual model tool in GMS (AQUAVEO, 2017b)

was then used to define the boundary conditions, recharge and structures effecting the groundwater conditions.

3.4.2 Manual calibration

MODFLOW was solved using the NWT-package with the xMD matrix solver for all model runs, using steady state conditions. Groundwater head observations in the upper and lower soil aquifers as well as in the rock aquifers was added to enable calibration. A manual calibration was performed to ensure that starting parameter values were reasonable, which was done by varying hydraulic conductivity and recharge and observing the effects in the model so that the computed groundwater head in the model was almost the same as the observed heads. Conductance of draining structures was also manually varied to attain leakage rates in line with measurements. The leakage rates were dependent on the hydraulic conductivity of the bedrock and deviates with about $\pm$ 1 l/min from the measured rates. The conductance was not related to the specified conductance from grouting performance calculations and deviated heavily from any pre-specified conductance.

3.4.3 Automatic Parameter Estimation calibration - PEST

The automatic calibration of the model was performed using the PEST 10.4 utility in GMS following the guides provided by Aquaevo (*GMS:Automated Parameter Estimation - XMS Wiki*, 2017). First, the model was parameterized using pilot points (PPs) interpolated with inverse distance interpolation. Parameters to be inversely calibrated with PEST were recharge for all recharge zones and hydraulic conductivity of bedrock, fractured bedrock and glacial till. Pilot point data sets for the parameters were created with PPs manually placed with denser placement intervals around observations and between observations and zonal boundaries as suggested by Doherty (2020). Each pilot point set was assigned a starting value and a max and min value that constrained the interval in which the parameters could vary. Starting values for the pilot points was the parameter values obtained from the manual calibration.

In order to allow PEST to run until a low error was achieved, the max number of iterations without improvement was set to three. The max number of PEST iterations was set to 25, a high number which was more then the estimated amount of iterations requried for the calibration to finish.

3.4.4 Stochastic inverse modeling

PEST Null Space Monte Carlo method was used to perform stochastic simulations and develop 20 calibrated MODFLOW models based on the inverse PEST calibrated model. NSMC uses Kriging as interpolation method, which is a method that uses a spatial correlation that assumes that points far apart will vary more, than points that are close to each other. This spatial correlation is described by a variogram, which was constructed by the pilot points data sets obtained with PEST. Each variogram consists of an experimental- and a model variogram, where the model

variogram is adjusted to match the experimental, see figure 3.2. The experimental variogram is calculated by GMS and is the variance of a point in relation to other points on the y-axis with point distance on the x-axis. The model variogram, when matched, describes the trend of the experimental variogram as a mathematical function. The model variogram is characterised by four factors: contribution, nugget, range and type of model function, where exponential and spherical was used the most. Nugget defines the interception of the y-axis, range is where the variogram levels of. Contribution defines the sill where variogram points below the sill indicates positive correlation. Some model variograms were not able to be fitted at all and arbitrary assumed experimental variograms had to be used.

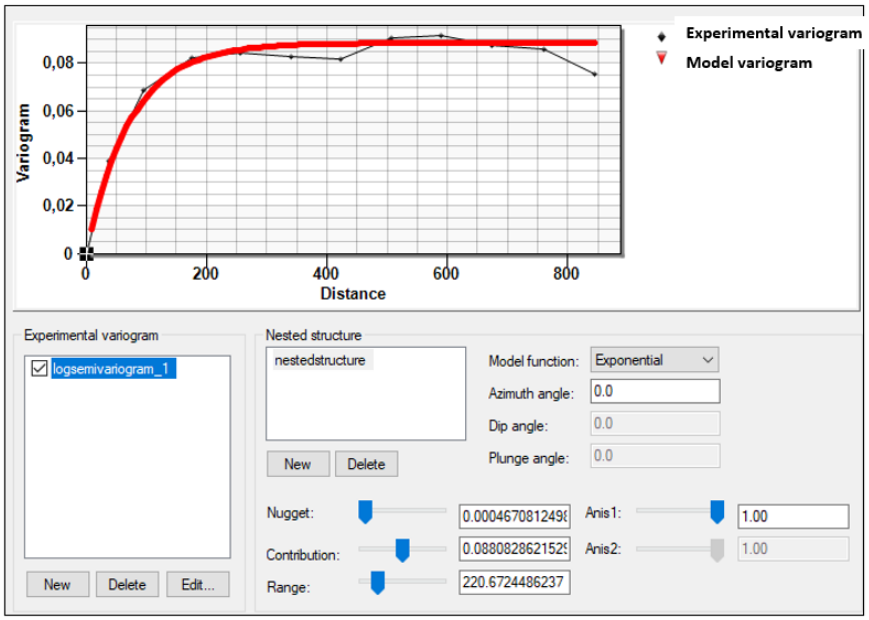

Figure 3.2: Experimental variogram and model variogram constructed in GMS 10.3.5 variogram editor.

If the PEST NSMC simulation was to run until three iterations was performed without improvement as in the previous PEST calibration, the run time was expected to be to long. In trial calibration using kriging interpolation with PEST calibration it was noticed that PEST begins at a similar error as the model calibrated with inverse distance weighted interpolation method finished at. The kriging interpolation calibrated model achieved a lower error than using inverse distance weighted interpolation method. The termination threshold error for when NSMC runs was to stop, was set to the achieved error with the PEST calibration minus 100 to allow the NSMC calibration to achieve slightly lower error then previous PEST calibration. With these settings, 20 calibrated models was computed with an expected run time of 72 hours.

To forecast the effect of tunnel leakage on the groundwater conditions, stochastic forward run simulations were performed with the 20 different parameter sets obtained with NSMC. The tunnel leakage was modelled with drain arcs in GMS, with a draining elevation at the bottom of the tunnels. The flow into the drains depends

on the their conductance, so an iterative process followed where the conductance was adjusted manually until the computed flow was similar to the desired leakage. The forward run was simulated and 20 different predictions of the drawdown were generated for each calibration case.

3.4.5 Statistical analysis

The mean and standard deviation of parameters and groundwater head of the stochastic runs was computed using the statistical analysis tool in GMS. The coefficient of variation for the hydraulic conductivity and recharge was calculated using equation 3.1.

$$CV = \frac{\sigma}{\mu} * 100[\%] \tag{3.1}$$

CV: Coefficient of variation
σ: Standard deviation
μ: Mean

3.5 Case studies

The working process of the two case studies have followed the flow chart in figure 3.1 and the general method described above.

3.5.1 Linné

Two calibration cases were used for Linné, case one and case two. Case one was calibrated with groundwater levels from before construction of the service tunnel. Case two uses tunnel leakage observations from when the tunnel hade been driven 495 meters and new groundwater levels from that time period.

Case	Observations used for service tunnel Linné
Case one	GW obs. points
Case two	GW obs. points + 20 l/min tunnel leakage

Table 3.1: Observations used for groundwater model Linné.

A 20x20 m horizontal grid covering 1.07 km^2 with 12 cells in the vertical direction originating at -200 m.a.s.l was used. The stratigraphy of the model can be seen from the south-west corner of the model in figure 3.3 and from a vertical view in figure 3.4.

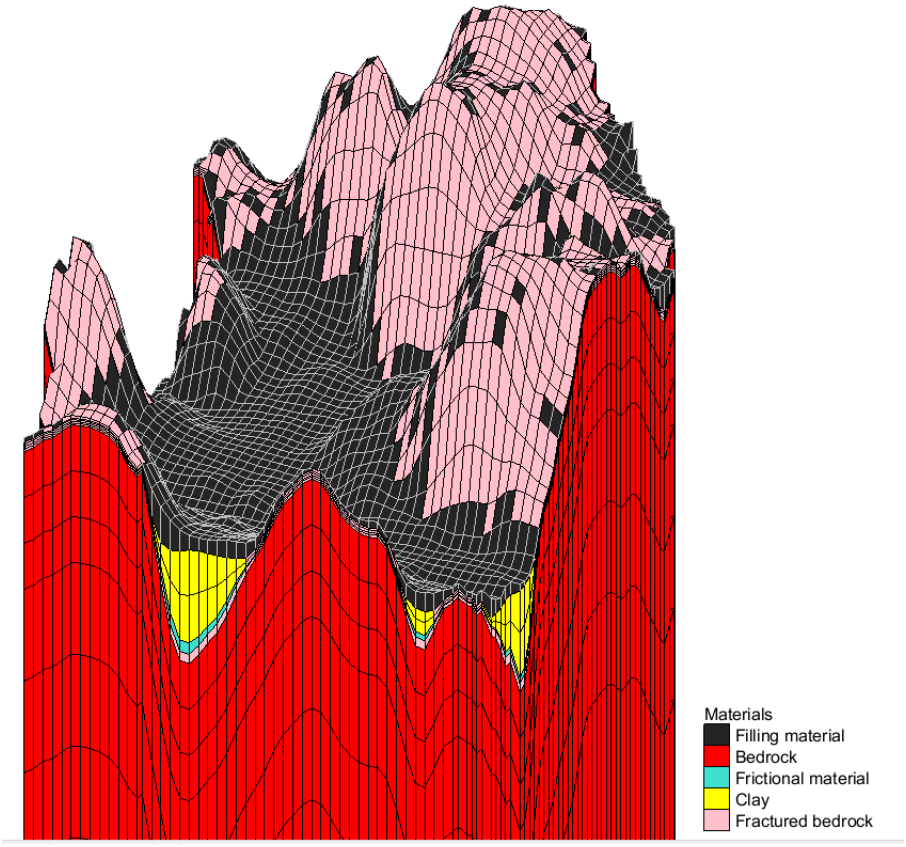

Figure 3.3: Linné Model stratigraphy viewed from south-west.

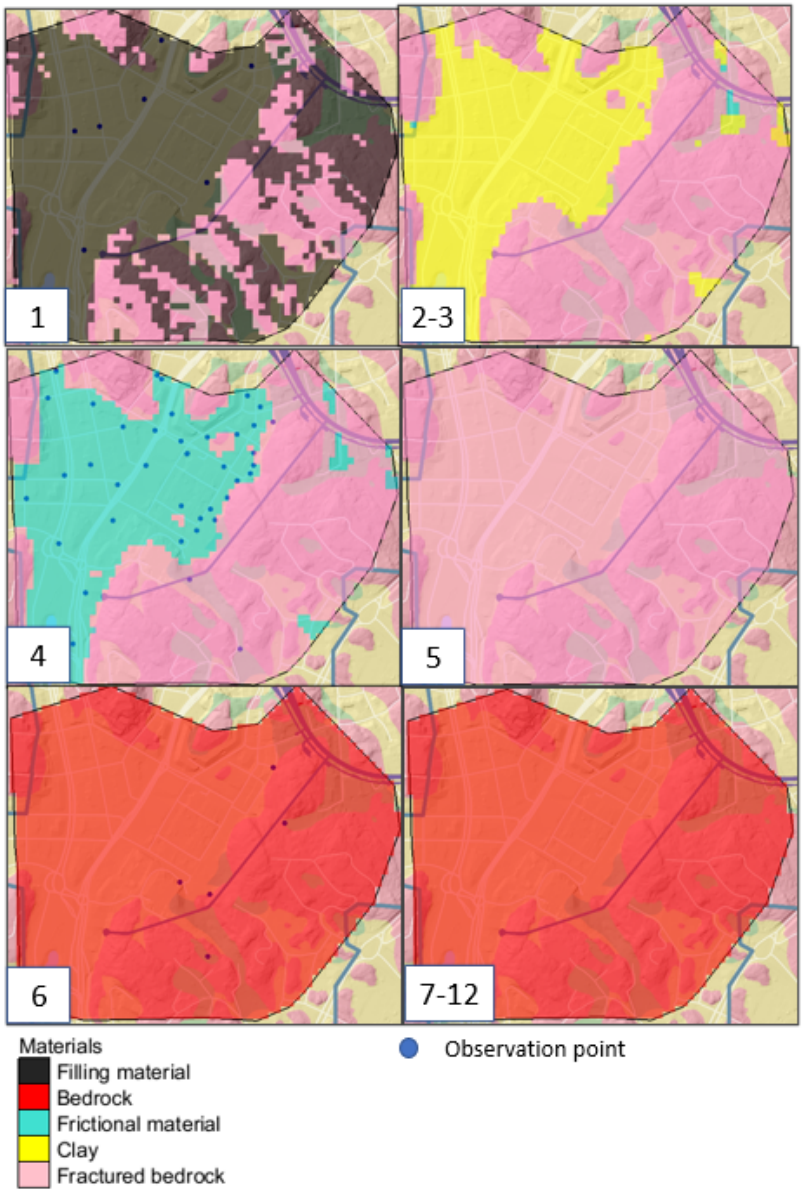

Figure 3.4: Materials for each layer and observation points used in layer one, four and six. Numbers indicating layer range.

The GMS conceptual model was delimited as in figure 3.5, with no flow boundaries at the water divides in the bedrock surrounding the valley of Annedal, with exception of the southeast boundaries which due to a lack of water dividers and information was drawn in a 400 m radius from the service tunnel. A constant head following the expected lower aquifer groundwater levels in figure 2.7 was placed in the depressions between the bedrock areas.

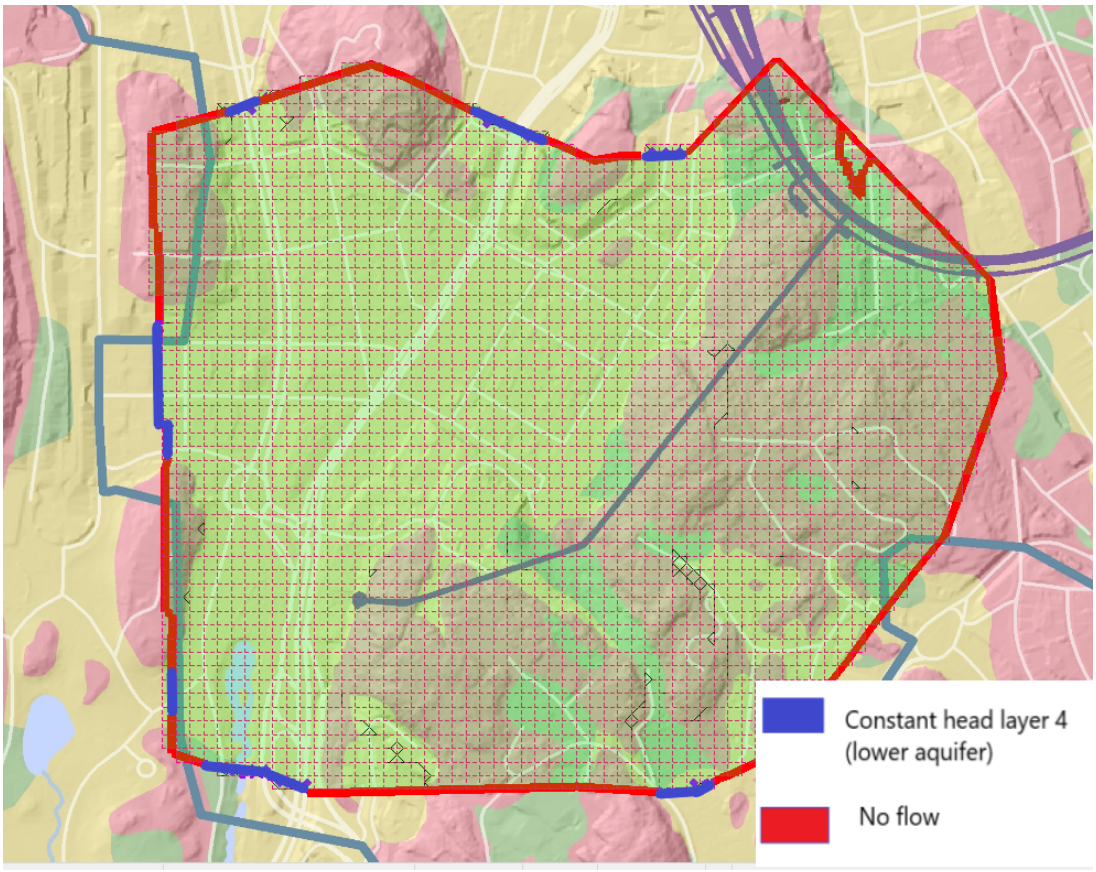

Figure 3.5: Model boundaries with background map of soil types and Linné service tunnel.

The model was divided into six recharge zones, see figure 3.6 [1]. The valley of Annedal and Linné with a low-permeable clay was considered as a low-recharge zone, zone six and the surrounding area with bedrock, zones 1-5, was considered to have higher recharge. The recharge rates used for calibration are displayed in table A.3. Shallow drainage was simulated by drain arcs -1 m below surface, see figure 3.6 [2]. Leakage from underground structures affecting the area was simulated with an estimated leakage of 4 l/min/100m.

The model was parameterized with PPs. Figure 3.7 displays the PPs for each of the parameters, where one set of PPs was used per parameterized material and one set PPs for each recharge zone, nine in total.

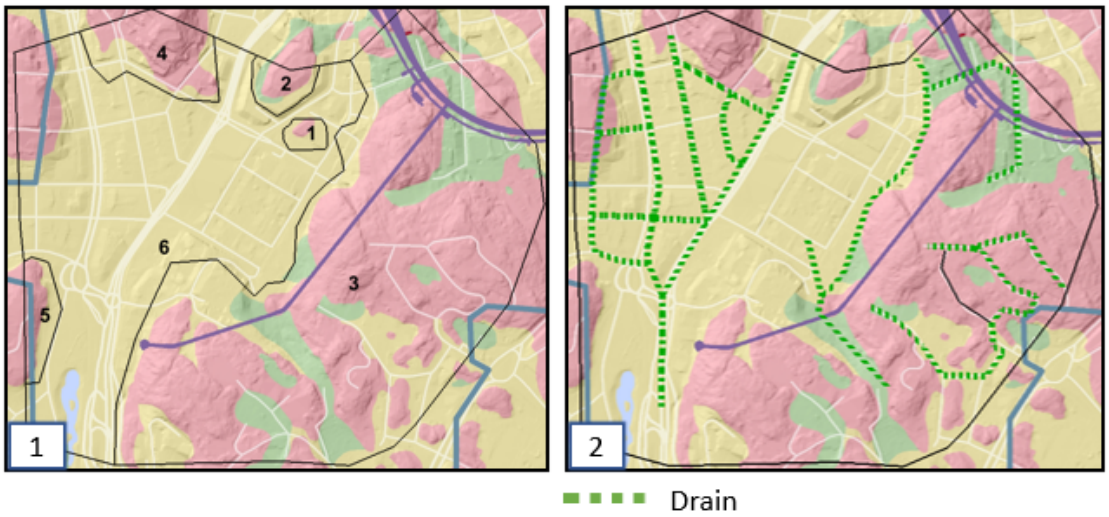

Figure 3.6: Recharge zones used for PEST [1] and shallow drains [2].

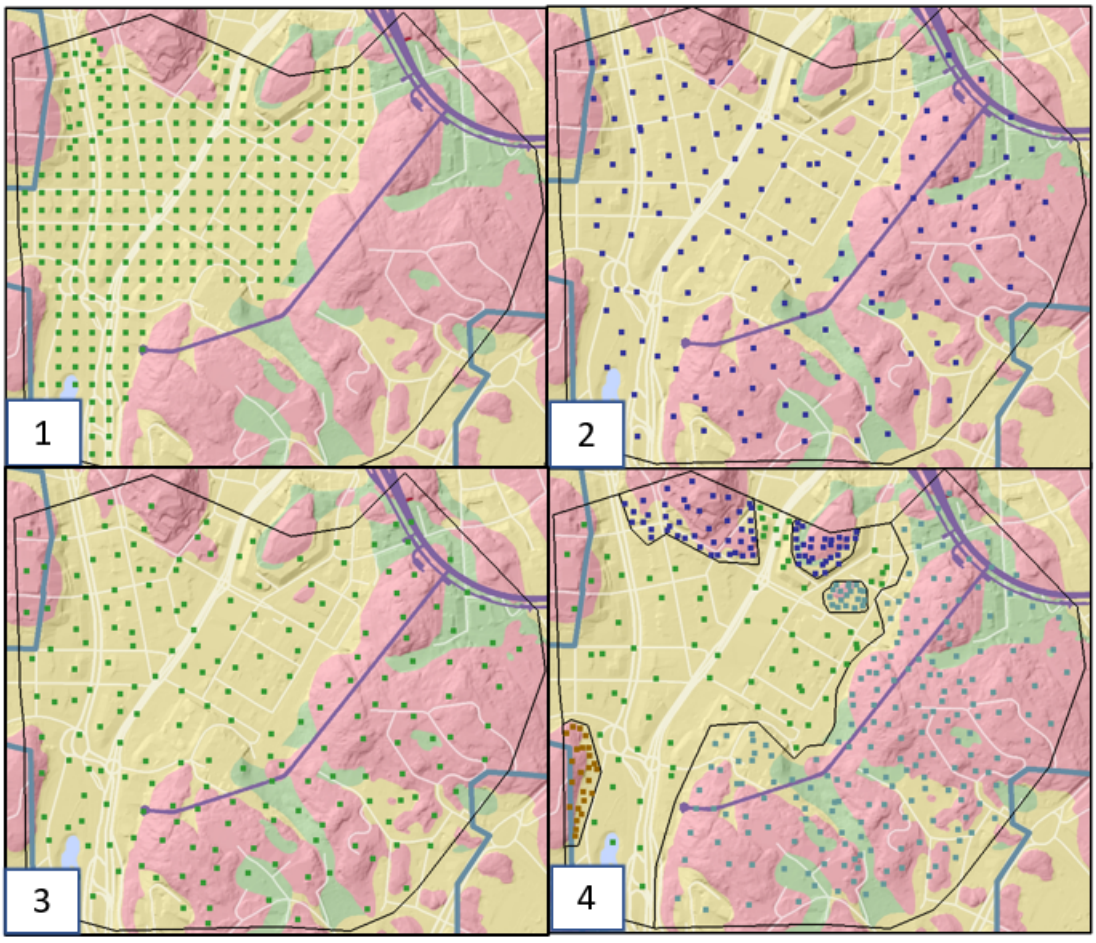

Figure 3.7: Pilot points used for parameterization of Linné model. Glacial till [1], fractured bedrock [2], bedrock [3] and recharge [4].

The PPs were assigned initial parameter values achieved from the manually cali-

brated model. Parameter values used for the inverse PEST calibration are shown in table A.1. The same parameter intervals was used for both case one and two. Material parameter invtervals used for NSMC simulation are found in table A.2.
51 groundwater observation wells were used, seven in top aquifer, 41 in the lower aquifer and five in the bedrock aquifer, see figure 3.4. Since the location of the bedrock aquifer is uncertain, the bedrock aquifer wells were arbitrarily placed in the top bedrock layer. For the inverse PEST calibration of case one, observation wells with long term mean groundwater levels were used, see figure 3.8 [1]. Case two was calibrated with mean groundwater levels from the service tunnel construction, with an additional 20 l/min tunnel leakage added as a draining arc in the model, seen below as a blue arc in figure 3.8 [2]. The service tunnel had been driven 495 meters, but only leakage measurements for 0-355 meters had been collected at the time of modelling. Three groundwater wells were reported as affected from the tunnel construction, se appendix A.1 for drawdown figures. The computed heads from NSMC calibration plotted against the observed heads can be found in appendix B.14, B.16, B.13 and B.15.

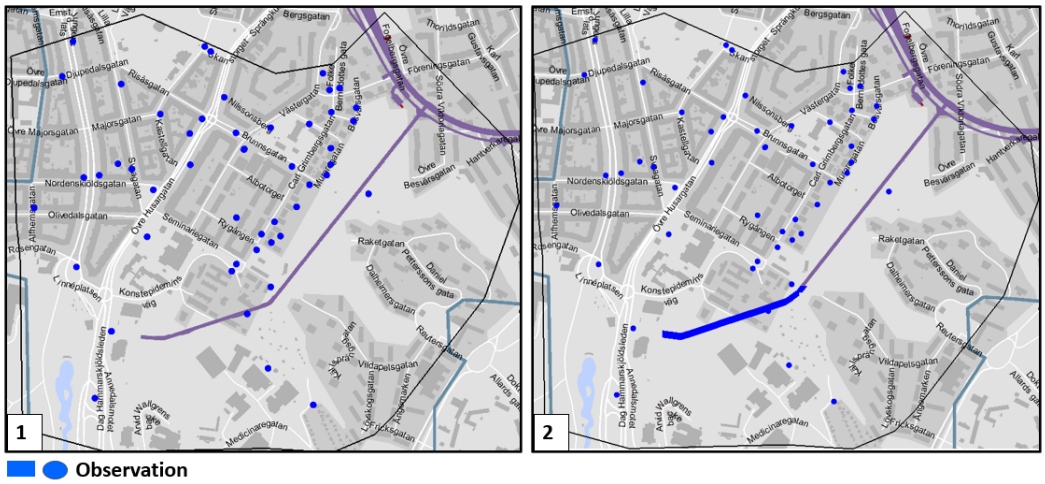

Figure 3.8: Observations used for case 1 [1] and case 2 [2].

Tunnel section	**Case one [l/min]**	**Case two [l/min]**
0m-355m	8.0	20
355m-955m	23.5	23.5
Total	31.5	43.5

Table 3.2: Leakage rates used for PEST NSMC forward run simulation of Linné model.

When calculating the effect of the entire tunnel with stochastic forward run, different leakage rates were used for case one and two, these are shown in table 3.2 below. Leakage rates for each section in case one were according to tunnel grouting calculations provided by Trafikverket. The leakage requirements from trafikverket is 30 l/min, but due to diffulties to reach the correct leakage when calibrating the leakage with drain arc conductance, 31.5 l/min was used. For case two, measured leakage on the first 0-355 meters was used and section 355-955 meters used the leakage according to Trafikverkets calculations, with a total leakage of 43.5 l/min.

3.5.2 Korsvägen model

A 20x20m horizontal grid with 10 cells in the vertical direction originating at -200 m.a.s.l was used for the model, making up an area of 1.65km^2. A section stretching eastward from Liseberget across the Mölndalsån valley showing the stratigraphy can be seen in figure 3.9 and the areal extent of the materials in the different layers with used observations points is seen in figure 3.10.

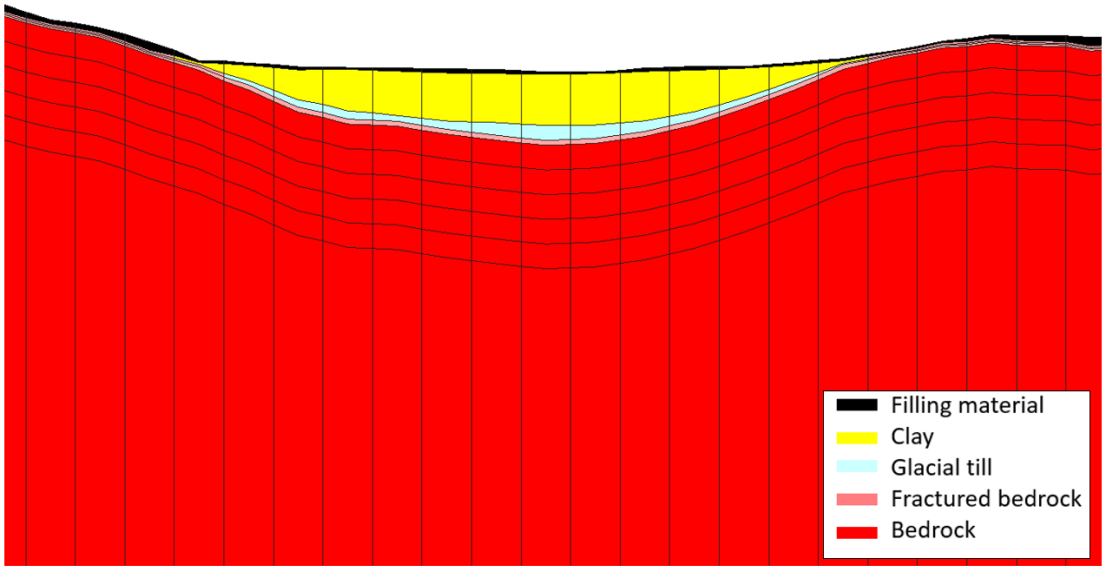

Figure 3.9: Example of model stratigraphy.

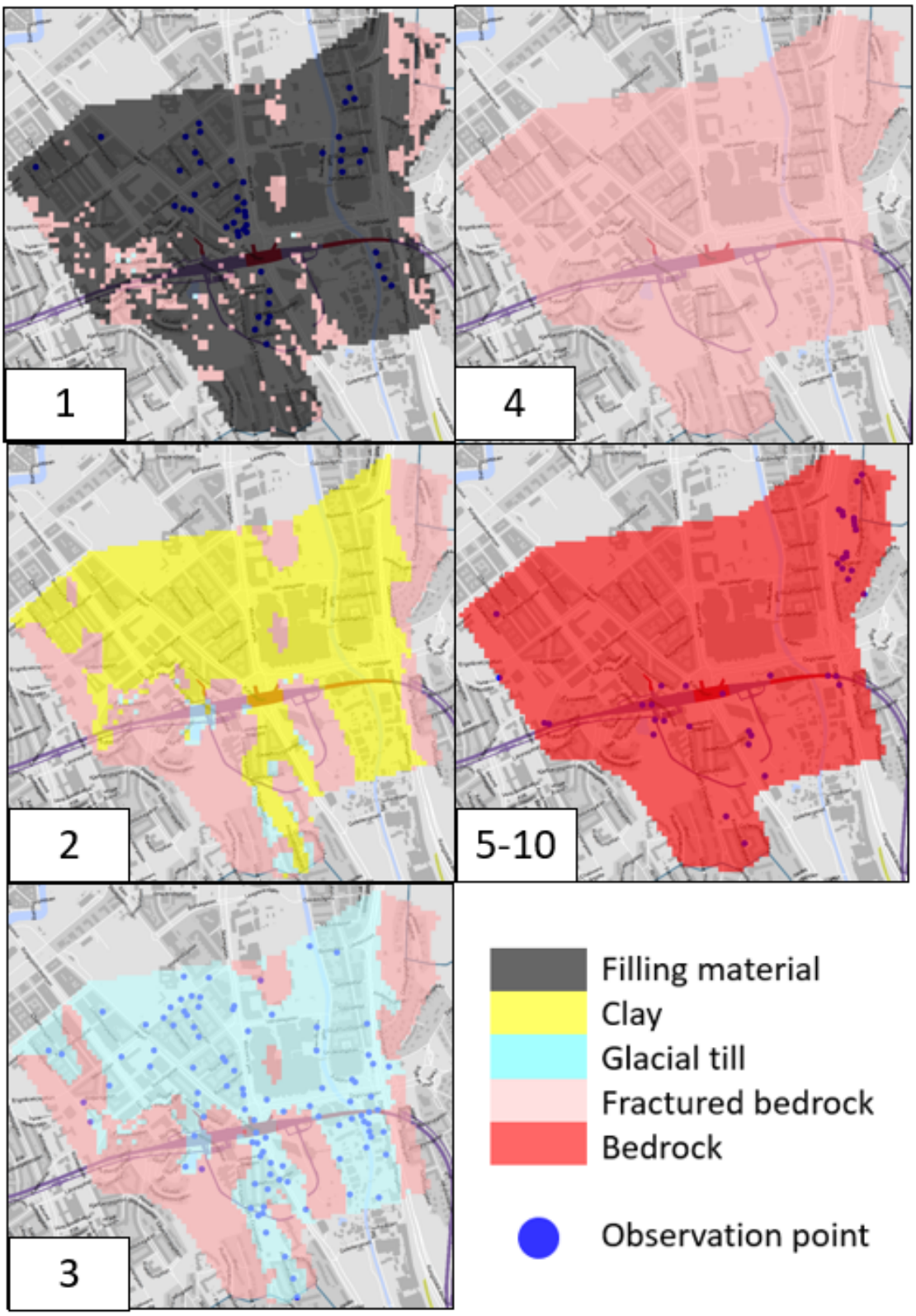

Figure 3.10: Materials and observation points of the different layers, numbers indicating layer. Observation points in [5-10] are only present in layer five.

The model was mainly delimited by using the water divides in the area and it was assumed that no flow would take place over them. A constant head was used where no water divides could be found, with the head being based on interpreted levels in figure 2.10. Mölndalsån also made up a constant head boundary, but only affecting the top layer in the model and the head was set according to measured levels by Mölndalsån.se (2020). The boundaries can be seen in figure 3.11.

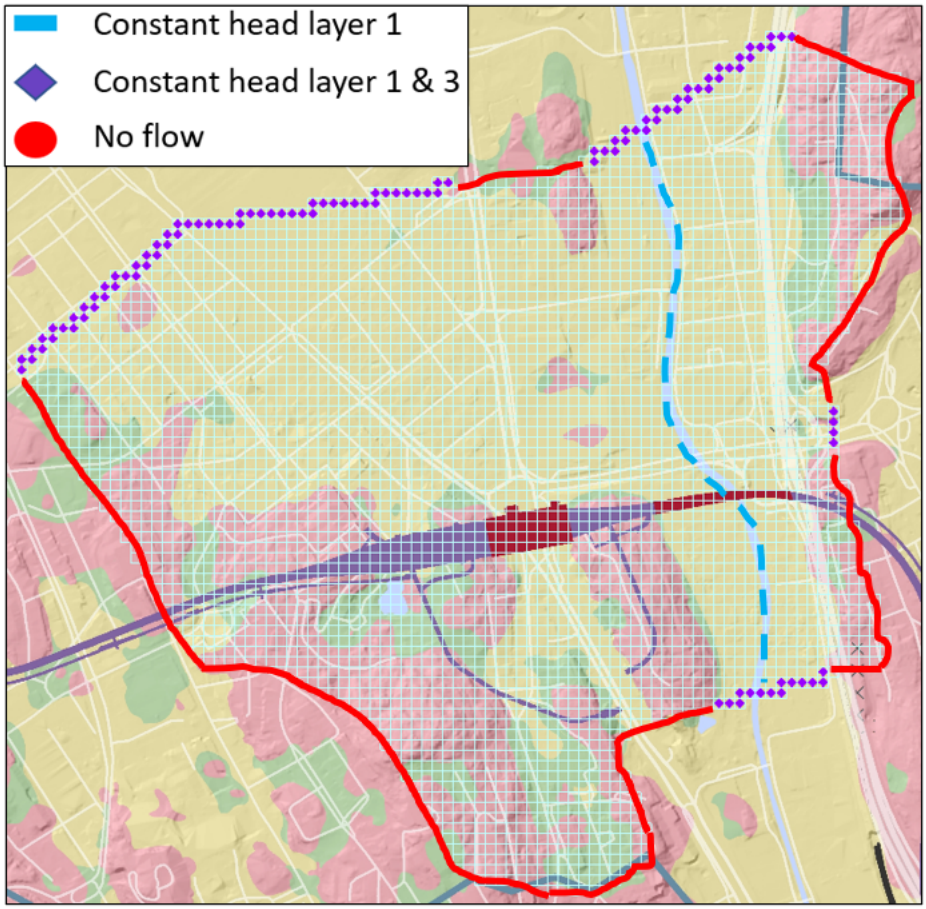

Figure 3.11: Model boundaries.

PPS was used for the calibration and the distribution of the PPs can be seen in figure 3.13.

Material	**Horizontal hydraulic conductivity [m/s]**
Filling material	10^{-5}
Clay	10^{-9}
glacial till	10^{-6} – 10^{-3}
Fractured rock	10^{-9} – 10^{-5}
Bedrock	$5 * 10^{-10}$ – 10^{-6}

Table 3.3: Hydraulic conductivity used for PEST calibration of Korsvägen.

The model area was divided into two different kinds of recharge zones. One with lower recharge rates caused by the presence of low permeable clay and another

one with higher recharge where no clay is present, see table 3.4 for the assumed parameter ranges. Figure 3.12 [1] shows the extent of the zones, where the shaded area is the "clay zone" and is the rest of the area the "no clay zone". All recharge was assigned to the top layer of the model and the ranges are based on the evaluation by Sundkvist and Wallroth (2016).

Zone	**Recharge [mm/yr]**
Clay	1 - 50
No clay	10 - 350

Table 3.4: Recharge rates for the two kinds of recharge zones at Korsvägen.

The two existing tunnels inside the model domain Chalmerstunneln and Gårdatunneln were modelled as drain arcs, as can be seen in figure 3.12 [3], where the arc to the left is Chalmerstunneln and the one to the right is Gårdatunneln. The built environment in large parts of the area means that especially the upper layer has greatly disturbed groundwater conditions. This fact is dealt with by adding shallow draining arcs to the model. These are placed along roads 1m below the ground surface, which can be seen in figure 3.12 [2].

The leakage from the existing tunnels Chalmerstunneln and Gårdatunneln are based on measurements, while the values for the service tunnels 206 and 207 are predicted ones based on grouting design and Västlänken's values is the maximum leakage demanded. Amount of leakage can be found in table 3.5. Calibration of tunnel inflows was done by changing conductance of the drain arcs. This was done for one of the NSMC runs, meaning that the conductance was the same in all models, while the actual leakage differed between the models.

Zone	**Leakage [l/min]**	**Leakage [l/min per 100m]**	**Conductance [m/s]**
Chalmerstunneln	8.2	2.48	10^{-8}
Gårdatunneln	120	8	$2 * 10^{-7}$
Västlänken	40.6	4.38	10^{-7}
206	10	1.79	$7 * 10^{-8}$
207	9.2	2.74	$7.5 * 10^{-8}$

Table 3.5: Leakage to existing and planned tunnels.

Calibration with NSMC was done based on a PEST calibrated model that used a narrower parameter interval than those seen in table 3.3. The first case was calibrated against historical head observations in the points that can be seen in figure 3.10, while the second case was calibrated with the heads at the end of a pumping test with a flow of 57l/min performed at the location seen in figure 3.14, which resulted in the drawdown found in appendix A.4. Observation wells inside the model domain that had a drawdown of more than 0.1m during the test were modified while the rest of the wells were kept at the same head as case one. The computed heads from NSMC calibration plotted against the observed heads can be

Figure 3.12: Recharge zones [1], shallow drainage [2], Chalmerstunneln Gårdatunneln [3], Västlänken [4]. Tunnels and drains in green.

found in appendix B.13, B.14, B.15 and B.16. The parameters obtained with these two calibration methods were then used to forecast the effect of the tunnel leakage. The service tunnels and the main tunnel were added to the model as drain arcs, which can be seen in figure 3.12 [4].

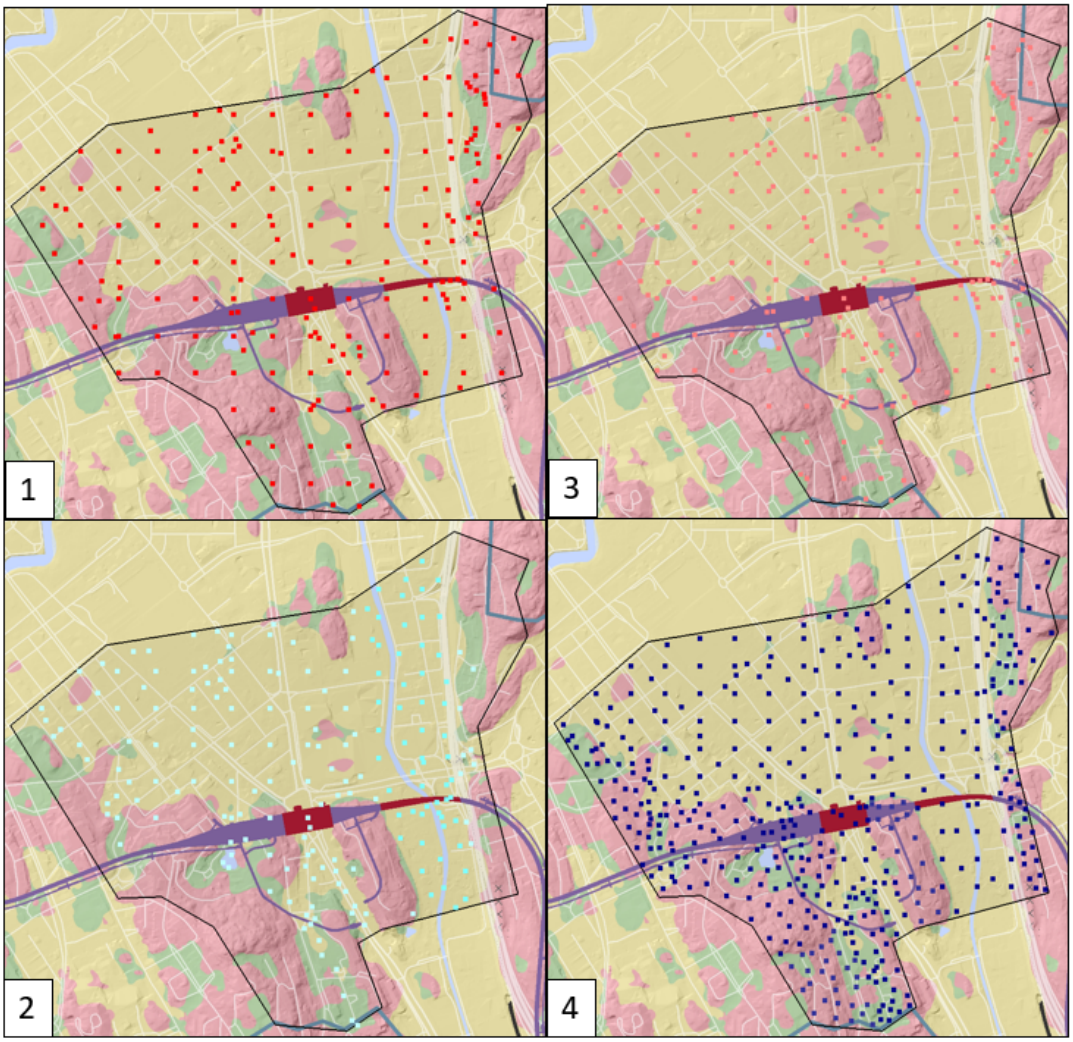

Figure 3.13: Pilot points for: Bedrock [1], glacial till [2], fractured bedrock [3], recharge [4].

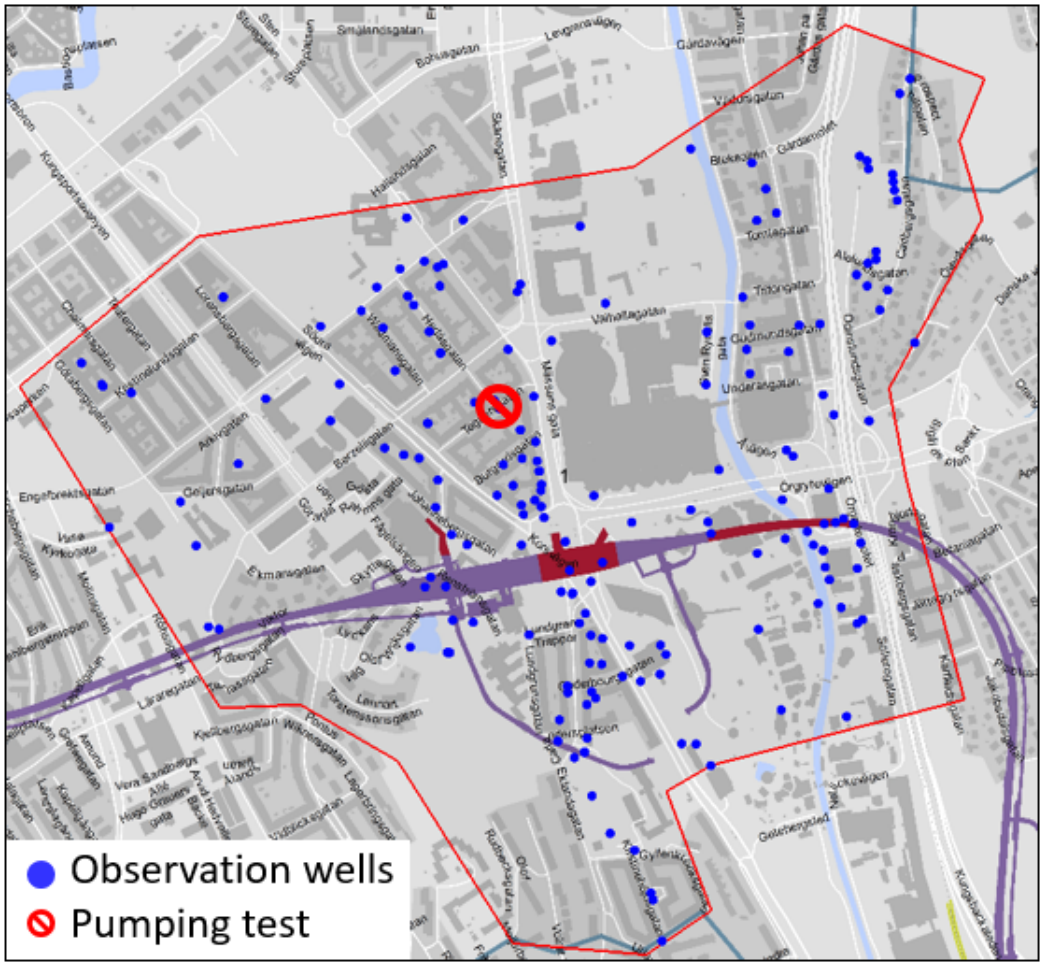

Figure 3.14: Observation wells and location of pumping test.

4
Results

The result from the stochastic simulations is presented in two parts, a parameter uncertainty part and a model outcome uncertainty part, for each of the two model areas. The parameter uncertainty is displayed as the coefficient of variation (cv) for recharge and hydraulic conductivity and histograms of the water budget. The model outcome uncertainty is displayed as the histograms of tunnel leakage, drawdown and maps with standard deviation of groundwater head. All figures compare the different types of calibration methods seen in table 4.1, with case one being the figures to the left and case two to the right in both model areas.

Area	**Case one**	**Case two**
Linné	Historical mean heads	Observed drawdown from partially built tunnel
Korsvägen	Historical mean heads	Pumping test with observed drawdown

Table 4.1: Calibration data used for each case and model area.

4.1 Linné

4.1.1 Parameter uncertainty

The cv of recharge is slightly higher in case two compared to case one, both in the clay zone and in the bedrock zone, see figure 4.1. The highest cv for both cases is located in the bedrock zone. The areas with a very low cv in the north east of case two have recharge levels that reaches the maximum value of the recharge calibration interval, which appendix B.4 displays. There are small circular areas with higher cv, which also indicates spots with extreme values in areas of uniform recharge. This is shown in appendix B.5, where it can be seen that the spots with high cv correlates with areas of very high recharge.

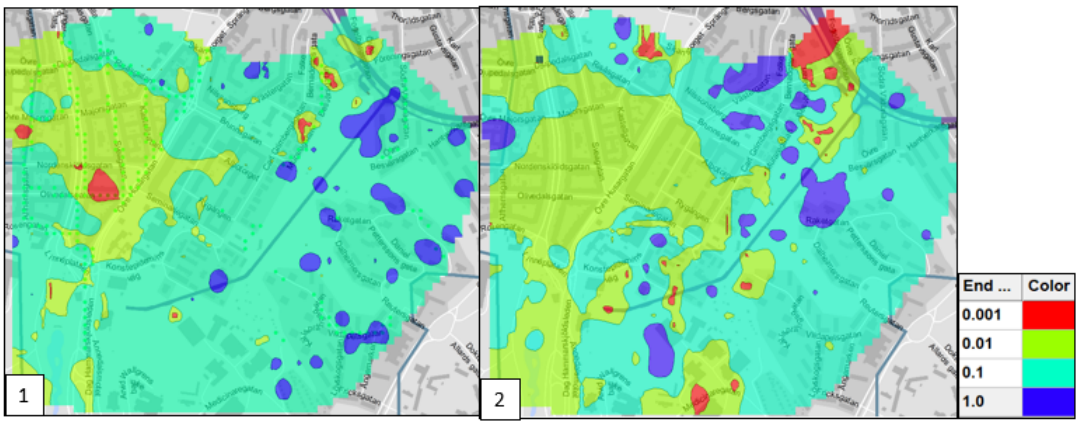

Figure 4.1: Coefficient of variation [%] of recharge in case one [1] and case two [2].

Figure 4.2 shows that there are differences in the coefficient of variation in hydraulic conductivity between case one and two. In case one the cv for fractured bedrock is below 1 % in large parts of the model, which as seen in the figure of min and max hydraulic conductivity in appendix B.1 is an area where the mean hydraulic conductivity is at the minimum value in the parameter interval used for calibration, $6*10^{-7}$ m/s. That value is close to the conductivity of bedrock and not as conductive as the fractured rock could be, indicating that the model might strive to decrease the flow in the model compared to case two.

The inverse PEST calibrated model calibrated before NSMC of case one has a hydraulic conductivity of fractured bedrock that is similar to the glacial till, see appendix B.2.

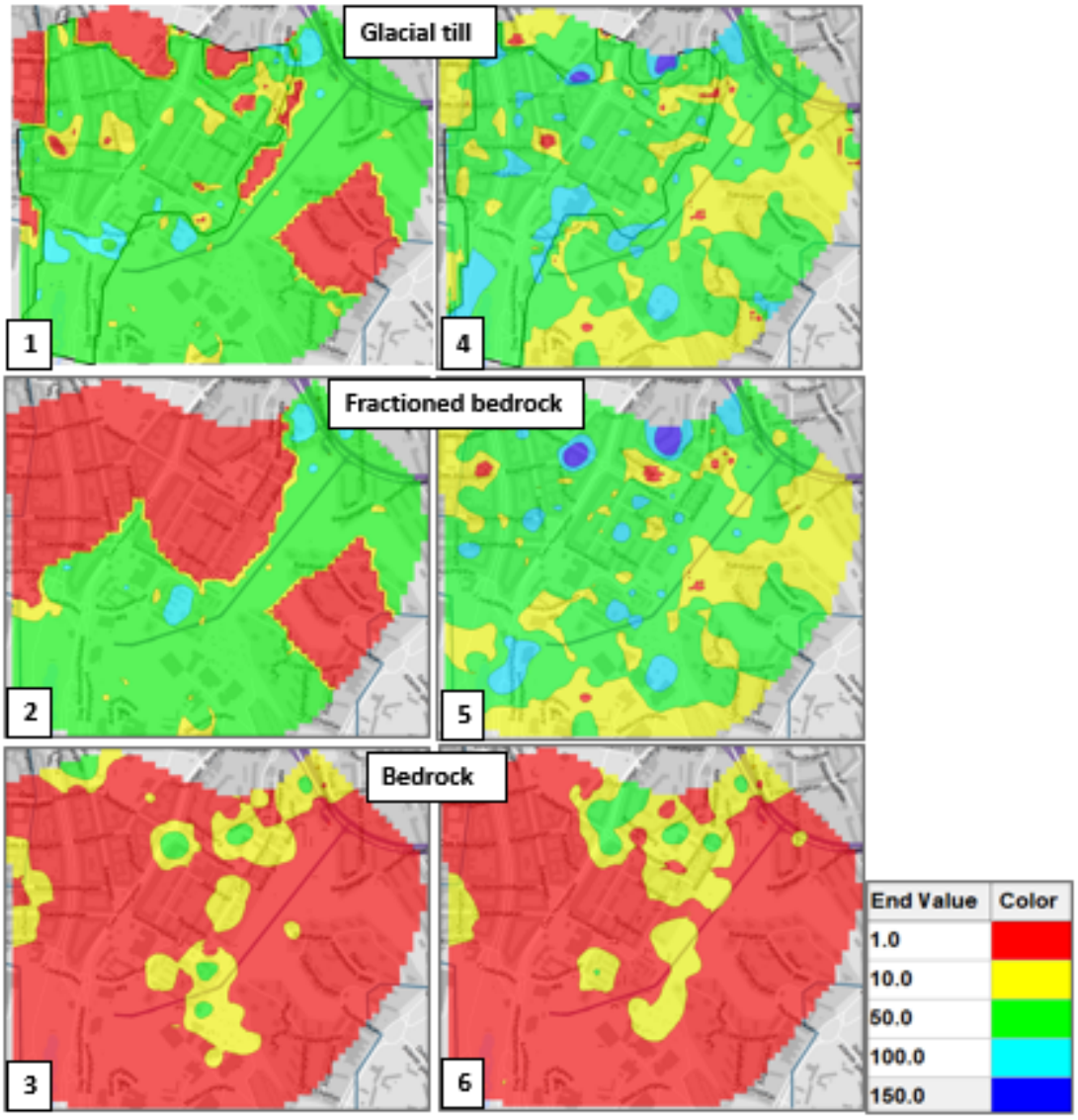

Figure 4.2: Coefficient of variation of hydraulic conductivity shown as % in layer four [1 and 4], layer five [2 and 5], and layer six [3 and 6]. The left column is case one and the right is case two. Area with glacial till in [1] and [4] is within the gray arc.

The distributions of the the water balance are shown in figure 4.3. The spread in recharge and drain is high in both cases compared to CHD in and out, but no extreme outliers are observed. The leakage in the first 355m of the tunnel in case two, which is the part with measured leakage, is about 250 % higher than in case one. This could be a reason to why the drain values are higher in case two. The CHD out (water out) and recharge are also higher in case two compared to case one. The tunnel leakage should not affect the flow over the constant head boundaries, nor the recharge. The recharge in case two however had a large zone in the north-east where maximum recharge levels are present, which was not observed in case one.

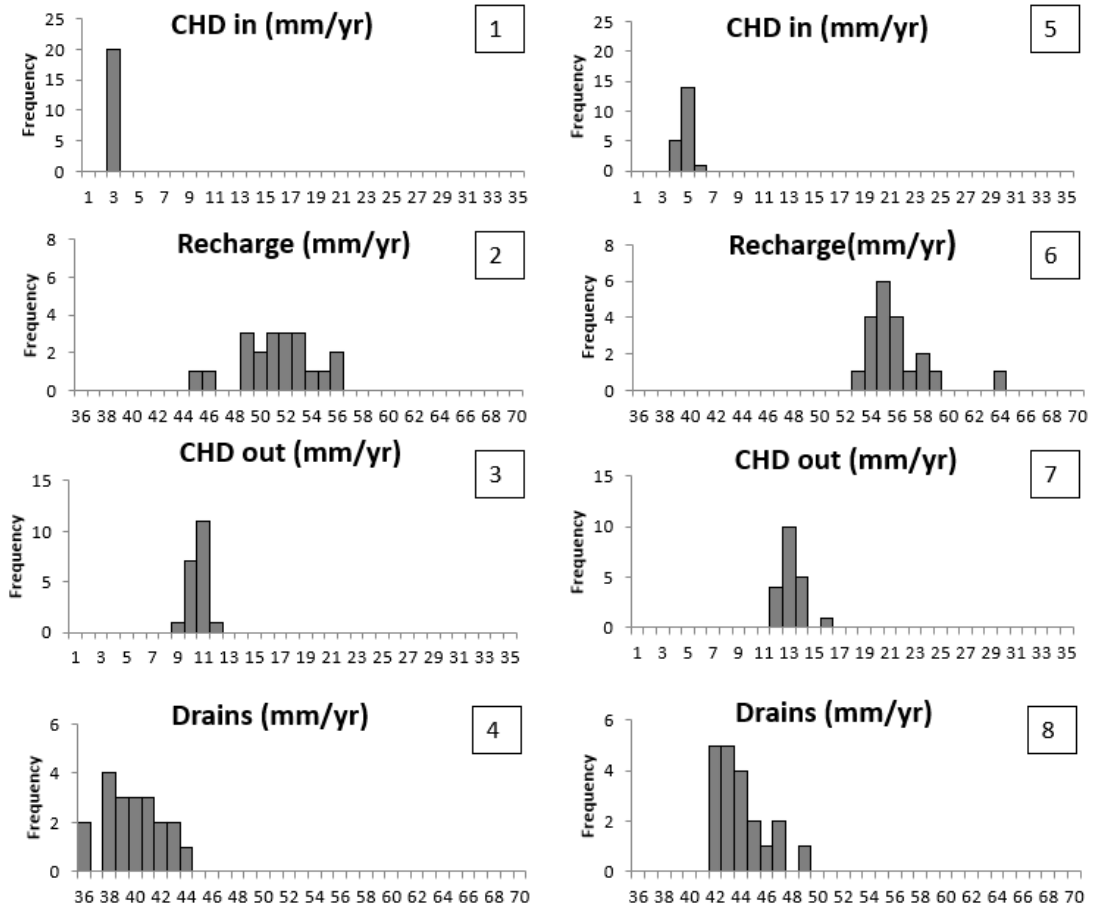

Figure 4.3: Water balance histograms. [1-4]: case one, [5-8]: case two. CHD is the water in/out at constant head boundaries. Drains includes service tunnel Linné and shallow drainage.

4.1.2 Model outcome uncertainty

The range of the leakage in service tunnel Linné is slightly larger for case two with 1,2 l/min/100m difference between min and max compared to a range of 0.8 l/min/100m in case one, see figure 4.4 below.

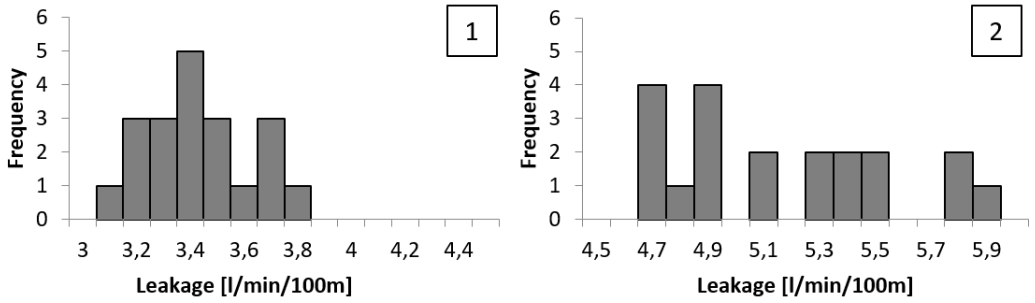

Figure 4.4: Leakage to service tunnel Linné, case one to the left [1] and case two to the right [2].

Figure 4.5 below displays the leakage divided in two sections, 0-355m for which case two was calibrated with measured leakage values in the initial inverse PEST calibration and 355-955m which was calculated values added in the forecast model in both cases. The range of leakage in both sections is wider in case two. Case one has a very uniform leakage range at 0-355m, whereas it is a more similar range between the models at 355-955m. As seen in the histogram the measured flow for 0-355m section in case two is higher than the calculated flow used in case one, which explains why the leakage distribution does not overlap. Studying the cv of the bedrock around the second part of the tunnel in figure 4.2 [3 and 6], the wide range of the leakage at 355-955m does not correlate with a high cv in bedrock. The cv for bedrock in case one is large around the 0-355m section and at the same time has a much smaller leakage range compared to the 355-955 stretch, which has a lower cv. The leakage is determined by the drain arc conductance and the bedrock hydraulic conductivity, for which a higher leakage requires a higher drain arc conductance. When manually calibrating the conductance to obtain the desired flow it was noted that for the larger leakage rates, it was that a low hydraulic conductivity of the bedrock that limited the flow into the arc. The wider spread in the range of leakage rates could therefore be explained by that those three sections with higher leakage rates being much more sensitive to variations in bedrock conductivity. If viewing the mean hydraulic conductivity of bedrock in appendix B.2, it can be noted that the hydraulic conductivity on case one is high above section 0-355m, compared to the 355-955m in both case one and two, making the leakage rate more sensitive to arc conductance rather than bedrock hydraulic conductivity.

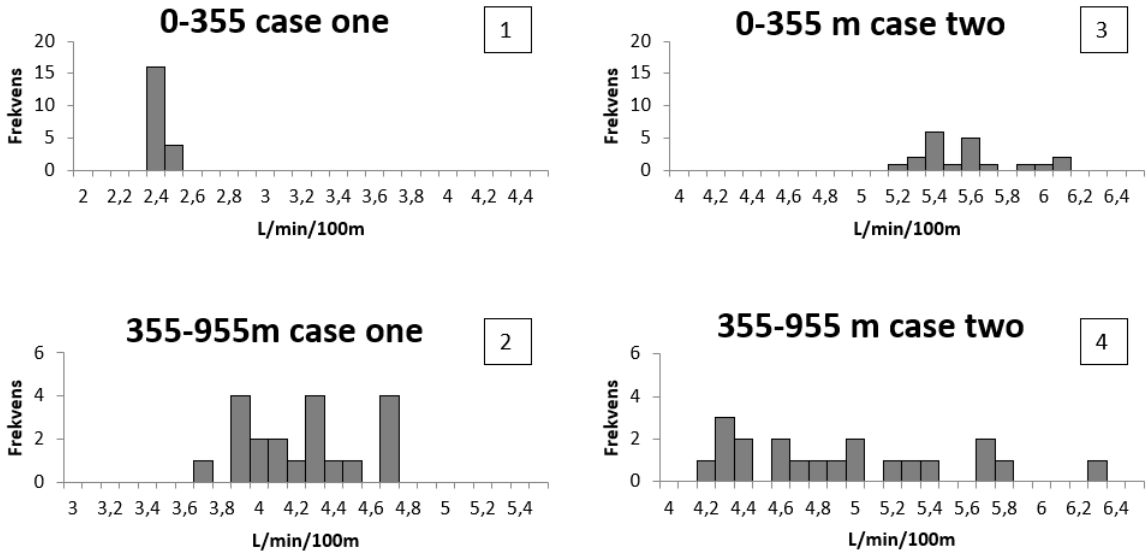

Figure 4.5: Leakage for first and second part of service tunnel Linné in the stochastic forecast model, case one to the left [1 and 2] and case two to the right [3 and 4].

In figure 4.6 the standard deviation of the head for the forecast is presented. The standard deviation of the head in the lower soil- and rock aquifer is higher in case two compared to case one. The standard deviation for the head in the rock aquifer is high for both cases at the second half of the service tunnel. Case two [4] have spots with a maximum standard deviation of 11.2 m, whilst case one [2] has a maximum of 8.6 m, which is much higher than the deviation in lower soil aquifer. This difference could be due to the higher density of observation wells in the lower soil aquifer, which governs the model output during calibration. In the area with high standard deviation in rock aquifer there is a high drainage from the tunnel, this in combination with few observation allows the model to vary the head a lot.

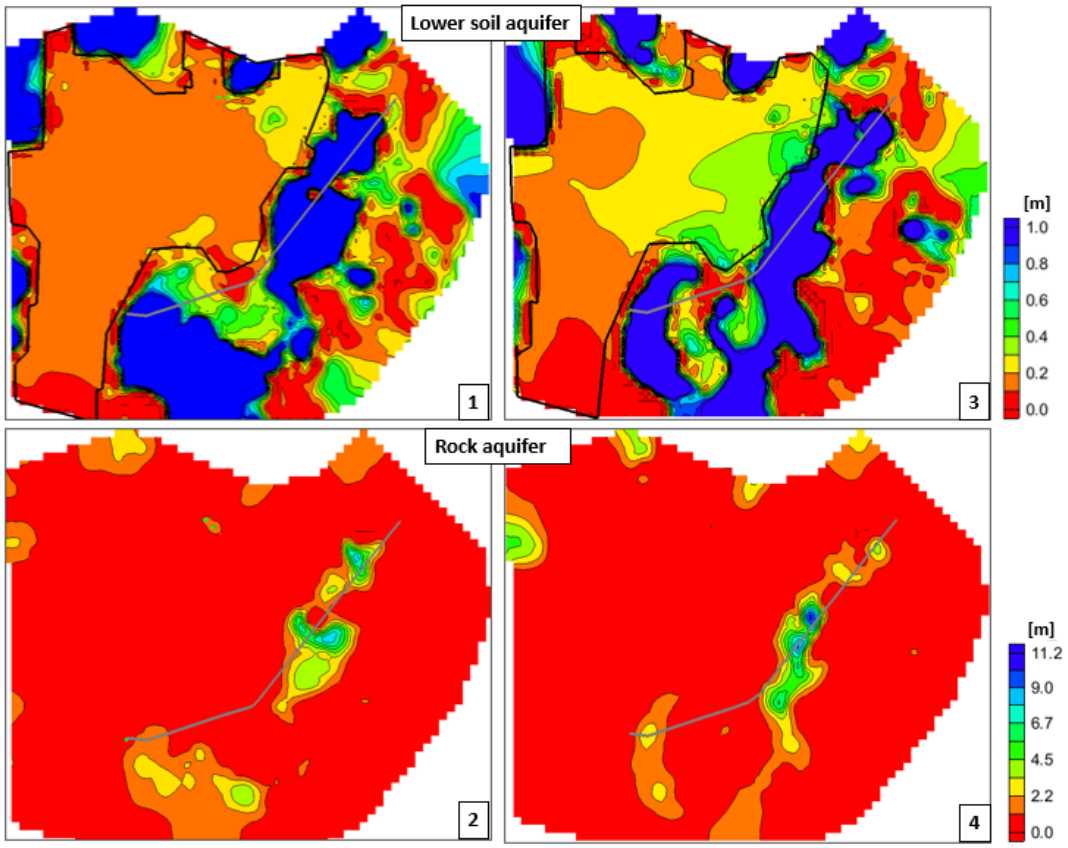

Figure 4.6: Standard deviation of groundwater head [m]. Layer four, representing the lower soil aquifer, [1] and [3]. Extent of lower soil aquifer marked with black line. Layer six representing the rock aquifer, [2] and [4].

In figure 4.7 the points used for comparison of drawdown distribution between the cases are displayed.

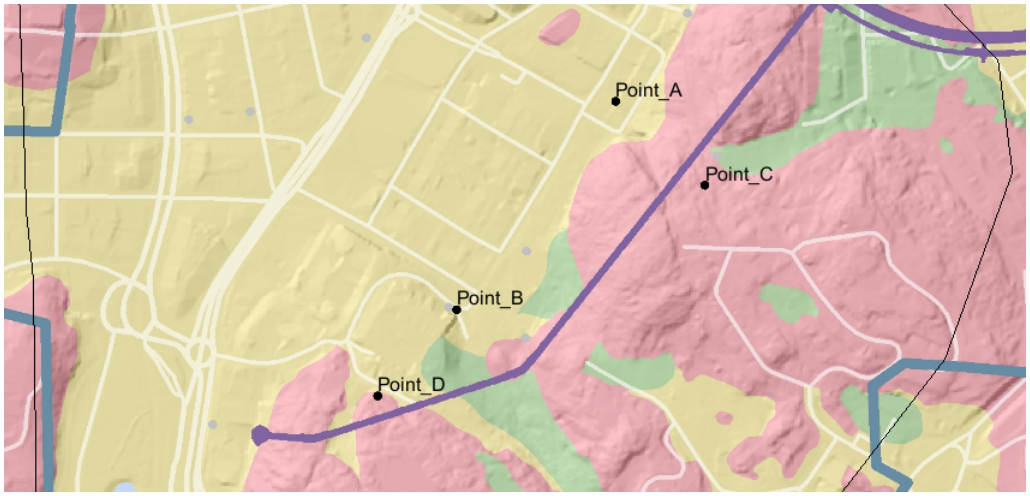

Figure 4.7: Points used for histogram of drawdown. Point A and B are in the lower soil aquifer and point C and D are in the rock aquifer.

In table 4.2 the groundwater head for when removing the tunnel leakage from the case two forecast model, to simulate the conditions without a tunnel is displayed. This is compared with the conditions produced by the case one calibration. As seen in the table, the difference in head in the lower soil aquifer, point A and B is low compared to the difference of head in the bedrock aquifer, point C and D.

Point	Case one	Case two	Difference
A	21.9	21.55	0.35
B	20.27	20.52	0.22
C	56.6	53.66	2.94
D	30.63	34.12	3.49

Table 4.2: Table of groundwater head [m] at each point used for comparison of drawdown. The head for case one is before applying drain arcs and performing forecast of tunnel influence. The head for case two is with all drain arcs removed from the forecast model and new stochastic forward run of the no-tunnel conditions.

In the lower soil aquifer, see figure 4.8, case two clearly have a greater spread in drawdown at both point A and B. Especially at point B where case one have a max frequency of 12 compared to a max frequency of four models with the same drawdown for case two. The same trend can not be seen in the rock aquifer, where at point C, case one have a wider spread compared to case two, see figure 4.9. At point D case one has a slightly higher drawdown frequency than case two, but a range of almost two meters in the dataset compared to one meter in case two.

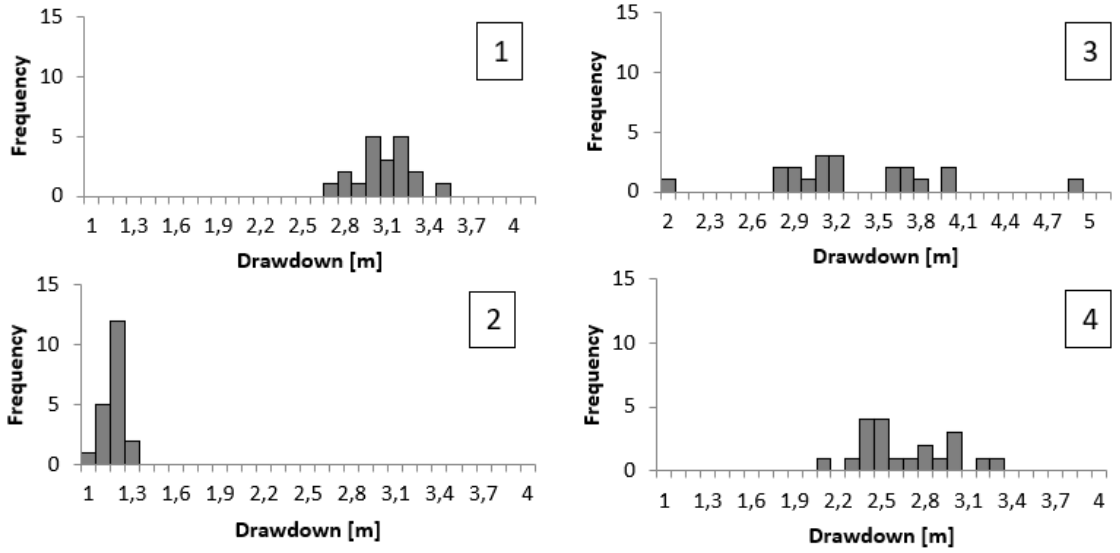

Figure 4.8: Drawdown in lower soil aquifer located at point A [1 and 3] and point B [2 and 4]. The left graphs are case one and the right ones case two.

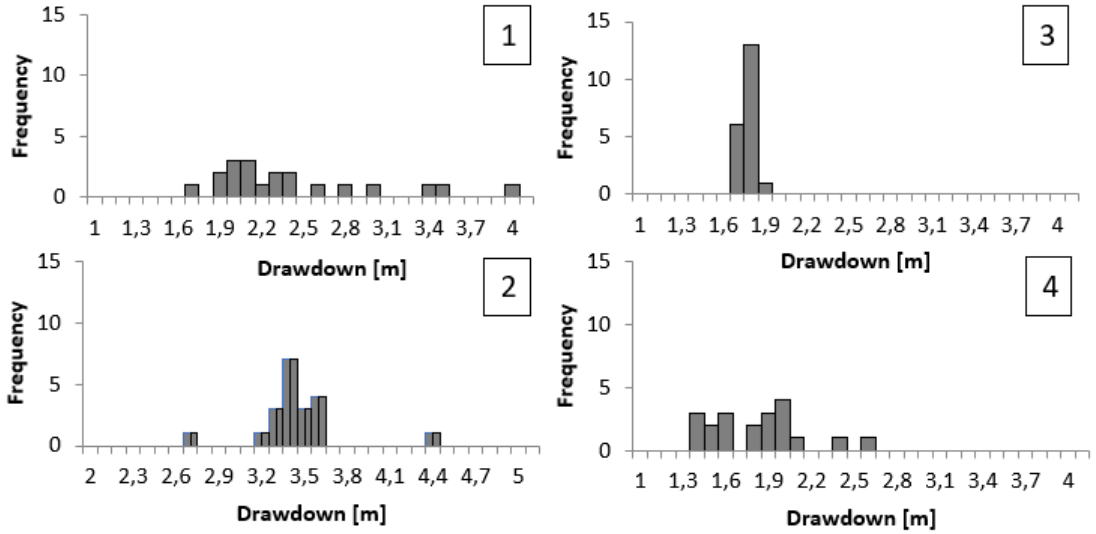

Figure 4.9: Drawdown in rock aquifer at point C [1 and 3] and point D [2 and 4]. The left graphs are case one and to the right case two.

The results show a difference in cv of hydraulic conductivity of glacial till and fractured bedrock where case two has a higher uncertainty than case one. The trend is also present in the distribution of leakage, with less spread in model one. The larger spread of leakage and hydraulic conductivity in case two combines into a larger spread in drawdown compared to case one. The lack of a trend in the distribution of drawdown in the rock aquifer could be due to the low variation of hydraulic conductivity in bedrock between the cases.

4.2 Korsvägen

4.2.1 Parameter uncertainty

A significant difference in the cv of the hydraulic conductivity in the glacial till between case one and two can be seen in figure 4.10. Large zones has a cv of over 100% in case one, while case two only reaches over 50% in a few places. The fractured rock has somewhat higher cv of hydraulic conductivity in case two compared to case one, while there are only minor differences between the cases for the bedrock. The glacial till manifests the largest cv of the three layers, followed by the fractured bedrock, with the smallest values found in the bedrock.

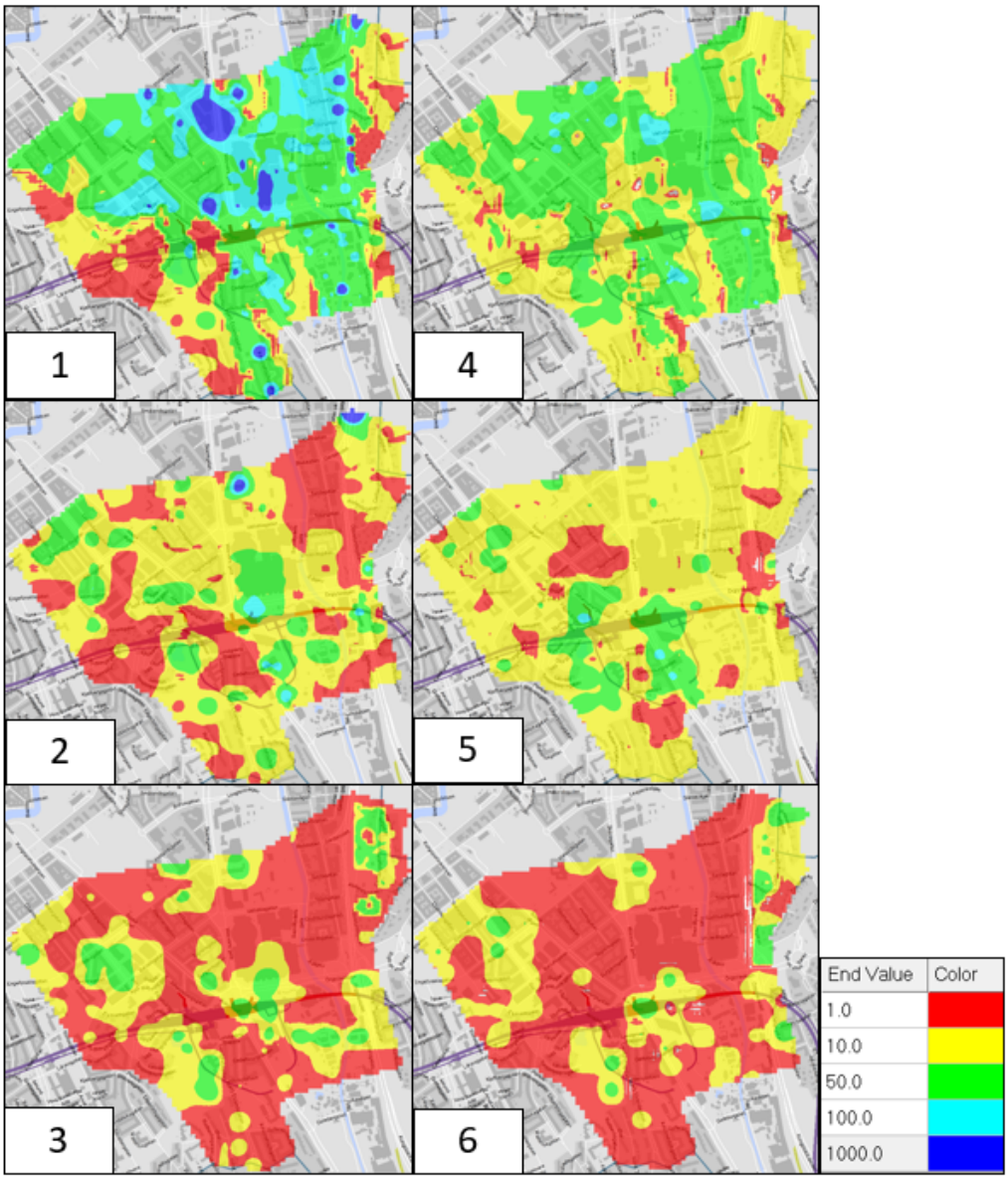

Figure 4.10: Coefficient of variation of hydraulic conductivity in the lower soil aquifer, layer three [1 and 4], fractured bedrock, layer four [2 and 5], and bedrock, layer five [3 and 6]. The left column is case one and the right case two.

The coefficient of variation for recharge can be seen in figure 4.11, where case one shows a slightly higher cv. It is also clear that the largest cv is found in the "no clay" recharge zones, that has much higher mean recharge rates compared to the other zone. It should be noted that the cv of recharge is much smaller than the cv of hydraulic conductivity, meaning that the hydraulic conductivity varies significantly more.

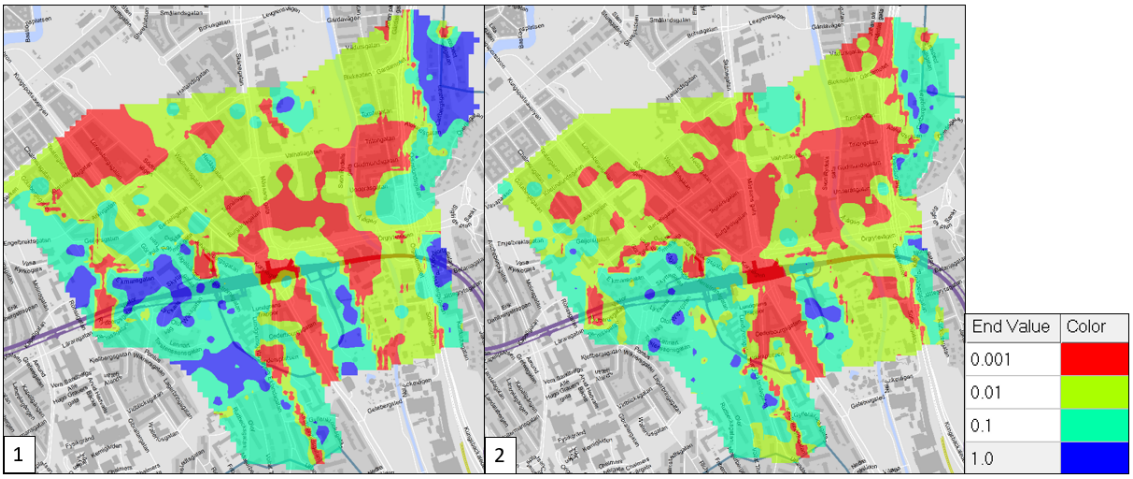

Figure 4.11: Coefficient of variation of recharge in case one [1] and case two [2].

A smaller spread of the calibrated parameters was obtained for the model calibrated with a pumping test compared to the model calibrated against historical mean heads, with variations of hydraulic conductivity being much larger than variation of recharge. A reason for the lower uncertainty obtained with calibration against the pumping test could be that the disturbed groundwater conditions limits the amount of possible solutions of the system. Less variations of hydraulic conductivity and recharge can produce the groundwater conditions during the pumping test compared to the first case, which leads to less spread.

The water balance of the two cases are similar, which can be seen in figure 4.12. There is a little less spread in the second case for all parts of water balance compared to the first case and somewhat less water flows through the second case. In all parts of the water balance except drains does the spread of case one overlap case two completely. The spread of drainage of the two cases do overlap to some extent, but the majority of case two runs have higher drainage, than the highest values of case one.

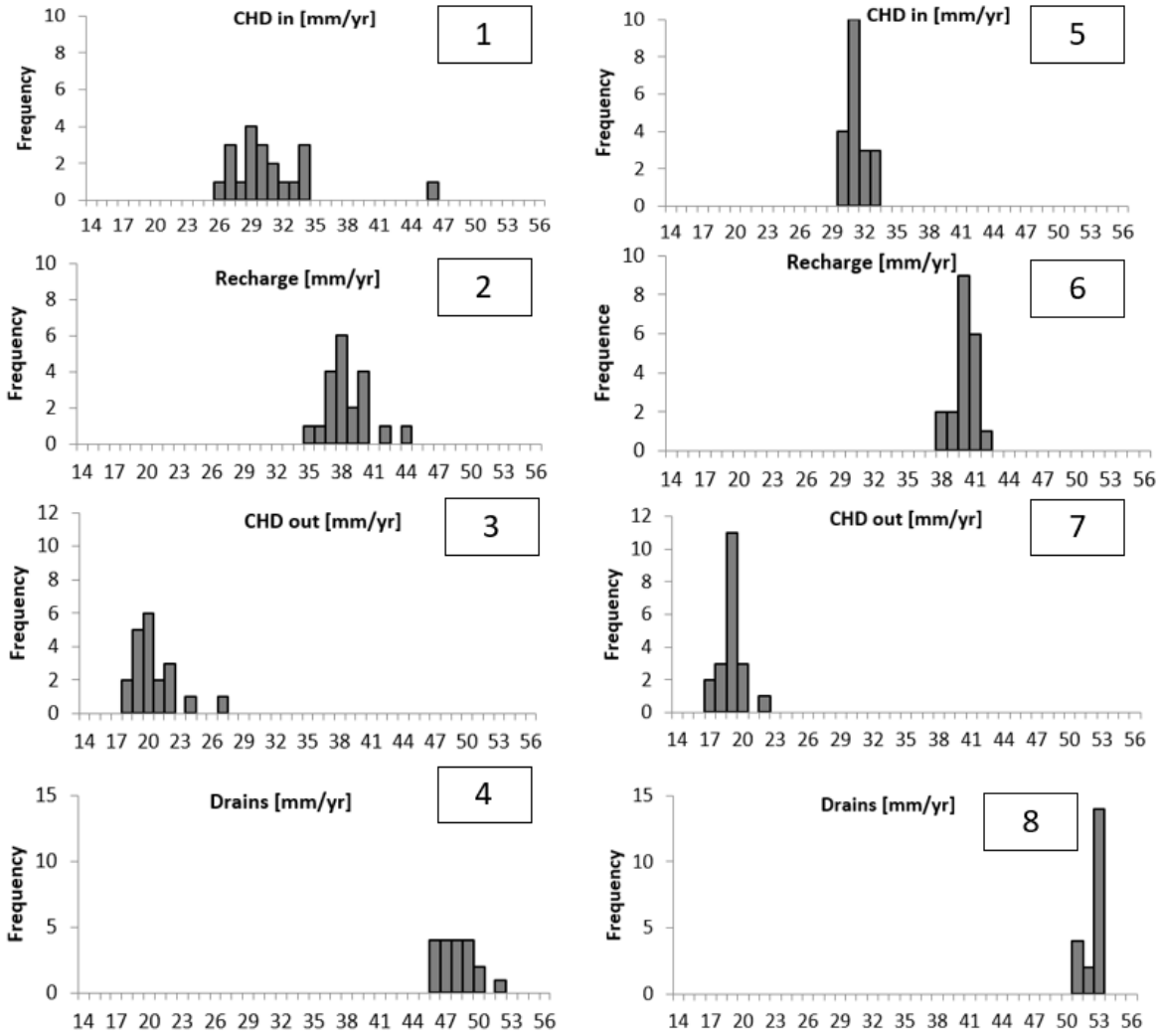

Figure 4.12: Water balance histogram. 1-4: case one, 5-8: case two. CHD is the water in/out at constant head boundaries. Drains includes all tunnels and shallow drainage.

4.2.2 Model outcome uncertainty

Leakage shown in figure 4.13 displays higher leakage rates for case two compared to case one, which probably explains the higher total drainage in case two. There is a slightly higher spread in the first case and the distributions of leakage for the two cases does not overlap each other. Calibration with the pumping test method forecasts a 27% higher leakage rate with the same conductance as case one. This is probably due to the fact the second case has a slightly higher hydraulic conductivity in the rock west of Korsvägen, meaning that it is the hydraulic conductivity that dictates the leakage in some parts of the tunnel and not the actual conductance of the drain. This larger spread in case one is likely caused by the fact that there is larger variation in the hydraulic conductivity of the rock that the tunnel passes through in case one compared to case two.

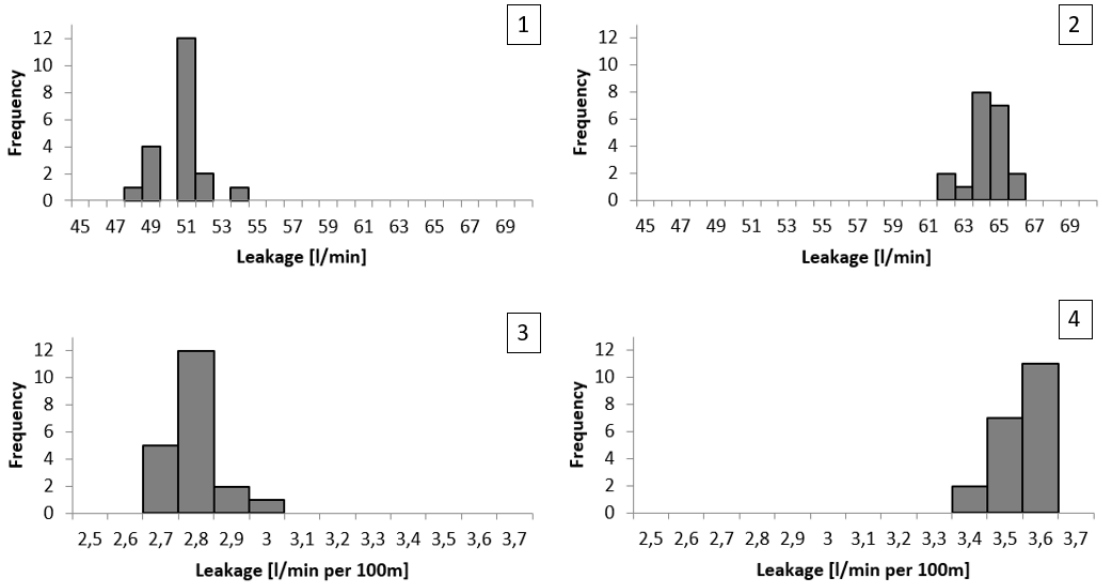

Figure 4.13: Combined leakage to Västlänken, 206 and 207. [1] and [3] are for case one and [2] and [4] for case two.

The standard deviation of the forecast head is clearly higher in the rock aquifer compared to the lower soil aquifer, as seen in figure 4.14. There is also generally higher standard deviation in both the rock- and lower soil aquifer in case one compared to case two. High values of standard deviation are found along the tunnels. At Korsvägen and to the south, there is a lower standard deviation in the lower soil aquifer for case two compared to the other case.

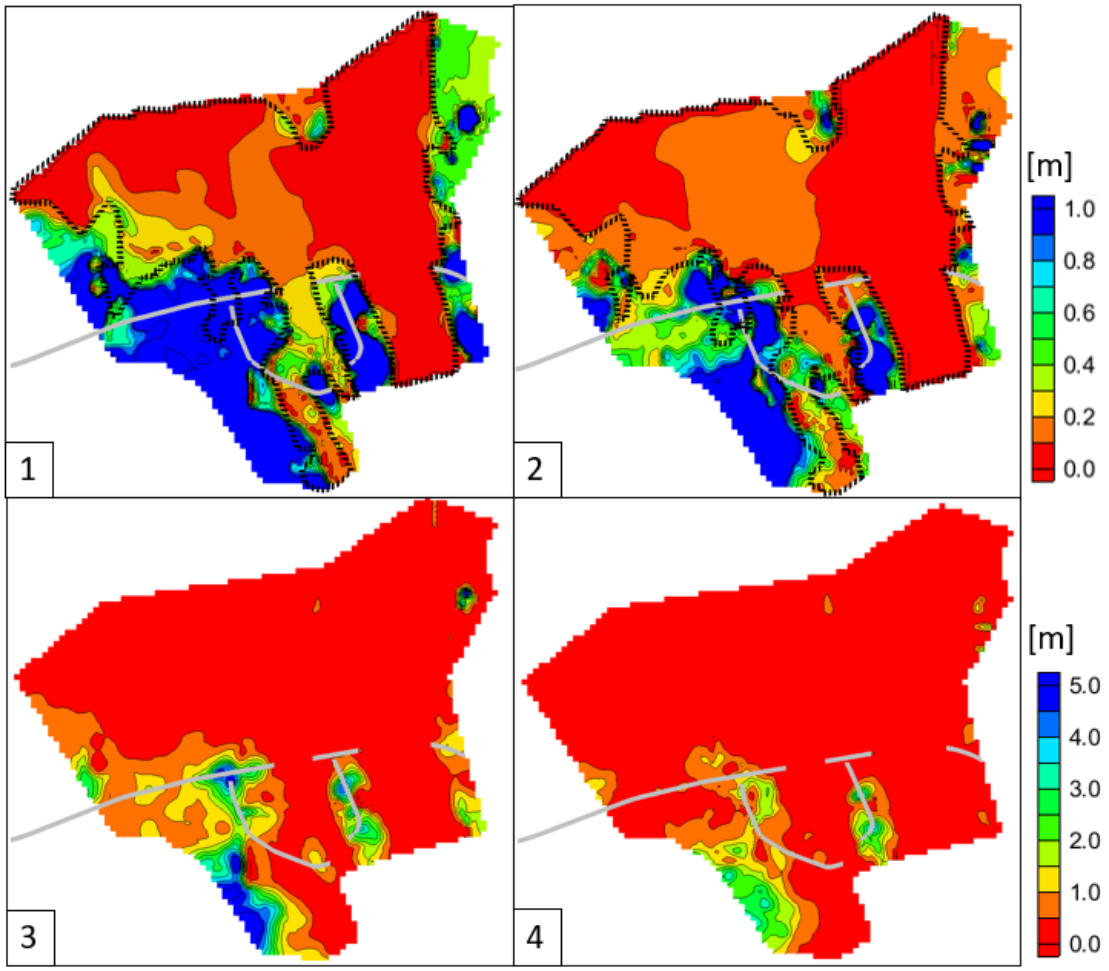

Figure 4.14: Standard deviation of forecast groundwater head in the lower soil aquifer, layer three [1-2] and in the rock aquifer, layer five [3-4], with case one to the left and case two to the right. Extent of lower soil aquifer marked with dashed line and position of the tunnels with grey lines. Note the different scales.

The maximum and minimum drawdown forecast with the two cases is displayed in figure 4.15 and shows that case two in general forecasts larger drawdown. This larger drawdown for case two is very clear for the lower soil aquifer when comparing both the maximum and minimum drawdown. Larger drawdown can also be seen in the rock close to the main tunnel west of Korsvägen for case two, while the southern and eastern part of the model domain does not exhibit any apparent differences between the cases.

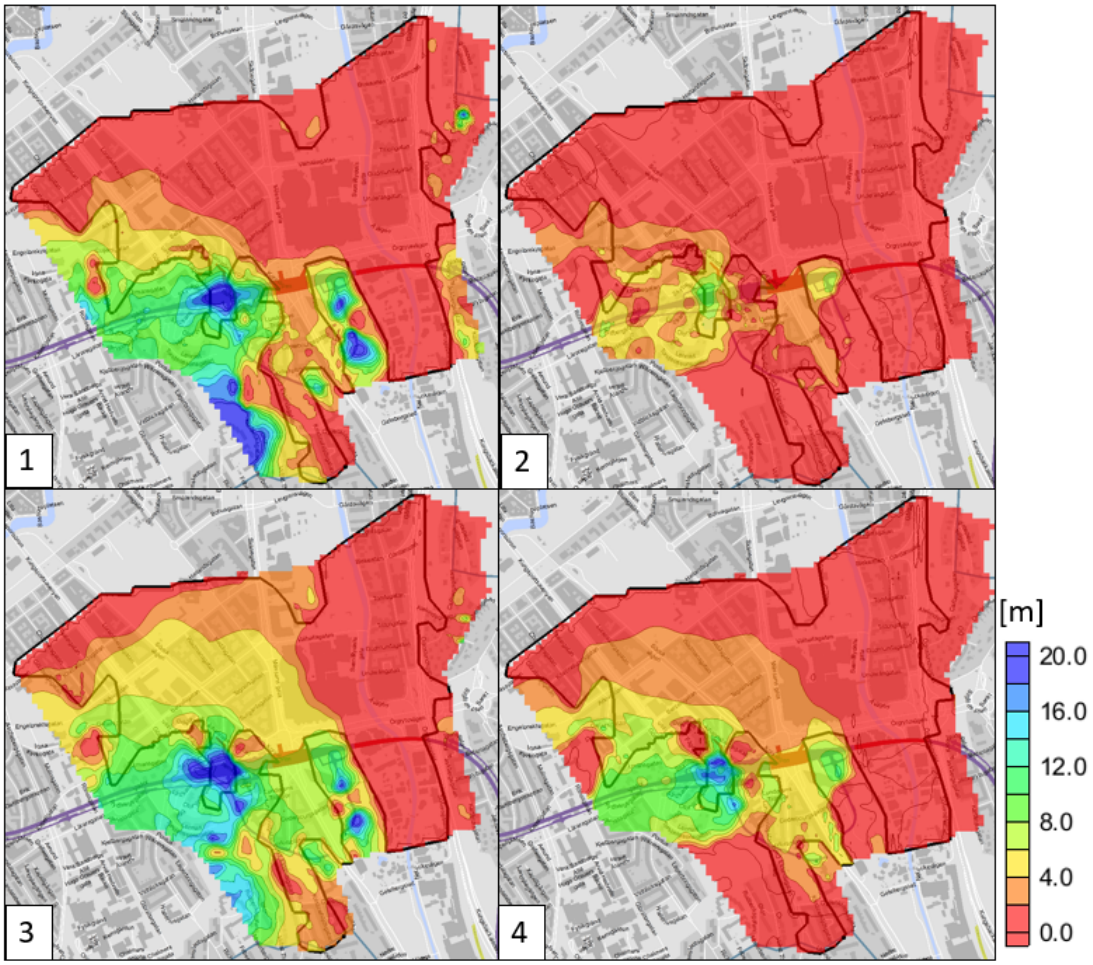

Figure 4.15: Maximum, [1 and 3] and minimum, [2 and 4] drawdown in layer three, with 1-2 from case one and 3-4 from case two. Extent of lower soil aquifer marked with the black line.

Two points, A and B in figure 4.18 are used to view the drawdown in the lower soil aquifer, layer three in the models. The drawdown, as shown in figure 4.16 is larger for the second case in both points and the spread of the drawdown does not overlap in any of the points. It can also be seen that the spread of the drawdown is larger for case one compared to case two at both point A and B. The higher leakage rate partly explains the larger drawdown in case two, but this larger drawdown is not seen across the whole model domain and the increased leakage is not proportional to the differences in drawdown. There is for example a 106 % larger drawdown in point B used for the histograms. Slightly higher conductivity of the glacial till and bedrock, leading to smaller gradients in case one could partly explain this difference.

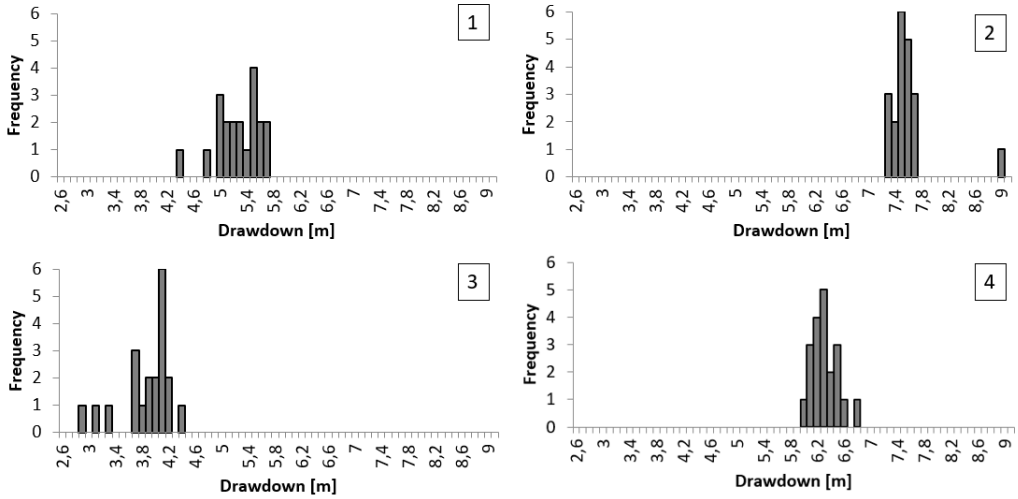

Figure 4.16: Drawdown in the lower soil aquifer at point A [1-2] and B [3-4]. The left graphs are for case one and the ones to the right are for case two.

The drawdown in the rock aquifer, layer five in the model is also displayed for two points, C and D in figure 4.18, as seen in figure 4.17. The rock aquifer shows the same trend as the lower soil aquifer, with larger drawdown for case two and also larger spread in case one at both examined points.

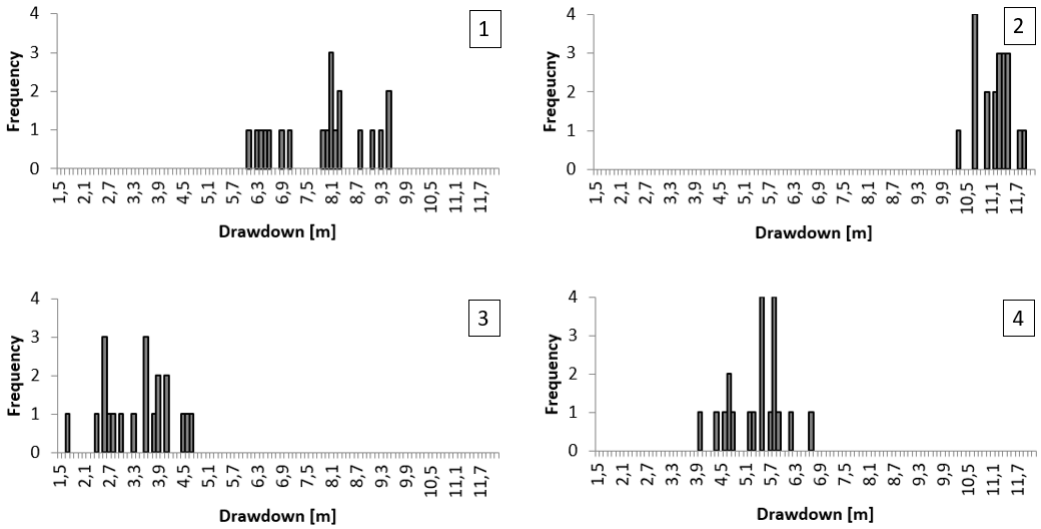

Figure 4.17: Drawdown in the rock aquifer at point C [1-2] and D [3-4]. The left graphs for case one and the ones to the right for case two.

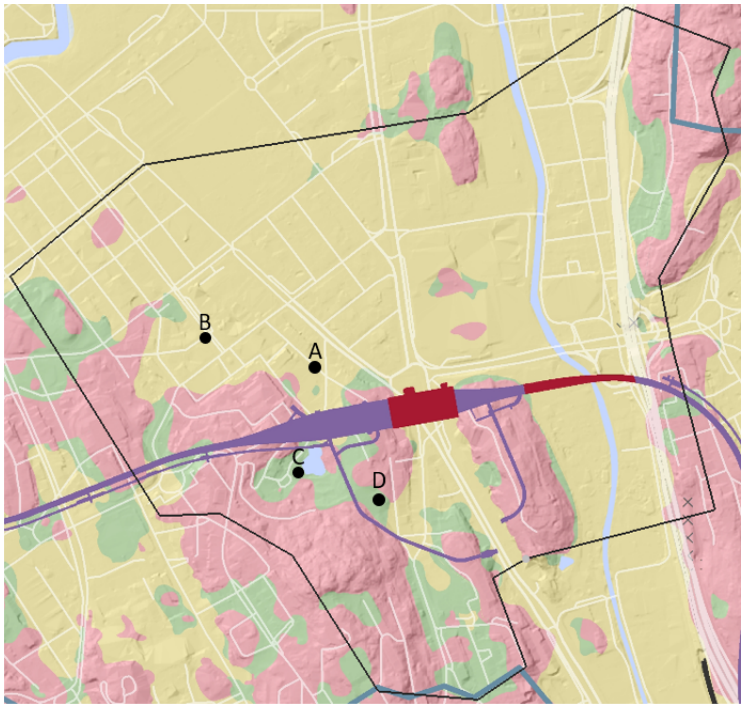

Figure 4.18: Location of points used for drawdown histograms.

The trend of less variation in case two can be seen when looking at the standard deviation of forecast head for both the lower soil- and rock aquifer, as well as when

looking at the spread of drawdown in both the aquifers. Since the only uncertainty incorporated in the model is the calibrated parameters, does the model outcome uncertainty consequently follow the same trend as the variations of the parameters, with less uncertainty for case two. The hydraulic conductivity varies more in the first case, which makes the leakage vary more and these two factors combines into a larger spread of the forecast drawdown in case one. It should however be noted that significantly larger drawdown was forecast by case two in both aquifers and that drawdown distributions of the two cases does not overlap.

5

Discussion

The results of the comparison for the model over service tunnel Linné demonstrates that adding measured tunnel leakage and calibrating with affected groundwater head observations does not decrease the uncertainties in the forecast of leakage induced drawdown from service tunnel Linnè, compared to calibration against historic mean groundwater head observations.

The correlations in the model for Korsvägen of both the parameter- and model outcome uncertainty indicates that using a pumping test for calibration instead of historic mean groundwater head observations decreases uncertainties associated with the calibrated parameters, but also that different calibration methods can give significantly contrasting forecasts of leakage induced drawdown.

Another approach to simulate the leakage into the tunnel could have been used. One way would be to use a drain as was done in this study, but edit the hydraulic conductivity of the material surrounding the tunnel to mimic the effect of grouting, instead of editing the drain conductance. This could possibly avoid the problem with largely different flow when using the same conductance.

Forecasting the effect from tunnel leakage using 37 % of the Linné service tunnel in calibration yields higher model uncertainty than using only historic mean head observations , while the model calibrated with a pumping test provides lower parameter uncertainty compared to using historic mean head observations. The fact that the pumping test calibration gave lower uncertainty, while the calibration with tunnel leakage gave higher uncertainty is probably due to much more observation points being affected by the pumping test, than what is the case for the tunnel leakage. The leakage that Linné model was calibrated with only affected the head in three observation wells, compared to 21 observations wells being affected by the pumping test in the Korsvägen model. This means that there are more observations that constrains the possible solutions in the Korsvägen model compared to the Linné model, leading to less variations of the calibrated parameters being able to produce a solution of the groundwater system.

It is important to note that this study only takes uncertainty of the calibrated parameters into account and as described in section 2.2.4 Uncertainties in groundwater modelling, there are many types of uncertainties surrounding groundwater modeling. The conceptual model uncertainties have by Dubus, Brown, and Beulke (2003) been seen to be the greatest source of uncertainty. This means that further studies would benefit from incorporating more types of uncertainty and one way could be

to create several conceptual models that are calibrated with different methods to get a more comprehensive measure of the uncertainty.

MODFLOW bases the flow equations on Darcy's law, that describes flow through a porous medium, but the intact bedrock is not porous and it is only trough the fractures that flow takes place. This means that modelling flow through bedrock with Darcy's law is a rough simplification of reality, which could effect modelling results. Higher values of conductivity should in reality follow weakness zones, but obtained calibrated hydraulic conductivity fields does not show any correlation between weakness zones and conductivity. How large impact this simplification of reality has on the outcome is not known.

20 models were created for each calibration method due to the large time consumption of the modelling, but these models should provide enough ground to show the general trends of the different methods. A larger amount of models would strengthen the credibility of the results and could potentially give slightly different results. More models would probably amplify the trends and more clearly show which models that are outliers. One other thing that could influence results is that the same residual error was not obtained with NSMC for the different methods. Higher residual error coincides with the model with the largest spread for both Korsvägen and Linné. This higher residual error could mean that a larger variation of the parameters is allowed when the solutions does not have to be as close to the observations as the more well calibrated model.

The variograms used for the kriging interpolation method was not able to be fitted to all data sets and arbitrary variograms had to be used. This adds another type of uncertainty that is not explored in this report and it is not known how large effect this has on the results.

Using observations during construction could be beneficial to generate better forecasts, but having more observations points than is the case for the Linné model, that is effected by the construction to calibrate the model would most likely be key to obtain more accurate predictions. Planning an observation point scheme before construction that can be used for calibration would probably be needed if this method was to be used for design of protective measures. Validation of the forecasts produced by the models could be an appropriate task for future studies. This would enable evaluation of the forecast accuracy of the different calibration methods and not only of the uncertainty, as was done in this study. Another way to incorporate more data from the construction into calibration is to use transient data, where more stages of the construction could be simulated, which could lead to less uncertain results when there are more constraints to the calibration. This transient method could also be applied to the pumping test in future research.

The time consumption of the calibration was a limiting factor during the work with this thesis and further studies on this topic would strongly benefit from a way of making calculations faster. More computing power is the obvious solution to this problem, but constructing the model in a way that makes the computing more efficient is also an alternative. Starting out with a coarse regional model to find the area of influence and then develop a smaller local model that uses the results from the

regional model as boundary conditions is one possible way to reduce computational time.

The results found in this study identifies the following topics for future research, summarized as bullet points:

- Perform calibration with transient data to add constraints that possibly could reduce uncertainties
- Incorporate analysis of conceptual uncertainties by using different conceptual models to evaluate the calibration methods.
- Analyze how the spatial density of observations used for calibration affects the parameter uncertainty.

6

Conclusion

This study could not find a clear link between parameter- and prediction uncertainties and method used for calibration. Calibration against a pumping test compared to historic mean groundwater heads reduced uncertainties, while calibration against tunnel leakage produced larger uncertainties compared to calibration against historic mean groundwater heads. These results signifies that calibration against a disturbance of the groundwater conditions does not always provide more accurate forecasts of drawdown than using historic mean groundwater head observations and that more observations not necessarily leads to reduced uncertainties. Future studies on this topic would probably benefit from calibrating against transient data and could also incorporate other types of uncertainties, such as conceptual model uncertainties into the analysis.

References

Ahlberg, P., & Lundgren, T. (1977). *Grundvattensänkning till följd av tunnelsprängning* (Tech. Rep.). Linköping: SWEDISH GEOTECHNICAL INSTITUTE.

Anderson, M., Woessner, W., & Hunt, R. (2015). *Applied Groundwater Modeling: Simulation of Flow and Advective Transport* (2nd ed.).

Andersson, M. P., Hunt, R. J., & Woessner, W. W. (2015). *Applied groundwater modelling : simulation of flow and advective transport* (Second edi ed.). Academic press.

AQUAVEO. (2017a). *GMS:Boundary Matching - XMS Wiki.* Retrieved from `https://www.xmswiki.com/wiki/GMS:Boundary_Matching`

AQUAVEO. (2017b). *GMS:Conceptual Model - XMS Wiki.* Retrieved from `https://www.xmswiki.com/wiki/GMS:Conceptual_Model`

Beven, K. (2005, 9). On the concept of model structural error. *Water Science and Technology*, *52*(6), 167–175. doi: 10.2166/wst.2005.0165

Chilton, J. (1999). *Groundwater in the Urban Environment* (21st ed.; JOHN CHILTON, Ed.). NOTTINGHAM: INTERNATIONAL ASSOSIATION OF HYDROGEOLOGISTS.

Doherty, J. (2018). *PEST Model-Independent Parameter Estimation User Manual Part I: PEST, SENSAN and Global Optimisers* (Tech. Rep.).

Doherty, J. (2020). *PESThomePage.org - FAQ.* Retrieved from `http://www.pesthomepage.org/PEST_FAQ.php`

Dubus, I. G., Brown, C. D., & Beulke, S. (2003, 12). Sources of uncertainty in pesticide fate modelling. *Science of the Total Environment*, *317*(1-3), 53–72. doi: 10.1016/S0048-9697(03)00362-0

Eklund, H. S. (2002). *Hydrogeologiska typmiljöer: verktyg för bedömning av grundvattenkvalitet, identifiering av grundvattenförekomster samt underlag för riskhantering längs vägar* (Unpublished doctoral dissertation). Chalmers university of technology.

Fetter, C. J. (2014). *Applied hydrogeology* (Fourth edi ed.). Harlow.

Gallagher, M., & Doherty, J. (2007, 2). Predictive error analysis for a water resource management model. *Journal of Hydrology*, *334*(3-4), 513–533. doi: 10.1016/j.jhydrol.2006.10.037

GMS:Automated Parameter Estimation - XMS Wiki. (2017). Retrieved from `https://www.xmswiki.com/wiki/GMS:Automated_Parameter_Estimation`

Gustafson, G. (2009). *Hydrogeologi för bergbyggare.* Göteborg.

Harbaugh, W., Arlen. (2005). MODFLOW-2005 , The U . S . Geological Sur-

vey Modular Ground-Water Model — the Ground-Water Flow Process. *U.S. Geological Survey Techniques and Methods*, 253. Retrieved from http://water.usgs.gov/software/ground_water.html/.

Hölting, B., & Coldewey, W. (2019). *Hydrogeology.* Springer, Berlin, Heidelberg. Retrieved from https://link-springer-com.proxy.lib.chalmers.se/book/10.1007%2F978-3-662-56375-5#toc

Knutssons, G., & Morfeldt, C.-O. (2002). *Grundvatten: Teori och tillämpning* (Third ed.; H. Svensson, Ed.). Stockholm: AB Svensk Byggtjänst.

Lissel, P. (2016). *PM Numeriska beräkningar* (Vol. 1; Tech. Rep. No. 1).

Lithén, J., & Wadsten, M. (2016). *PM Hydrogeologi berg Underlagsdokument till PM Hydrogeologi, ansökan om tillstånd till vattenverksamhet* (Tech. Rep.). Göteborg.

Lithén, J., Wadsten, M., Östergaard, S. H., & Persson, K. (2016). *PM Hydrogeologi jord* (Tech. Rep.).

Mölndalsån.se. (2020). *Flöden och nivåer i Mölndalsån.* Retrieved from http://molndalsan.se/#

Moore, C., & Doherty, J. (2006, 4). The cost of uniqueness in groundwater model calibration. *Advances in Water Resources*, *29*(4), 605–623. doi: 10.1016/j.advwatres.2005.07.003

Niwsonger, R. G., Panday, S., & Ibaraki, M. (2011). MODFLOW-NWT, a newton formulation for MODFLOW-2005. In *Section a, groundwater book 6, modelling techniques* (chap. 37). Virginia: U.S. Geological survey.

PEST Model-independence. (n.d.). Retrieved from http://www.pesthomepage.org/Model-independence.php

Ramböll. (2014). VÄSTLÄNKEN SERVICETUNNEL-PROFIL.

Raposo, J. R., Molinero, J., & Dafonte, J. (2010, 11). Quantitative evaluation of hydrogeological impact produced by tunnel construction using water balance models. *Engineering Geology*, *116*(3-4), 323–332. doi: 10.1016/j.enggeo.2010.09.014

SSPA. (n.d.). *PEST.* Retrieved from https://www.sspa.com/software/pest

Sundell, J. (2018). Risk Assessment of Groundwater Drawdown in Subsidence Sensitive Areas.

Sundkvist, U. (2016). PM Hydrogeologiska beräkningar. , *TRV 2016/3*(44), 1–44.

Sundkvist, U., & Wallroth, T. (2016). Ansökan om tillstånd enligt miljöbalken för anläggandet av Västlänken och Olskroken planskildhet Göteborgs Stad, Mölndals stad, Västra Götalands län. PM Hydrogeologi. (TRV 2016/3151). Retrieved from www.trafikverket.se

Tiedeman, C. R., Hill, M. C., D'Agnese, F. A., & Faunt, C. C. (2003, 1). Methods for using groundwater model predictions to guide hydrogeologic data collection, with application to the Death Valley regional groundwater flow system. *Water Resources Research*, *39*(1). Retrieved from http://doi.wiley.com/10.1029/2001WR001255 doi: 10.1029/2001WR001255

Trafikverket. (2014). *Järnvägsplan, Västlänken, Planbeskrivning* (Tech. Rep. No. TRV 2013/92333).

Vestin, T., & Lindström, M. (2020). *Kontrollprogram grundvatten, månadsrapport för februari 2020* (Tech. Rep.). Göteborg: Trafikverket.

Walker, W., Harremoës, P., Rotmans, J., van der Sluijs, J., van Asselt, M., Janssen, P., & Krayer von Krauss, M. (2003, 3). Defining Uncertainty: A Conceptual Basis for Uncertainty Management in Model-Based Decision Support. *Integrated Assessment*, *4*(1), 5–17. doi: 10.1076/iaij.4.1.5.16466

Wallroth, T., Larsson, K., Hjalmarsson, H., Högsta, U., Sanell, K., & Lindblad-Påsse, A. (2016). Ansökan om tillstånd enligt miljöbalken för anläggandet av Västlänken och Olskroken planskildhet, Teknisk Beskrivning. (2016/3151). Retrieved from `www.trafikverket.se`

XMS Wiki. (2017). *GMS:MODFLOW Packages Supported in GMS.* Retrieved from `https://www.xmswiki.com/wiki/GMS:MODFLOW_Packages_Supported_in_GMS`

Yoo, C., Lee, Y. J., Kim, S. H., & Kim, H. T. (2012, 5). Tunnelling-induced ground settlements in a groundwater drawdown environment - A case history. *Tunnelling and Underground Space Technology*, *29*, 69–77. doi: 10.1016/j.tust.2012.01.002

A

Appendix 1

A.1 Linné

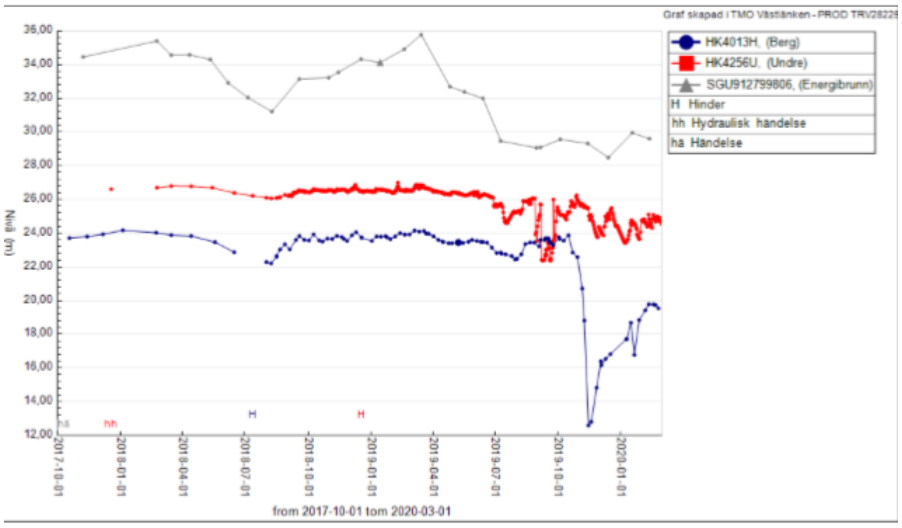

Figure A.1: Measured groundwater head at three observations wells at time of tunnel construction (Vestin & Lindström, 2020).

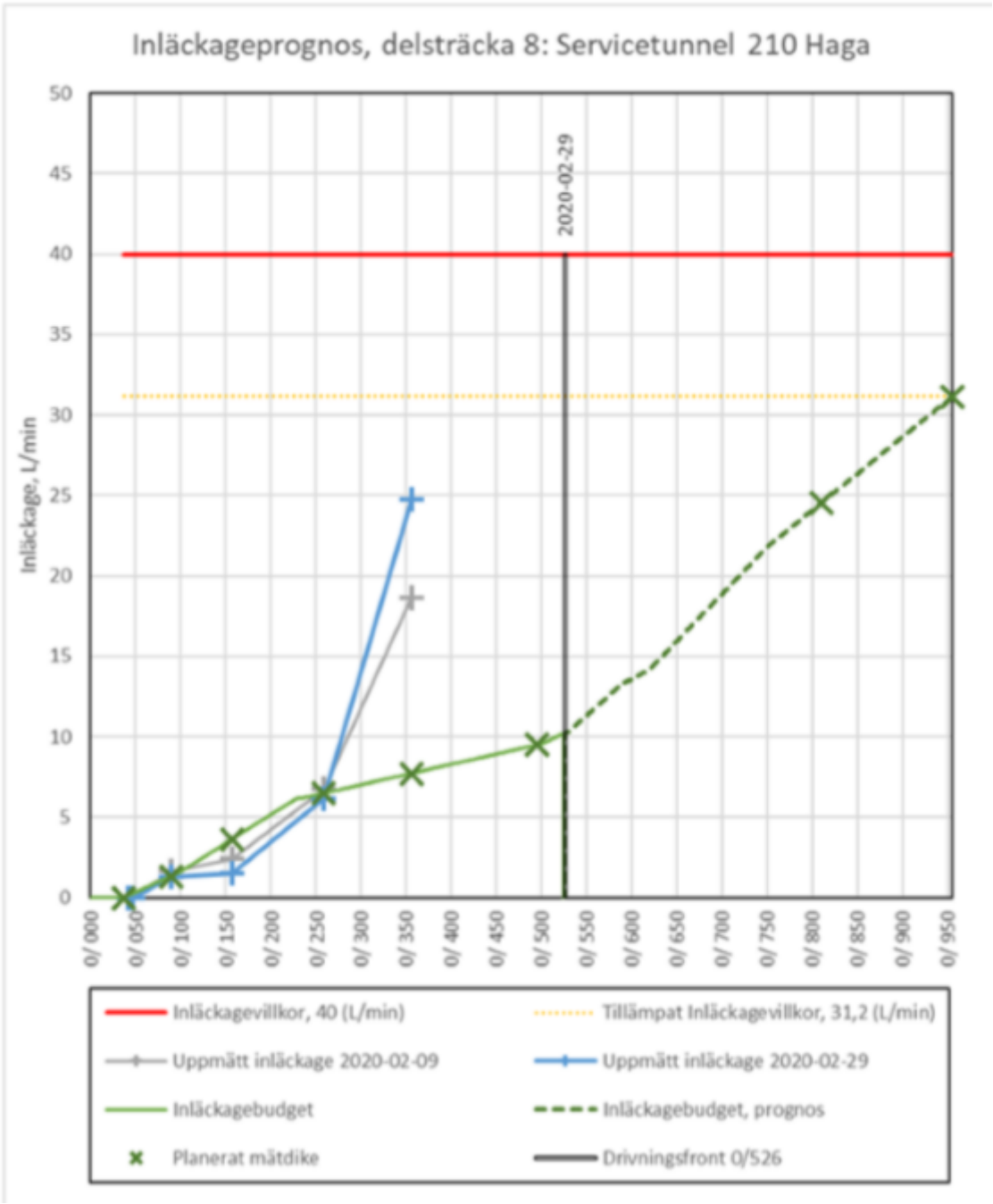

Figure A.2: Measured tunnel leackage (l/min) and graph of allowed tunnel leakage from leakage budget (Vestin & Lindström, 2020).

Materials	Pilot points [m/s]	Calibration intervals [m/s]
Filling material		10^{-5}
Clay		10^{-8}
Glacial till	$1.5 * 10^{-5}$	$6.7 * 10^{-6}$ – $2.5 * 10^{-5}$
Fractured rock	$3 * 10^{-6}$	$6.7 * 10^{-7}$ – $2.5 * 10^{-5}$
Bedrock	$2 * 10^{-8}$	$8.7 * 10^{-9}$ – $6.7 * 10^{-7}$

Table A.1: Hydraulic conductivity values used for PEST calibration of Linné

Materials	Pilot points [m/s]	Calibration intervals [m/s]
Filling material		10^{-5}
Clay		10^{-8}
Glacial till	From PEST calibration	$6 * 10^{-6}$ – $3 * 10^{-5}$
Fractured rock	From PEST calibration	$6 * 10^{-7}$ – $3 * 10^{-5}$
Bedrock	From PEST calibration	$8 * 10^{-9}$ – $7 * 10^{-7}$

Table A.2: Hydraulic conductivity values used for NSMC simulation of Linné

Recharge zone	Manual	PEST	NSMC
1	$4 * 10^{-9}$	$3.9 * 10^{-10}$-$8.2 * 10^{-9}$	$2 * 10^{-10}$-$8.5 * 10^{-9}$
2	$4 * 10^{-9}$	$1.5 * 10^{-9}$-$8.2 * 10^{-9}$	$1 * 10^{-9}$-$8.5 * 10^{-9}$
3	$5 * 10^{-9}$	$1.7 * 10^{-9}$-$8.2 * 10^{-9}$	$1 * 10^{-9}$-$8.5 * 10^{-9}$
4	$4 * 10^{-9}$	$1.5 * 10^{-9}$-$8.2 * 10^{-9}$	$1 * 10^{-9}$-$8.5 * 10^{-9}$
5	$3 * 10^{-9}$	$9.8 * 10^{-10}$-$8.2 * 10^{-9}$	$9 * 10^{-10}$-$8.5 * 10^{-9}$
6	$1 * 10^{-9}$	$6 * 10^{-12}$-$6.5 * 10^{-9}$	$6 * 10^{-12}$-$6.5 * 10^{-9}$

Table A.3: Recharge rate $[m^3/s]$ at manual, PEST and NSMC calibration of Linné

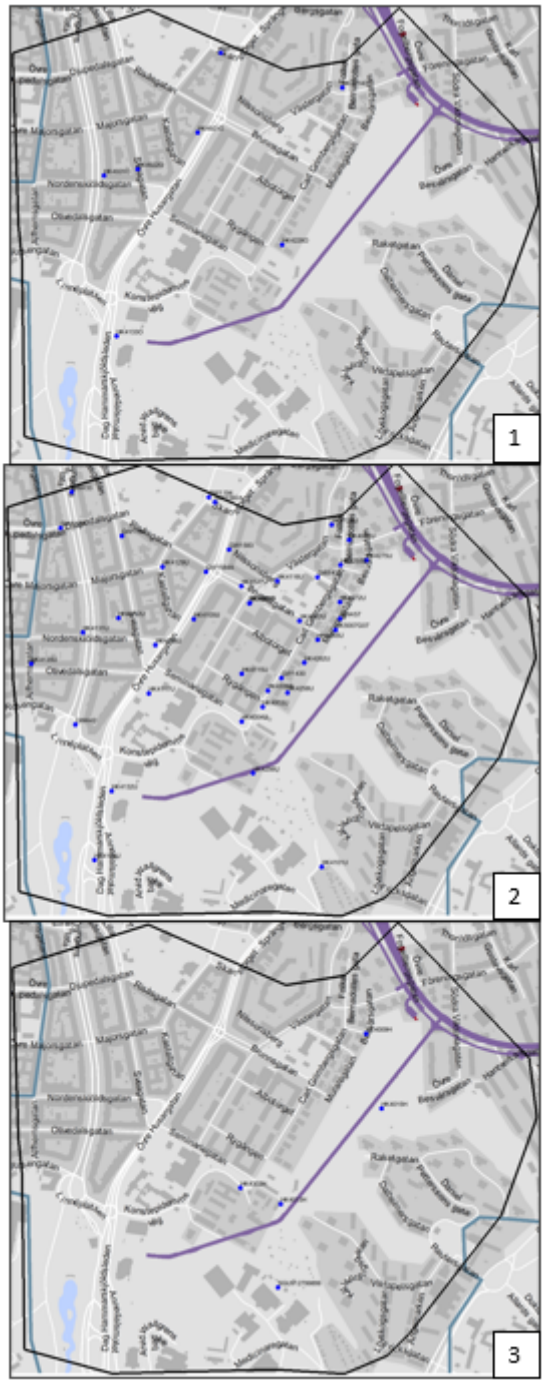

Figure A.3: Observations wells used for Linné, with [1] upper aquifer in layer one, [2] lower soil aquifer in layer four, [3] rock aquifer in layer six.

A.2 Korsvägen

Observation point	Distance from pump [m]	Drawdown [m]
KK4249B	0	12,09
KK4248U	0,7	7,58
KK4234B	100	2,66
KK4246U	131	1,96
GW1044	18	1,705
KK4229U	144	1,4
GW1618	100	1,59
KK4233U	208	1,22
KK4201U	186	1,17
TY30GW	210	1,08
KK4013U	288	0,7
KK4001B	288	0,61
TY501GW	341	0,58
GW2137	264	0,56
KK4012U	288	0,51
KK4231U	242	0,48
KK4106U	507	0,4
GW502	351	0,18
TY33GW	461	0,16
KK4110U	302	0,16
KK4235B	394	0,14
KK4242U	101	0,14

Figure A.4: Drawdown at the end of pumping test.

B

Appendix 2

B.1 Linné

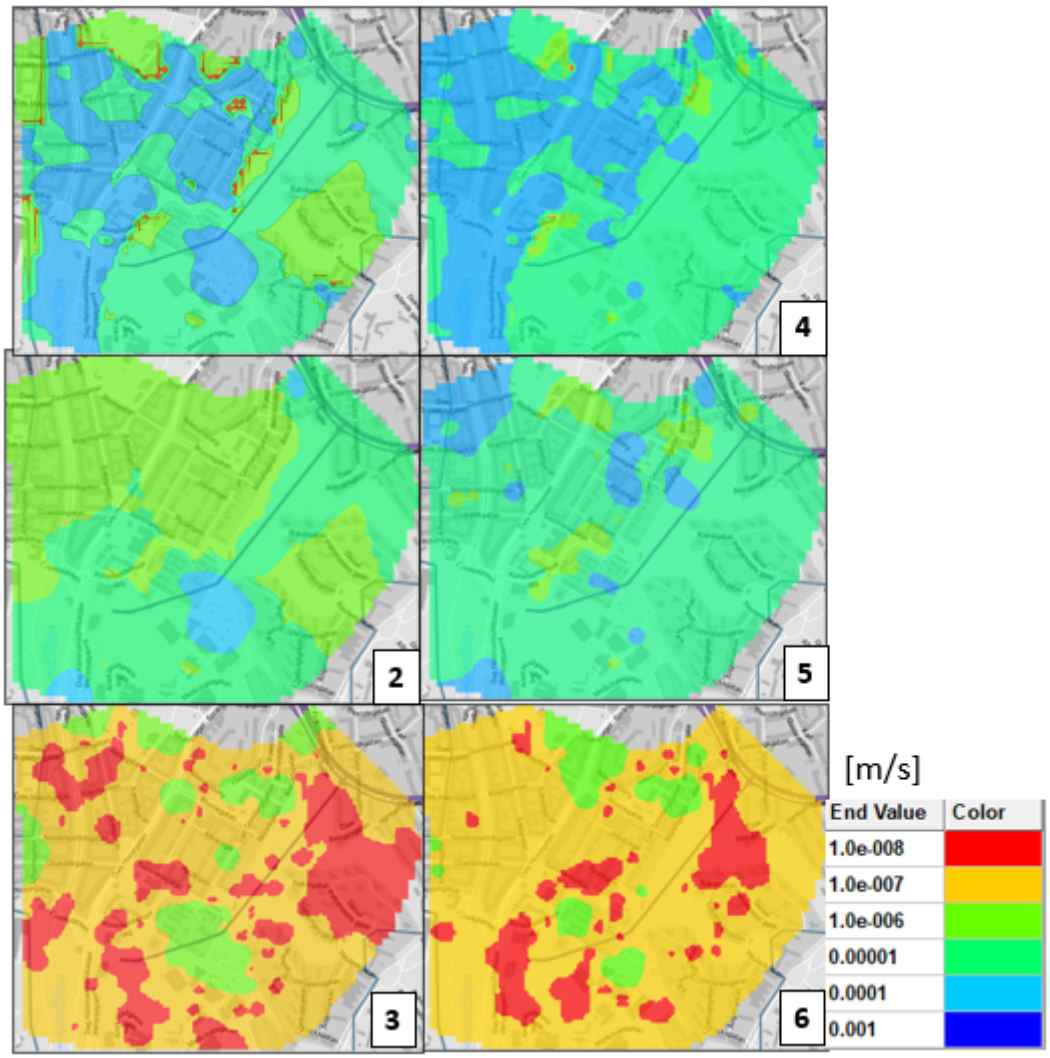

Figure B.1: Mean hydraulic conductivity in m/s of glacial till [1&4], fractured bedrock [2&5] and bedrock [3&6]. Case one to the left and case two to the right.

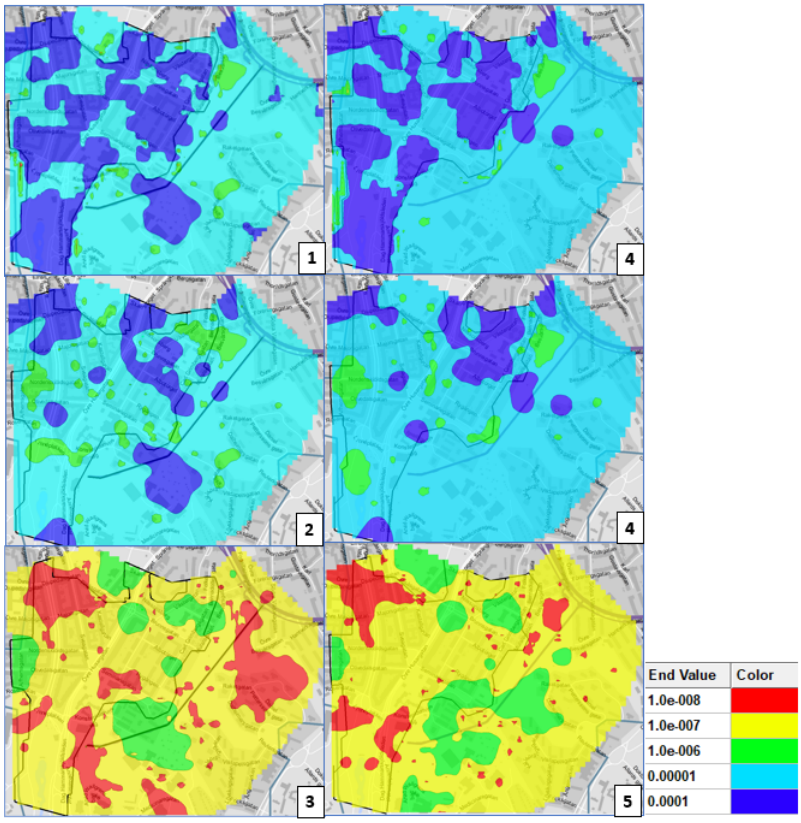

Figure B.2: PEST calibrated models using inverse distance weighted interpolation before NSMC. Hydraulic conductivity in m/s of glacial till [1&4], fractured bedrock [2&5] and bedrock [3&6]. case one to the left and case two to the right.

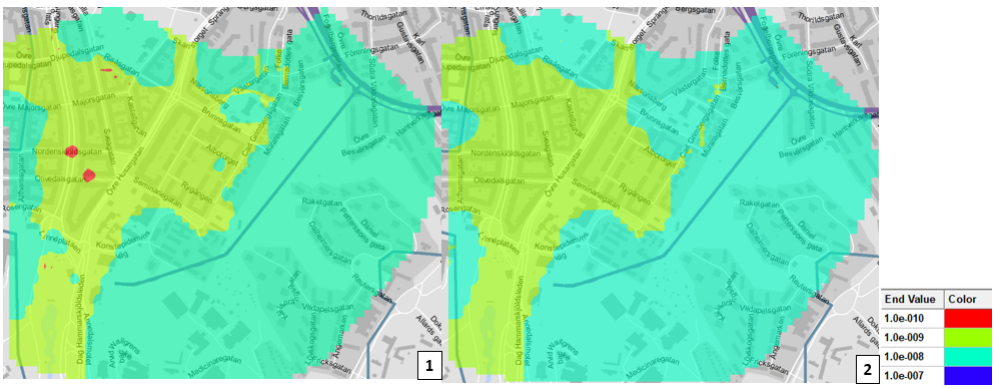

Figure B.3: Mean recharge in m/s for case one to the left and case two to the right.

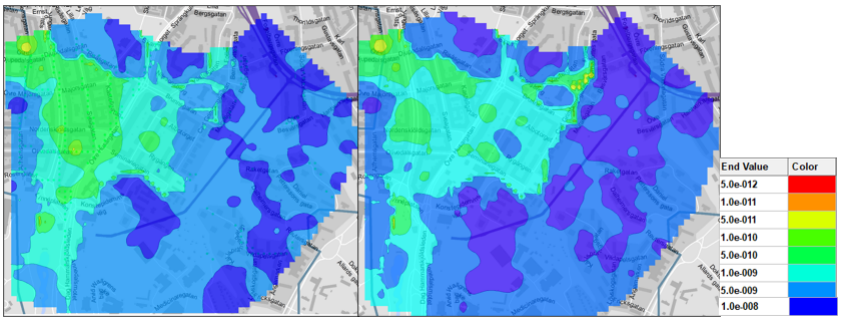

Figure B.4: PEST calibrated models using inverse distance weighted interpolation before NSMC. Recharge in m/s for case one to the left and case two to the right.

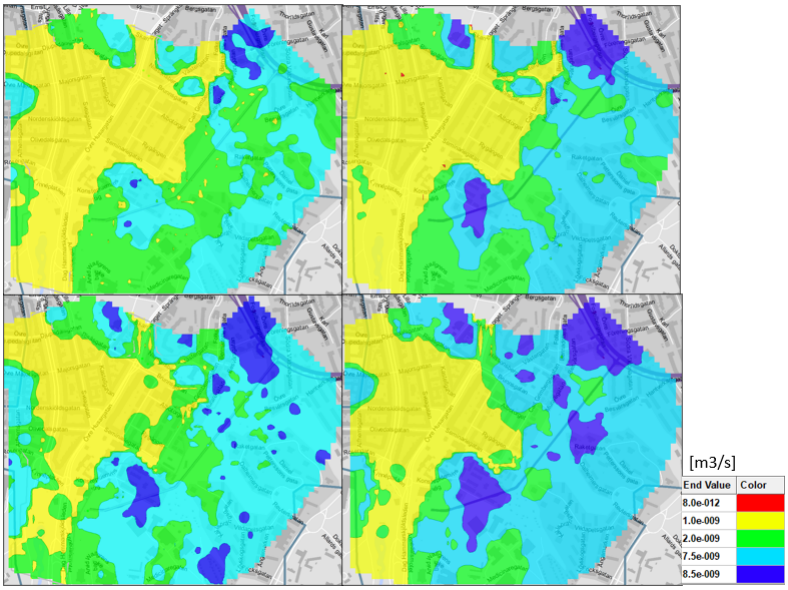

Figure B.5: Recharge [m/s] with legend focused on min and max values. Min recharge of NSMC datasets [1 & 3] and max recharge of NSMC datasets. Case one to the left and case two to the right.

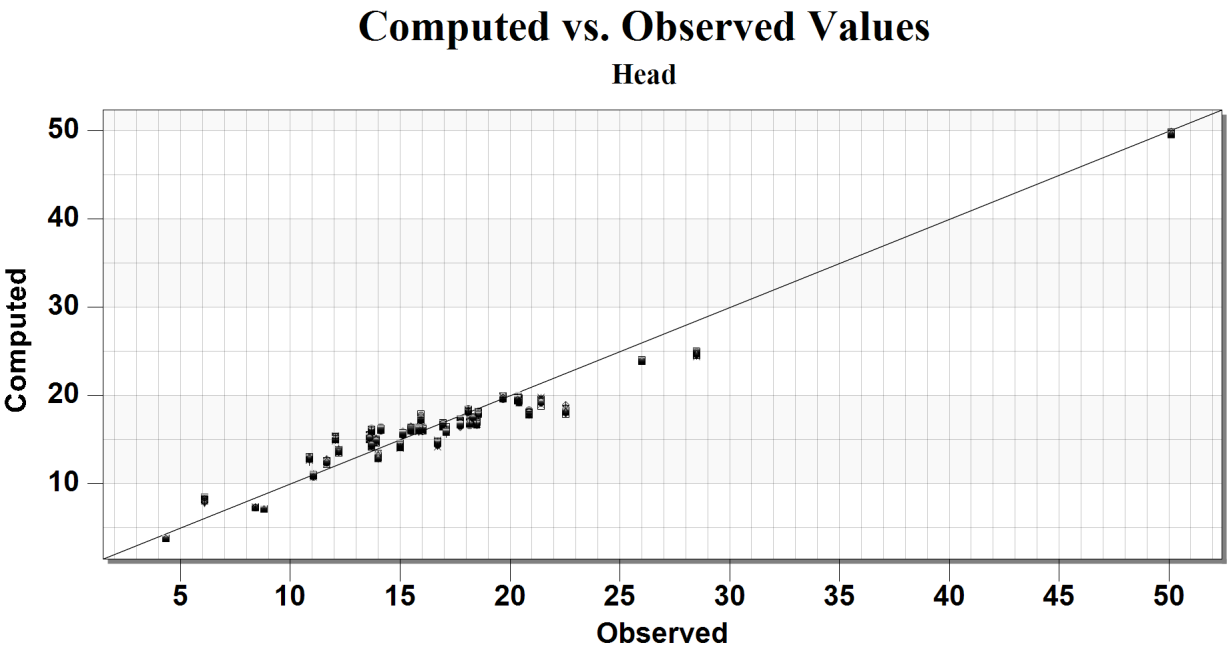

Figure B.6: Computed versus observed heads in the lower soil aquifer for calibration case one of the Linné model.

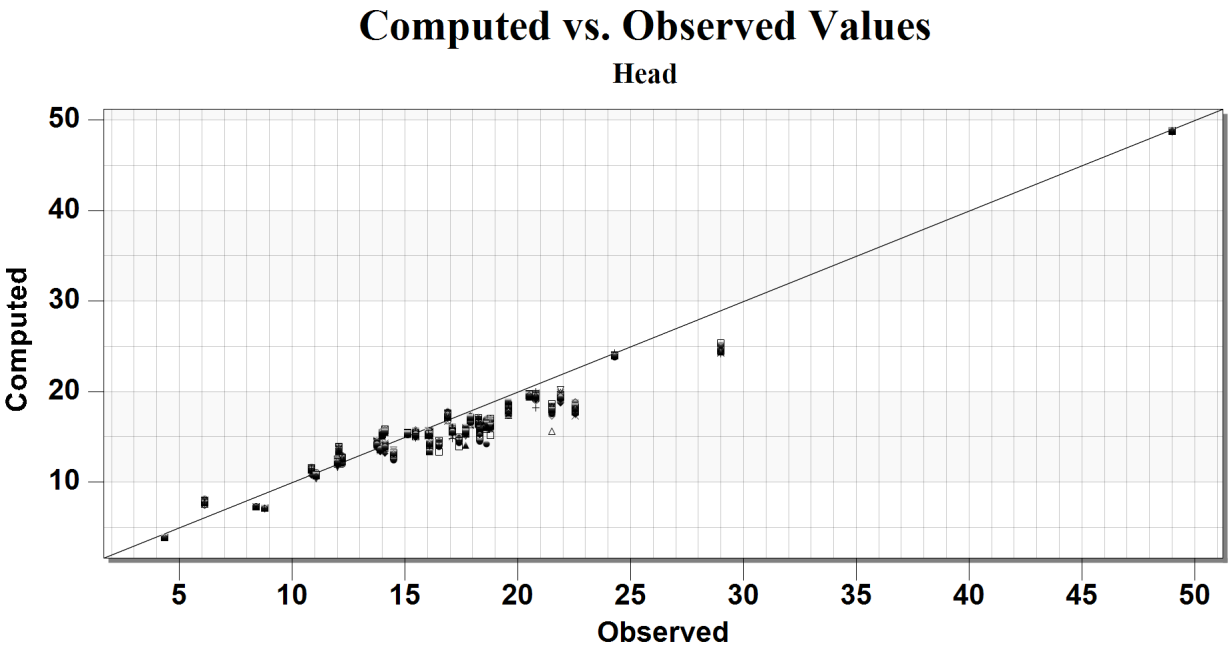

Figure B.7: Computed versus observed heads in the lower soil aquifer for calibration case two of the Linné model.

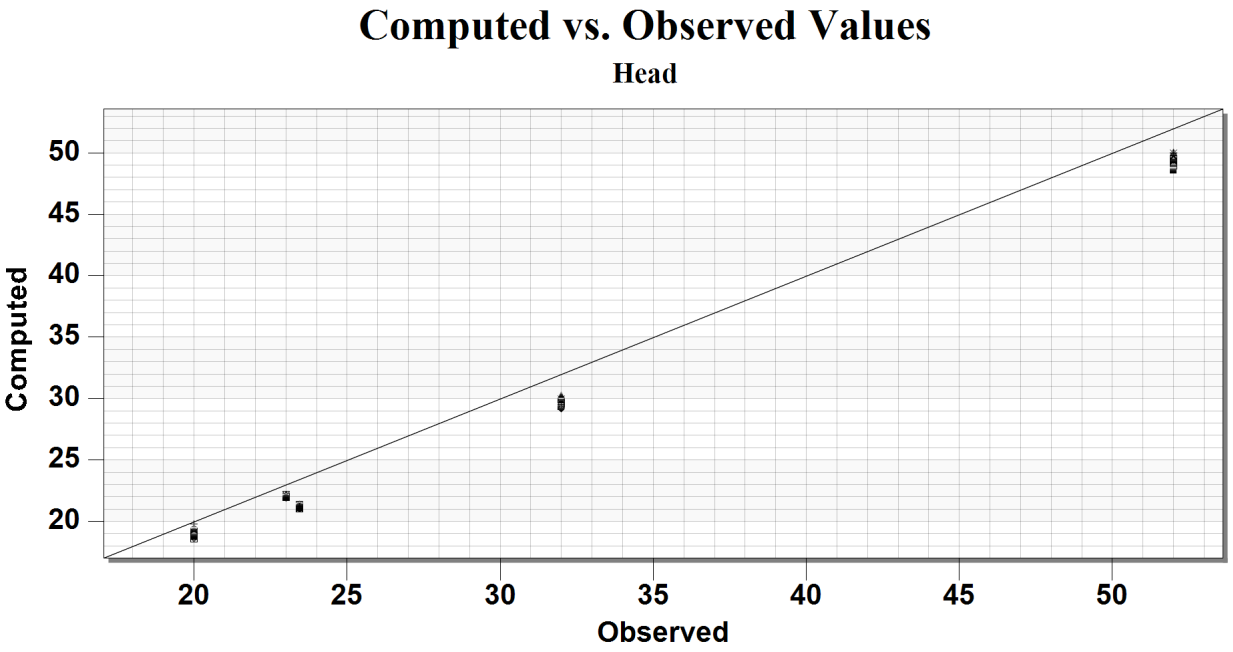

Figure B.8: Computed versus observed heads in rock aquifer for calibration case one of the Linné model.

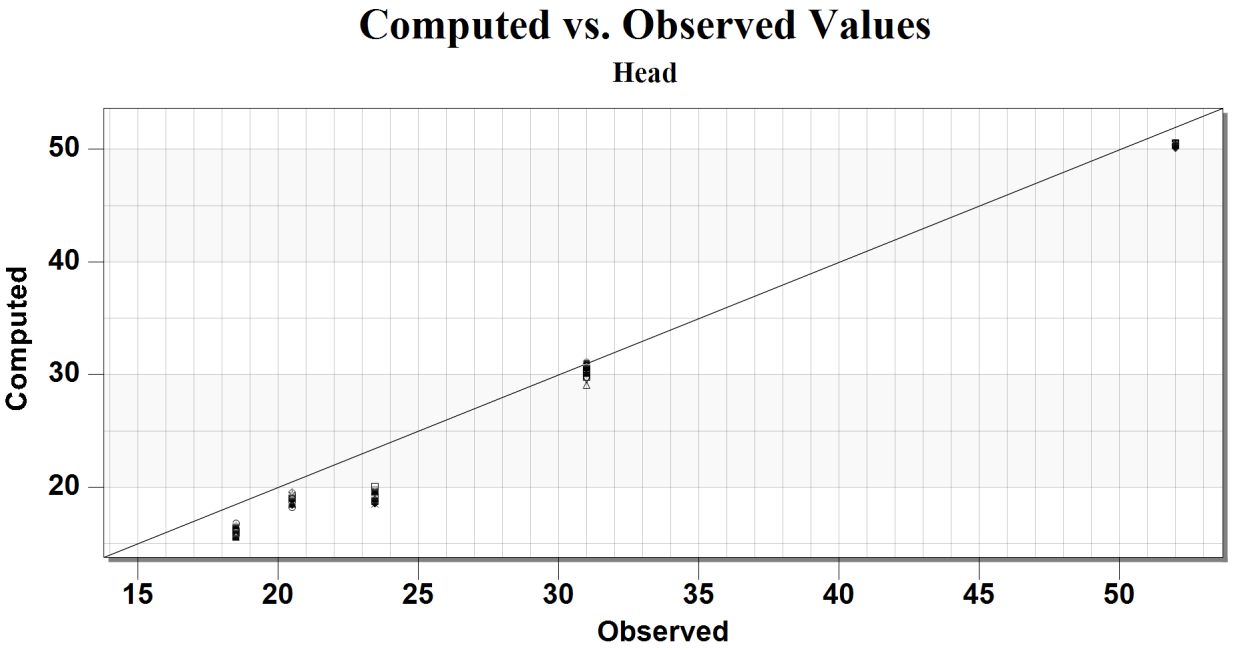

Figure B.9: Computed versus observed heads in the rock aquifer for calibration case two of the Linné model.

B.2 Korsvägen

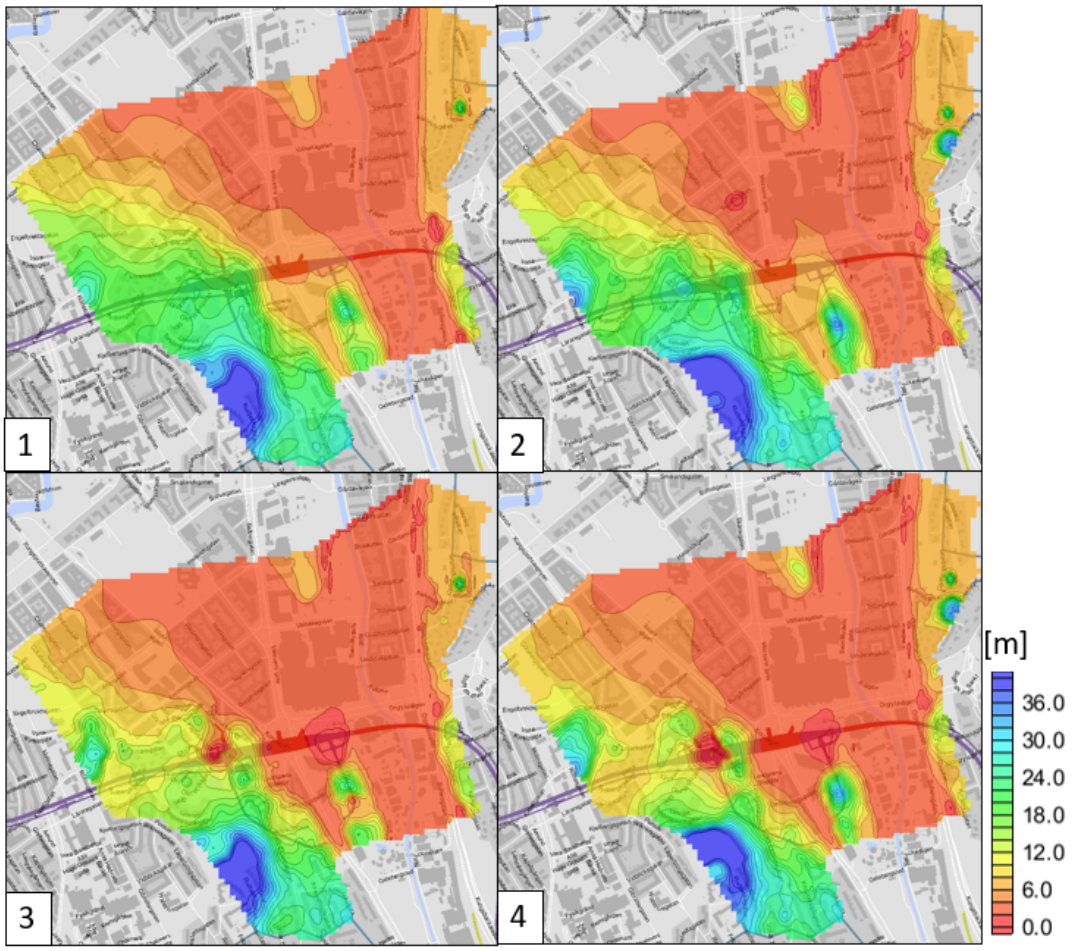

Figure B.10: Mean head observations after calibration [1&2] and forecast [3&4]. case one to the left and case two to the right.

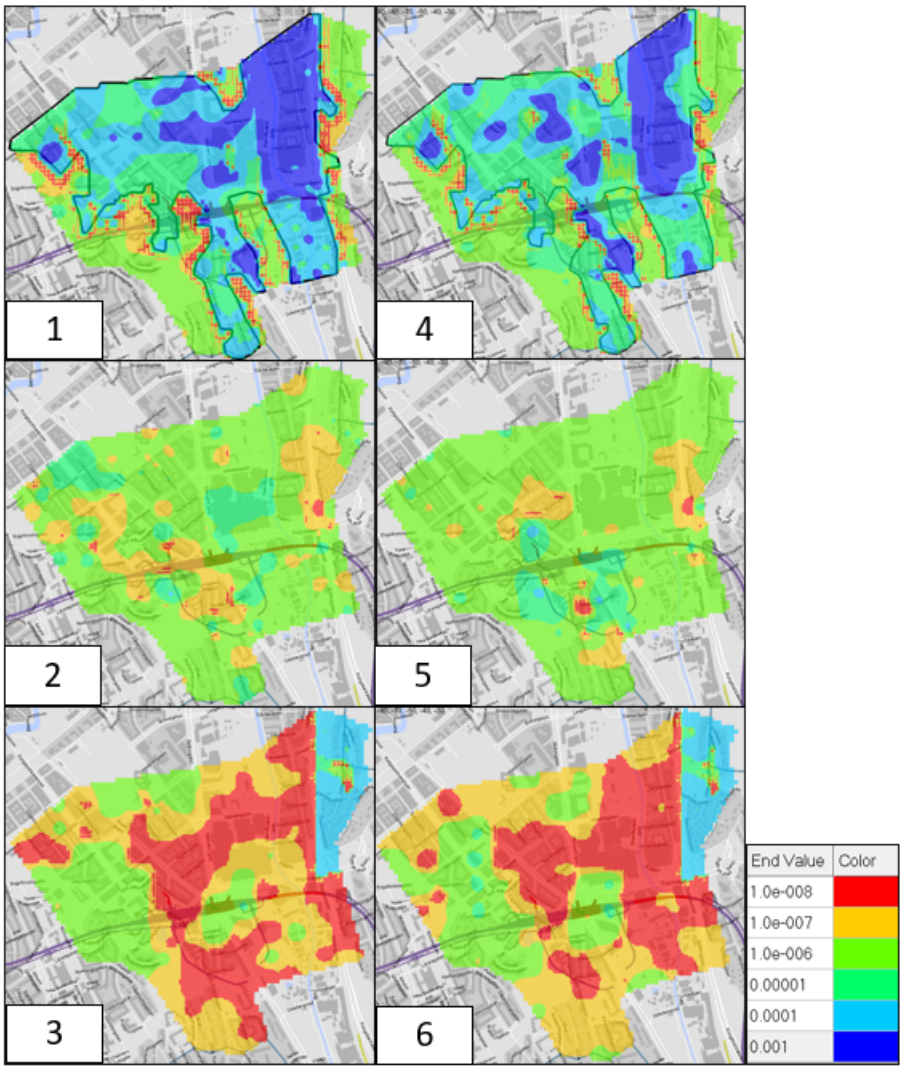

Figure B.11: Mean hydraulic conductivity in m/s of glacial till [1&4], fractured bedrock [2&5] and bedrock [3&6]. case one to the left and case two to the right.

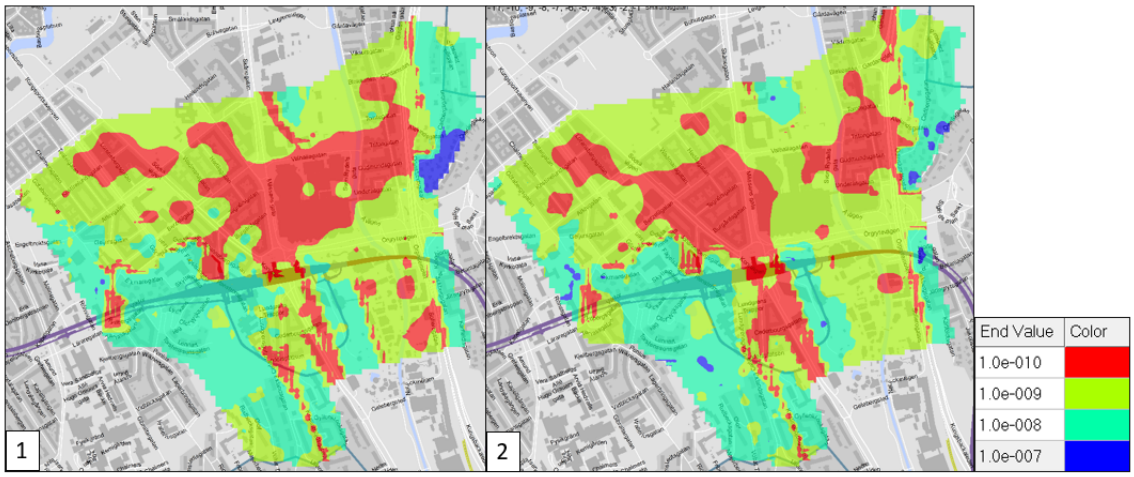

Figure B.12: Mean recharge in m/s for case one to the left and case two to the right.

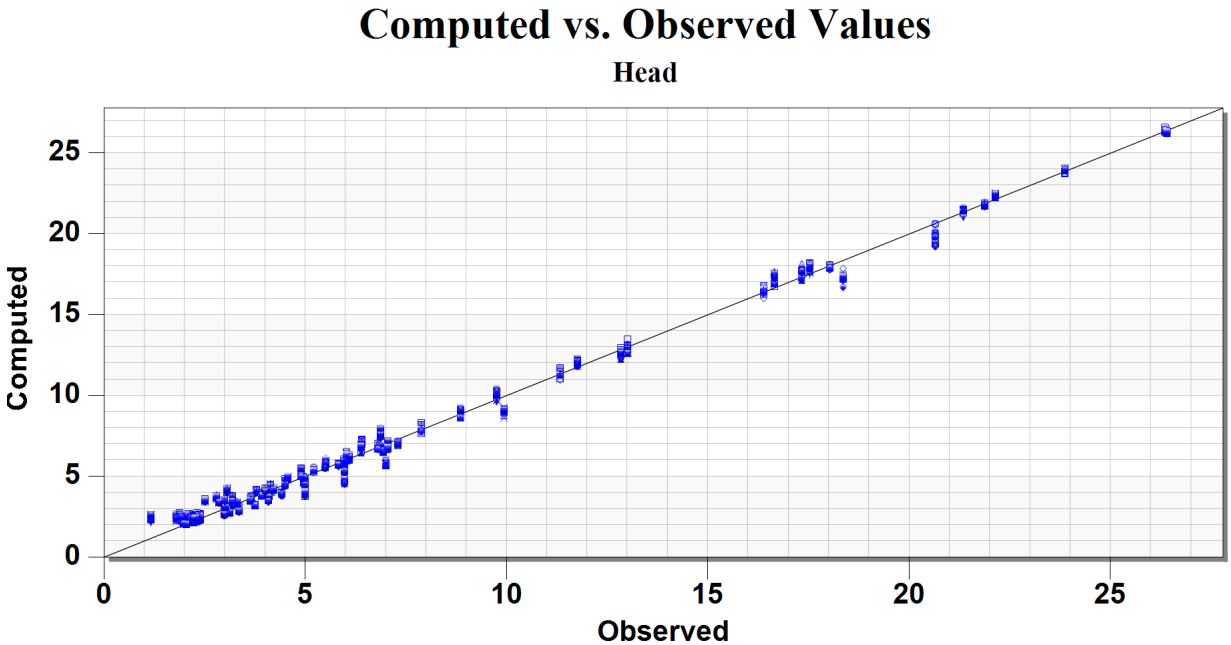

Figure B.13: Computed versus observed heads in the lower soil aquifer for calibration case one of the Korsvägen model.

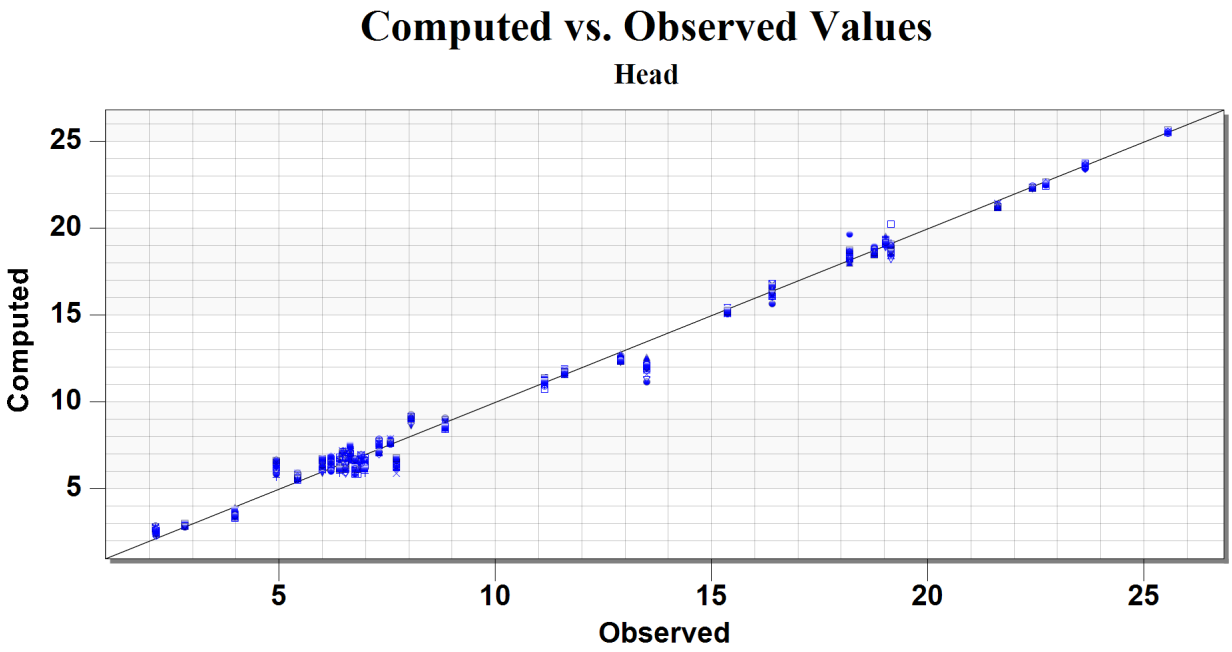

Figure B.14: Computed versus observed heads in the rock aquifer for calibration case one of the Korsvägen model.

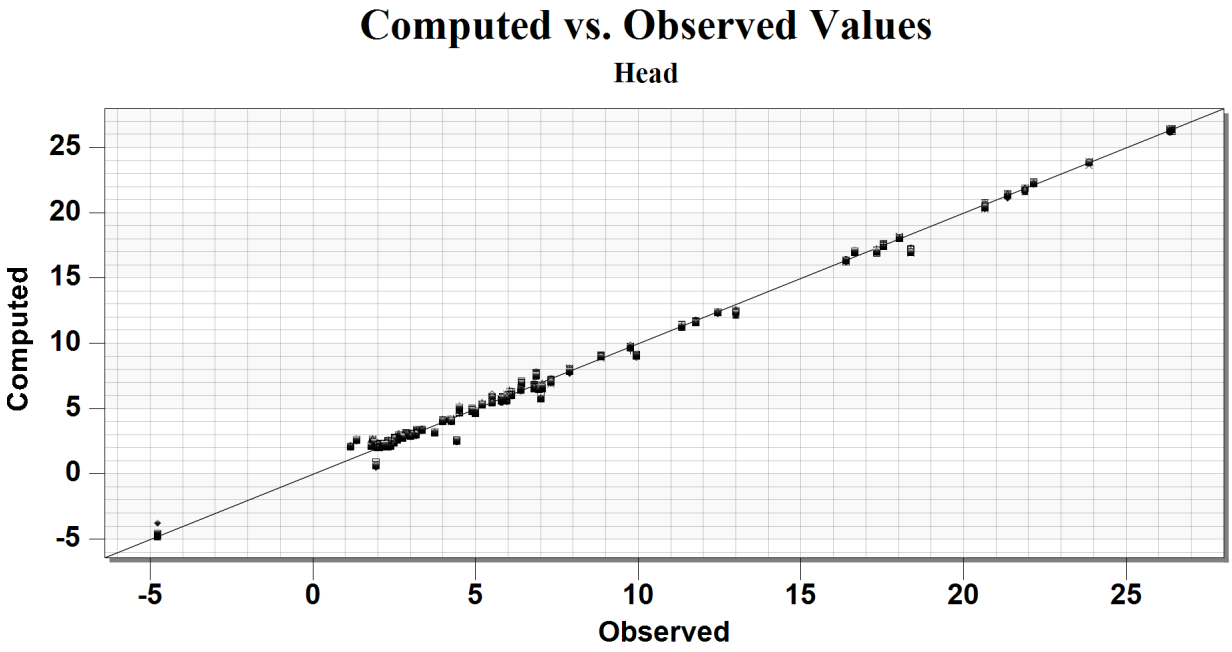

Figure B.15: Computed versus observed heads in the lower soil aquifer for calibration case two of the Korsvägen model.

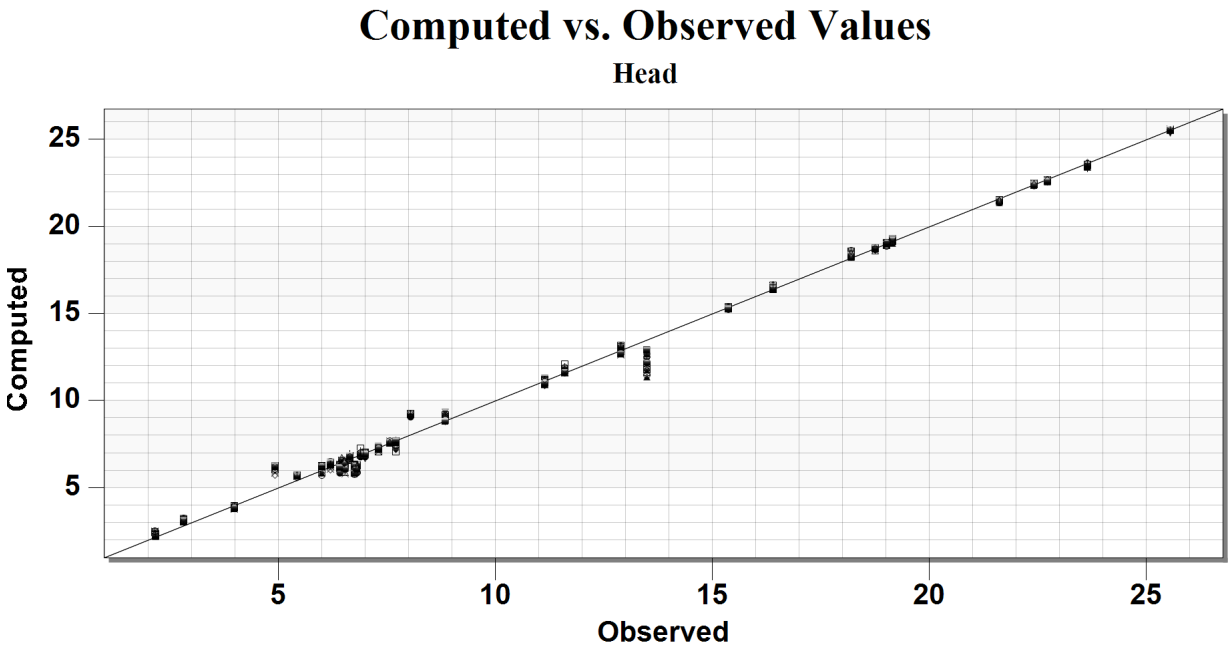

Figure B.16: Computed versus observed heads in the rock aquifer for calibration case two of the Korsvägen model.